

New Physics Patterns in ε'/ε and ε_K with Implications for Rare Kaon Decays and ΔM_K

Andrzej J. Buras*

TUM Institute for Advanced Study, Lichtenbergstr. 2a, D-85748 Garching, Germany
Physik Department, TU München, James-Franck-Straße, D-85748 Garching, Germany

* E-mail: aburas@ph.tum.de

Abstract

The Standard Model (SM) prediction for the ratio ε'/ε appears to be significantly below the experimental data. Also ε_K in the SM tends to be below the data. Any new physics (NP) removing these anomalies will first of all have impact on flavour observables in the K meson system, in particular on rare decays $K^+ \rightarrow \pi^+\nu\bar{\nu}$, $K_L \rightarrow \pi^0\nu\bar{\nu}$, $K_L \rightarrow \mu^+\mu^-$ and $K_L \rightarrow \pi^0\ell^+\ell^-$ and ΔM_K . Restricting the operators contributing to ε'/ε to the SM ones and to the corresponding primed operators, NP contributions to ε'/ε are quite generally dominated either by QCD penguin (QCDP) operators $Q_6(Q'_6)$ or electroweak penguin (EWP) operators $Q_8(Q'_8)$ with rather different implications for other flavour observables. Our presentation includes general models with tree-level Z and Z' flavour violating exchanges for which we summarize known results and add several new ones. We also briefly discuss few specific models. The correlations of ε'/ε with other flavour observables listed above allow to differentiate between models in which ε'/ε can be enhanced. Various DNA-tables are helpful in this respect. We find that simultaneous enhancements of ε'/ε , ε_K , $\mathcal{B}(K_L \rightarrow \pi^0\nu\bar{\nu})$ and $\mathcal{B}(K^+ \rightarrow \pi^+\nu\bar{\nu})$ in Z scenarios are only possible in the presence of both left-handed and right-handed flavour-violating couplings. In Z' scenarios this is not required but the size of NP effects and the correlation between $\mathcal{B}(K_L \rightarrow \pi^0\nu\bar{\nu})$ and $\mathcal{B}(K^+ \rightarrow \pi^+\nu\bar{\nu})$ depends strongly on whether QCDP or EWP dominate NP contributions to ε'/ε . In the QCDP case possible enhancements of both branching ratios are much larger than for EWP scenario and take place only on the branch parallel to the Grossman-Nir bound, which is in the case of EWP dominance only possible in the absence of NP in ε_K . We point out that QCDP and EWP scenarios of NP in ε'/ε can also be uniquely distinguished by the size and the sign of NP contribution to ΔM_K , elevating the importance of the precise calculation of ΔM_K in the SM. We emphasize the importance of the theoretical improvements not only on ε'/ε , ε_K and ΔM_K but also on $K_L \rightarrow \mu^+\mu^-$, $K_L \rightarrow \pi^0\ell^+\ell^-$, and the $K \rightarrow \pi\pi$ isospin amplitudes $\text{Re}A_0$ and $\text{Re}A_2$ which would in the future enrich our analysis.

Contents

1	Introduction	3
2	Basic formula for ε'/ε	6
3	Strategy	10
3.1	Present	10
3.2	Future	11
4	Z Models	12
4.1	Preliminaries	12
4.2	Left-handed Scenario (LHS)	13
4.2.1	ε'/ε	13
4.2.2	ε_K , ΔM_K and $K_L \rightarrow \mu^+ \mu^-$	14
4.2.3	$K^+ \rightarrow \pi^+ \nu \bar{\nu}$ and $K_L \rightarrow \pi^0 \nu \bar{\nu}$	15
4.3	Right-handed Scenario (RHS)	16
4.3.1	ε'/ε	16
4.3.2	ε_K , ΔM_K and $K_L \rightarrow \mu^+ \mu^-$	17
4.3.3	$K^+ \rightarrow \pi^+ \nu \bar{\nu}$ and $K_L \rightarrow \pi^0 \nu \bar{\nu}$	17
4.4	General Z Scenarios	18
4.4.1	ε'/ε	18
4.4.2	ε_K , ΔM_K and $K_L \rightarrow \mu^+ \mu^-$	18
4.4.3	$K^+ \rightarrow \pi^+ \nu \bar{\nu}$ and $K_L \rightarrow \pi^0 \nu \bar{\nu}$	19
4.4.4	Phenomenology	20
4.5	Summary of NP Patterns in Z Scenarios	23
5	Z' Models	24
5.1	Preliminaries	24
5.2	Z' with QCD Penguin Dominance (LHS)	26
5.2.1	ε'/ε	26
5.2.2	ε_K , ΔM_K and $K_L \rightarrow \mu^+ \mu^-$	27
5.2.3	$K^+ \rightarrow \pi^+ \nu \bar{\nu}$ and $K_L \rightarrow \pi^0 \nu \bar{\nu}$	28
5.3	Z' with QCD Penguin Dominance (RHS)	30
5.4	Z' with QCD Penguin Dominance (General)	30
5.4.1	ε'/ε	30
5.4.2	ε_K and ΔM_K	31
5.4.3	Implications	31
5.5	A heavy G'	32
5.6	Z' with Electroweak Penguin Dominance	33
5.6.1	The case of $\Delta_R^{qq}(Z') = \mathcal{O}(1)$	33
5.6.2	The case of $\Delta_R^{qq}(Z') \ll 1$	36
5.7	The Impact of $Z - Z'$ mixing	36
5.8	Z' Outside the Reach of the LHC	37
5.8.1	QCD Penguin Dominance	37
5.8.2	Electroweak Penguin Dominance	38

5.9	Summary of NP Patterns in Z' Scenarios	39
6	Hybrid Scenarios: Z and Z'	40
7	Selected Models	43
7.1	Preliminaries	43
7.2	Models with Minimal Flavour Violation	43
7.3	A Model with a Universal Extra Dimension	44
7.4	Littlest Higgs Model with T-Parity	44
7.5	331 Models	44
7.6	More Complicated Models	45
8	New Physics in $\text{Re}A_0$ and $\text{Re}A_2$	46
9	2018 Visions	47
9.1	$\kappa_{\varepsilon'} = 1.0$ and $\kappa_{\varepsilon} = 0.4$	47
9.2	$\kappa_{\varepsilon'} = 1.0$ and $\kappa_{\varepsilon} = 0.0$	47
10	Outlook and Open Questions	48
A	More Information on Renormalization Group Evolution	51
A.1	QCD Penguins	51
A.2	Electroweak Penguins	52
A.3	Beyond the LHC Scales	53
B	ε_K and ΔM_K	53
B.1	General Formulae	53
B.2	Z and Z' Cases	54
C	$K^+ \rightarrow \pi^+ \nu \bar{\nu}$ and $K_L \rightarrow \pi^0 \nu \bar{\nu}$	55
C.1	General Formulae	55
C.2	Z and Z' Cases	56
D	$K_L \rightarrow \mu^+ \mu^-$	57
D.1	General Formulae	57
D.2	Z and Z' Cases	57
E	$K_L \rightarrow \pi^0 \ell^+ \ell^-$	58
	References	58

1 Introduction

The ratio ε'/ε measures the size of the direct CP violation in $K_L \rightarrow \pi\pi$ decays relative to the indirect CP violation described by ε_K and is rather sensitive to new physics (NP). In the Standard Model (SM) ε' is governed by QCD penguins (QCDP) but receives also an important destructively interfering contribution from electroweak penguins (EWP). Beyond the SM the structure of NP contributions to ε'/ε is in general different as often only the EWP operators contribute in a significant manner. But, one can also construct scenarios in which NP contributions from QCDP dominate. This is for instance the case of certain Z' models which we will present in detail below. Moreover, there exist models in which NP contributions to ε'/ε can be dominated by new operators which can be neglected within the SM. A prominent example is the chromomagnetic penguin operator in supersymmetric models.

The present status of ε'/ε in the SM has been reviewed recently in [1, 2], where references to rich literature can be found. After the new results for the hadronic matrix elements of QCDP and EWP $(V - A) \otimes (V + A)$ operators from RBC-UKQCD lattice collaboration [3–5] and the extraction of the corresponding matrix elements of penguin $(V - A) \otimes (V - A)$ operators from the CP-conserving $K \rightarrow \pi\pi$ amplitudes one finds [1]

$$(\varepsilon'/\varepsilon)_{\text{SM}} = (1.9 \pm 4.5) \times 10^{-4}. \quad (1)$$

This result differs with 2.9σ significance from the experimental world average from NA48 [6] and KTeV [7, 8] collaborations,

$$(\varepsilon'/\varepsilon)_{\text{exp}} = (16.6 \pm 2.3) \times 10^{-4}, \quad (2)$$

suggesting evidence for NP in K decays.

As demonstrated in [9] these new results from lattice-QCD are supported by the large N approach, which moreover allows to derive upper bounds on the matrix elements of the dominant penguin operators. This implies [1, 9]

$$(\varepsilon'/\varepsilon)_{\text{SM}} \leq (8.6 \pm 3.2) \times 10^{-4}, \quad (\text{large } N), \quad (3)$$

still 2σ below the experimental data. Additional arguments for this bound will be given in Section 2.

While, the improvement on the estimate of isospin corrections, final state interactions (FSI) [10–15] and the inclusion of NNLO QCD corrections could in principle increase ε'/ε with respect to the one in (1), it is rather unlikely that values of ε'/ε violating the upper bound in (3) will be found within the SM. After all, until now, lattice QCD confirmed most of earlier results on K meson flavour physics obtained in the large N approach (see [2, 16]).

In particular a recent analysis of FSI in this approach in [17] gives additional support for these expectations. As stated in this paper, it turns out that beyond the strict large N limit, FSI are likely to be important for the $\Delta I = 1/2$ rule, in agreement with [10–15], but much less relevant for ε'/ε . It appears then that the SM has significant difficulties in explaining the experimental value of ε'/ε . This implies that NP models in which this ratio can be enhanced with respect to its SM value are presently favoured.

Now, the renormalization group effects play a very important role in the analysis of ε'/ε . They have been known already for more than twenty years at the NLO level [18–23] and present technology could extend them to the NNLO level if necessary. First steps in this direction have been taken in [24–26]. The situation with hadronic matrix elements is another story and even if significant progress on their evaluation has been made over the last 25 years, the present status is clearly not satisfactory. Still, both the large N approach and lattice QCD show that hadronic matrix elements of QCD and EWP $(V - A) \otimes (V + A)$ operators, Q_6 and Q_8 respectively, are by far the largest among those of contributing operators with the relevant matrix element $\langle Q_8 \rangle_2$ being larger than $\langle Q_6 \rangle_0$ in magnitude by roughly a factor of two.

With the Wilson coefficient y_6 of Q_6 being roughly by a factor of 90 larger than y_8 of Q_8 (see [1]) one would expect the Q_6 operator to be by far the dominant one in ε'/ε . That this does not happen is due to the factor

$$\frac{\text{Re}A_2}{\text{Re}A_0} = \frac{1}{22.4} \quad (4)$$

which in the basic formula for ε'/ε in (5) suppresses the Q_6 contribution relative to the Q_8 one. As a result strong cancellation between these two dominant contributions to ε'/ε in the SM takes place so that contributions of other less important $(V - A) \otimes (V - A)$ operators matter. A detailed anatomy of such contributions has been presented in [1].

Beyond the SM quite often the Wilson coefficients of Q_6 and Q_8 and of the primed operators Q'_6 and Q'_8 ¹ in the NP contribution to ε'/ε are of the same order and then operators Q_8 and/or Q'_8 win easily this competition because of the suppression of the Q_6 and Q'_6 contributions by the factor in (4) and the fact that their hadronic matrix elements are smaller than the ones of Q_8 and Q'_8 . Therefore retaining only the latter contributions in the NP part is a reasonable approximation if one wants to make a rough estimate of ε'/ε with the accuracy of 10%. Only in the presence of a flavour symmetry which assures the flavour universality of diagonal quark couplings, Q_6 and/or Q'_6 win this competition because the contribution of $Q_8(Q'_8)$ is then either negligible or absent. In such cases Q_6 and/or Q'_6 are by far the dominant contributions to ε'/ε .

This simplification in the renormalization group analysis, pointed out in [27], and present in many extensions of the SM, allows for a quick rough estimate of the size of NP contributions to ε'/ε in a given model. Moreover, the absence of cancellations between QCD and electroweak penguin contributions in the NP part makes it subject to much smaller theoretical uncertainties than it is the case within the SM. Then leading order renormalization group analysis is sufficient, in particular, for finding the sign of NP contribution as a function of model parameters, generally couplings of NP to quarks. This sign is in most cases not unique because of the presence of free parameters represented by new couplings in a given model. But requiring that NP enhances ε'/ε relative to its SM value, determines the signs of these couplings with implications for other observables in the K meson system. As ε'/ε is only sensitive to imaginary couplings, we will simultaneously assume that there is a modest anomaly in ε_K , which together with ε'/ε will allow us to determine both imaginary and real flavour violating couplings of Z and Z' implied by these anomalies. This in turn will give us predictions for NP contributions to $K_L \rightarrow \pi^0 \nu \bar{\nu}$,

¹These operators are obtained from Q_6 and Q_8 through the interchange of $V - A$ and $V + A$.

$K^+ \rightarrow \pi^+ \nu \bar{\nu}$, $K_L \rightarrow \mu^+ \mu^-$ and ΔM_K implied by these anomalies. In certain models the enhancement of ε'/ε implies uniquely enhancement or suppression of other observables or even eliminates significant NP contributions from them. In this manner even patterns of deviations from SM predictions can identify the favoured NP models.

This strategy of identifying NP through quark flavour violating processes has been proposed in [28] and graphically represented in terms of DNA-charts. But the case of ε'/ε has not been discussed there in this manner and we would like to do it here in the form of DNA-tables, see Tables 3 and 4, concentrating fully on the K meson system. But as we will see this system by itself can already give us a valuable insight into physics beyond the SM. The implications for other meson systems require more assumptions on the flavour structure of NP and will be considered elsewhere. A recent study of the impact of K physics observables on the determination of the Unitarity triangle can be found in [29].

Our paper is organized as follows. In Section 2 we recall the basic formula for ε'/ε that is valid in all extensions of the SM and recall the relevant hadronic matrix elements of the operators $Q_6(Q'_6)$ and $Q_8(Q'_8)$. In Section 3 we present our strategy for addressing the sizable ε'/ε anomaly and a modest ε_K anomaly with the hope that it will make our paper more transparent. In Section 4 we discuss models in which NP contributions to ε'/ε come dominantly from tree-level Z exchanges and identify a number of scenarios for flavour-violating Z couplings that could provide the required enhancement of ε'/ε with concrete implications for other flavour observables listed above. In Section 5 we generalize this discussion to models with tree-level Z' exchanges and discuss briefly the effects of $Z - Z'$ mixing. We also consider there the case of G' , a colour octet of heavy gauge bosons. In both sections we demonstrate how these different models can be differentiated with the help of other observables. Of particular interest is the case of $M_{Z'}$ outside the reach of the LHC if the flavour structure of a given model is such that the suppression by Z' propagator is compensated by the increase of flavour-violating couplings. We also stress that for $M_{Z'} \geq 10$ TeV renormalization group effects imply additional significant enhancements of both QCDP and EWP contributions to ε'/ε . In Section 6 we briefly discuss scenarios in which contributions of both Z and Z' are present even in the absence of significant $Z - Z'$ mixing. This is the case of models in which in addition to Z' also new heavy fermions, like vector-like quarks, are present implying through the mixing with SM quarks flavour-violating Z couplings. While our discussion is rather general, in Section 7 we give examples of specific Z and Z' models, in which one can reach clear cut conclusions and briefly summarize more complicated models. In Section 8 we discuss possible implications of NP in the $K \rightarrow \pi\pi$ isospin amplitudes $\text{Re}A_0$ and $\text{Re}A_2$. In Section 9 we contemplate on the implications of the possible discovery of NP in $K^+ \rightarrow \pi^+ \nu \bar{\nu}$ by NA62 experiment in 2018 in the presence of ε'/ε anomaly, dependently on whether NP in ε_K is present or absent. Finally in Section 10 we summarize most important findings and give a brief outlook for the coming years and list most important open questions. Several appendices contain a collection of useful formulae.

Our paper differs from other papers on flavour physics in K meson system in that we do not obtain the results for ε'/ε and ε_K as output of a complicated analysis but treat them as input parametrizing the size of NP contributions to them by two parameters of $\mathcal{O}(1)$: $\kappa_{\varepsilon'}$ and κ_{ε} . See Section 3 for the explicit formulation of this strategy.

Our paper differs also from many papers on rare processes present in the literature in

that it does not contain a single plot coming from a sophisticated numerical analysis. The uncertainty in the QCDP contribution to ε'/ε in the SM leaves still a very large room for NP in ε'/ε and a detailed numerical analysis would only wash out the pattern of NP required to enhance ε'/ε . The absence of sophisticated plots is compensated by numerous simple analytic formulae and DNA-tables that should allow model builders to estimate quickly the pattern of NP in the K meson system in her or his favourite model. Our goal is to present the material in such a manner that potential readers can follow all steps in detail.

Finally, our paper differs also from the recent literature on flavour physics which is dominated by the anomalies in most recent data for $B \rightarrow K(K^*)\ell^+\ell^-$ and $B \rightarrow D(D^*)\tau\nu_\tau$ reported by LHCb, BaBar and Belle. The case of ε'/ε is different as the data is roughly fifteen years old and the progress is presently done by theorists, not experimentalists. But as the recent papers [1, 3, 4, 9] show, ε'/ε after rather silent ten years is striking back, in particular in correlation with $K^+ \rightarrow \pi^+\nu\bar{\nu}$ and $K_L \rightarrow \pi^0\nu\bar{\nu}$ [30, 31] on which the data [32–34] will improve significantly in the coming years. Moreover, as we will see in the context of our presentation, theoretical improvements not only on ε'/ε but also on ε_K , ΔM_K , $K_L \rightarrow \mu^+\mu^-$, $K_L \rightarrow \pi^0\ell^+\ell^-$, and the $K \rightarrow \pi\pi$ isospin amplitudes $\text{Re}A_0$ and $\text{Re}A_2$ will give us new insights in NP at short distance scales.

2 Basic formula for ε'/ε

The basic formula for ε'/ε reads [1]

$$\frac{\varepsilon'}{\varepsilon} = -\frac{\omega_+}{\sqrt{2}|\varepsilon_K|} \left[\frac{\text{Im}A_0}{\text{Re}A_0} (1 - \hat{\Omega}_{\text{eff}}) - \frac{1}{a} \frac{\text{Im}A_2}{\text{Re}A_2} \right], \quad (5)$$

with (ω_+, a) and $\hat{\Omega}_{\text{eff}}$ given as follows

$$\omega_+ = a \frac{\text{Re}A_2}{\text{Re}A_0} = (4.53 \pm 0.02) \times 10^{-2}, \quad a = 1.017, \quad \hat{\Omega}_{\text{eff}} = (14.8 \pm 8.0) \times 10^{-2}. \quad (6)$$

Here a and $\hat{\Omega}_{\text{eff}}$ summarize isospin breaking corrections and include strong isospin violation ($m_u \neq m_d$), the correction to the isospin limit coming from $\Delta I = 5/2$ transitions and electromagnetic corrections [35–37]. $\hat{\Omega}_{\text{eff}}$ differs from Ω_{eff} in [35, 36] which includes contributions of EWP. Here they are present in $\text{Im}A_0$ and of course in $\text{Im}A_2$. Strictly speaking ε'/ε is a complex quantity and the expression in (5) applies to its real part but its phase is so small that we can drop the symbol “Re” in all expressions below in order to simplify the notation.

The amplitudes $\text{Re}A_{0,2}$ are then extracted from the branching ratios on $K \rightarrow \pi\pi$ decays in the isospin limit. Their values are given by

$$\text{Re}A_0 = 33.22(1) \times 10^{-8} \text{ GeV}, \quad \text{Re}A_2 = 1.479(3) \times 10^{-8} \text{ GeV}. \quad (7)$$

For the analysis of NP contributions in our paper the only relevant operators are the following QCDP and EWP $(V - A) \otimes (V + A)$ operators

QCD–Penguins:

$$Q_5 = (\bar{s}d)_{V-A} \sum_{q=u,d,s,c,b,t} (\bar{q}q)_{V+A} \quad Q_6 = (\bar{s}_\alpha d_\beta)_{V-A} \sum_{q=u,d,s,c,b,t} (\bar{q}_\beta q_\alpha)_{V+A} \quad (8)$$

Electroweak Penguins:

$$Q_7 = \frac{3}{2} (\bar{s}d)_{V-A} \sum_{q=u,d,s,c,b,t} e_q (\bar{q}q)_{V+A} \quad Q_8 = \frac{3}{2} (\bar{s}_\alpha d_\beta)_{V-A} \sum_{q=u,d,s,c,b,t} e_q (\bar{q}_\beta q_\alpha)_{V+A}. \quad (9)$$

The primed operators Q'_i are obtained from Q_i through the interchange of $V - A$ and $V + A$. Summation over colour indices α and β is understood. In the case of Z models top quark contribution should be omitted.

Eventually, if we are only interested in signs of NP contributions to ε'/ε and approximate estimates of their magnitudes, only $Q_6(Q'_6)$ will be relevant for $\text{Im}A_0$ and only contribution of $Q_8(Q'_8)$ for $\text{Im}A_2$. Thus we only need two hadronic matrix elements:

$$\langle Q_6(m_c) \rangle_0 = -4\sqrt{\frac{3}{2}} \left[\frac{m_K^2}{m_s(m_c) + m_d(m_c)} \right]^2 (F_K - F_\pi) B_6^{(1/2)} = -0.58 B_6^{(1/2)} \text{ GeV}^3 \quad (10)$$

$$\langle Q_8(m_c) \rangle_2 = \sqrt{2}\sqrt{\frac{3}{2}} \left[\frac{m_K^2}{m_s(m_c) + m_d(m_c)} \right]^2 F_\pi B_8^{(3/2)} = 1.06 B_8^{(3/2)} \text{ GeV}^3. \quad (11)$$

This approximate treatment would not be justified within the SM because of strong cancellations between QCDP and EWP contributions. But as we explained above such cancellations are absent in many extensions of the SM and for sure in the models considered by us.

The choice of the scale $\mu = m_c$ is convenient as it is used in analytic formulae for ε'/ε in [1]. But otherwise the precise value of μ is not relevant as the dominant μ dependence of the Wilson coefficients and of the matrix elements of Q_6 and Q_8 operators has a simple structure being dominantly governed by the μ dependence of involved quark masses. As a result of this the μ dependence of the parameters $B_6^{(1/2)}$ and $B_8^{(3/2)}$ is negligible for $\mu \geq 1 \text{ GeV}$ [22]. The matrix elements of primed operators differ only by sign from the ones given above. The numerical values in (10) and (11) are given for the central values of [38, 39]

$$m_K = 497.614 \text{ MeV}, \quad F_\pi = 130.41(20) \text{ MeV}, \quad \frac{F_K}{F_\pi} = 1.194(5), \quad (12)$$

$$m_s(m_c) = 109.1(2.8) \text{ MeV}, \quad m_d(m_c) = 5.44(19) \text{ MeV}. \quad (13)$$

The values of other parameters are collected in Table 1.

Recently significant progress on the values of $B_6^{(1/2)}$ and $B_8^{(3/2)}$ has been made by the RBC-UKQCD collaboration, who presented new results on the relevant hadronic matrix elements of the operators Q_6 [4] and Q_8 [3]. These results imply the following values for $B_6^{(1/2)}$ and $B_8^{(3/2)}$ [1, 45]

$$B_6^{(1/2)} = 0.57 \pm 0.19, \quad B_8^{(3/2)} = 0.76 \pm 0.05, \quad (\text{RBC-UKQCD}) \quad (14)$$

G_F	$1.16637(1) \times 10^{-5} \text{ GeV}^{-2}$	M_W	80.385 GeV
$\sin^2 \theta_W$	0.23116(13)	M_Z	91.1876 GeV
$ \epsilon_K $	$2.228(11) \times 10^{-3}$	m_K	0.4976 GeV
ΔM_K	$3.483 \times 10^{-15} \text{ GeV}$	\hat{B}_K	0.750(15) [16, 39]
$\lambda = V_{us} $	0.2252(9)	$B_6^{(1/2)}$	0.70
$\alpha_s(M_Z)$	0.1185(6)	$B_8^{(3/2)}$	0.76
$\tilde{\kappa}_\epsilon$	0.94 ± 0.02	η_2	0.5765(65) [44]
$\tilde{r}(M_Z)$	1.068	$\text{Re}\lambda_t$	$-3.0 \cdot 10^{-4}$
$\tilde{r}(3 \text{ TeV})$	0.95	$\text{Im}\lambda_t$	$1.4 \cdot 10^{-4}$

Table 1: Values of theoretical and experimental quantities used as input parameters. See also (12) and (13).

to be compared with their values in the strict large N limit of QCD [46–48]

$$B_6^{(1/2)} = B_8^{(3/2)} = 1, \quad (\text{large } N \text{ Limit}). \quad (15)$$

But, in this analytic, dual approach to QCD, one can demonstrate explicitly the suppression of both $B_6^{(1/2)}$ and $B_8^{(3/2)}$ below their large- N limit and derive conservative upper bounds on both $B_6^{(1/2)}$ and $B_8^{(3/2)}$ which read [9]

$$B_6^{(1/2)} < B_8^{(3/2)} < 1 \quad (\text{large-}N). \quad (16)$$

While this approach gives $B_8^{(3/2)}(m_c) = 0.80 \pm 0.10$, the result for $B_6^{(1/2)}$ is less precise but there is a strong indication that $B_6^{(1/2)} < B_8^{(3/2)}$, with typical values $B_6^{(1/2)} \approx 0.5 - 0.6$ at scales $\mathcal{O}(1 \text{ GeV})$, in agreement with (14)²

We should emphasize that this suppression of $B_6^{(1/2)}$ and $B_8^{(3/2)}$ results from the meson evolution of the density-density operators Q_6 and Q_8 from $\mu \approx 0$ (strict large N limit) to scales $\mathcal{O}(1 \text{ GeV})$, where the hadronic matrix elements are multiplied by the Wilson coefficients. The scale dependence of both parameters is logarithmic but the one of $B_6^{(1/2)}$ is stronger than of $B_8^{(3/2)}$ implying at scales $\mathcal{O}(1 \text{ GeV})$ the inequalities in (16). This pattern of scale dependence of both parameters is consistent with the one for $\mu > 1 \text{ GeV}$ [22] that can be found by usual renormalization group methods. But the scale dependence for $\mu > 1 \text{ GeV}$ is weaker than for lower scales, as expected. For further details, see [9].

It is probably useful to recall at this stage that the recent finding of ε'/ε in the SM being below its experimental value has been signalled already by early analyses, among them in [54–56], which used $B_6^{(1/2)} = B_8^{(3/2)} = 1$. See [57] for an early review. The new result in (16) tells us that this is an upper bound on these two parameters and the recent lattice and large N calculations show that these parameters are significantly below this bound making ε'/ε in the SM even smaller than previously expected.

²On the other hand a number of other large N approaches [49–51] violates strongly the bounds in (16) with $B_6^{(1/2)}$ in the ballpark of 3 and $B_8^{(3/2)} > 1$ in striking disagreement with lattice results. Similar comment applies to $B_8^{(3/2)}$ in the dispersive approach [52, 53].

On the other hand, it has been advocated by the chiral perturbation theory practitioners [10, 11, 13–15] that final state interactions (FSI), not included in the large N approach in the leading order, effectively increase the value of $B_6^{(1/2)}$ by roughly a factor of 1.5 and suppress $B_8^{(3/2)}$ by roughly 10% bringing SM prediction for ε'/ε close to the experimental result in (2). However, the recent analysis in [17] demonstrates that this claim in the case of $B_6^{(1/2)}$ cannot be justified. In fact, as pointed out in that paper, within a pure effective (meson) field approach like chiral perturbation theory the dominant current-current operators governing the $\Delta I = 1/2$ rule and the dominant density-density (four-quark) QCD penguin operator Q_6 governing ε'/ε cannot be disentangled from each other. Therefore, without an UV completion, that is QCD at short distance scales, the claim that the isospin amplitude $\text{Re}A_0$ and $B_6^{(1/2)}$ are enhanced through FSI in the same manner, as done in [10, 11, 13–15], cannot be justified. But in the context of a dual QCD approach, which includes both long distance dynamics and the QCD at short distance scales, such a distinction is possible. One finds then that beyond the strict large N limit FSI are likely to be important for the $\Delta I = 1/2$ rule but much less relevant for ε'/ε [17].

It should also be emphasized that the estimates in [10, 11, 13–15] omitted the non-factorizable contributions to $B_6^{(1/2)}$ and $B_8^{(3/2)}$, represented by meson evolution mentioned above and calculated in [9]. As stressed above, the inclusion of them in the hadronic matrix elements is mandatory in order for the calculations of matrix elements and of Wilson coefficients to be compatible with each other.

These findings diminish significantly hopes that improved treatment of FSI within lattice QCD approach and dual QCD approach would bring the SM prediction for ε'/ε to agree with the experimental data, opening thereby an arena for important NP contributions to this ratio and giving strong motivation for the analysis presented in our paper.

Unfortunately, due to cancellations between various contributions, the error on ε'/ε in the SM remains to be substantial. From present perspective we do not expect that this error can be reduced significantly by using large N approach or other analytical approaches. Therefore, the efforts to find out the room left for NP contributions in ε'/ε will be led in the coming years by lattice QCD. But it would be important to have at least second lattice group, beyond RBC-UKQCD, which would take part in these efforts. As this may take still several years, it is useful to develop some strategies to be able to face NP in ε'/ε , if the present results on ε'/ε in the SM from lattice QCD and large N approach will be confirmed by more precise lattice calculations. One such strategy is proposed below.

This information is sufficient for our analysis which as the main goal has the identification of NP patterns in flavour observables in a number of models implied by the desire to enhance ε'/ε over its SM value in a significant manner. In particular those models are

of interest which can provide a positive shift in ε'/ε by at least 5×10^{-4} .

3 Strategy

3.1 Present

In our paper the central role will be played by ε'/ε and ε_K for which in the presence of NP contributions we have

$$\frac{\varepsilon'}{\varepsilon} = \left(\frac{\varepsilon'}{\varepsilon}\right)^{\text{SM}} + \left(\frac{\varepsilon'}{\varepsilon}\right)^{\text{NP}}, \quad \varepsilon_K \equiv e^{i\varphi_\varepsilon} [\varepsilon_K^{\text{SM}} + \varepsilon_K^{\text{NP}}]. \quad (17)$$

In view of uncertainties present in the SM estimates of ε'/ε and to a lesser extent in ε_K we will fully concentrate on NP contributions. Therefore in order to identify the pattern of NP contributions to flavour observables implied by the ε'/ε anomaly in a transparent manner, we will proceed in a given model as follows:

Step 1: We assume that NP provides a positive shift in ε'/ε :

$$\left(\frac{\varepsilon'}{\varepsilon}\right)^{\text{NP}} = \kappa_{\varepsilon'} \cdot 10^{-3}, \quad 0.5 \leq \kappa_{\varepsilon'} \leq 1.5, \quad (18)$$

with the range for $\kappa_{\varepsilon'}$ indicating the required size of this contribution. But in the formulae below, $\kappa_{\varepsilon'}$ will be a free parameter. This step will determine the imaginary parts of flavour-violating Z and Z' couplings to quarks as functions of $\kappa_{\varepsilon'}$.

Step 2: In order to determine the relevant real parts of the couplings involved, in the presence of the imaginary part determined from ε'/ε , we will assume that in addition to the ε'/ε anomaly, NP can also affect the parameter ε_K . We will describe this effect by the parameter κ_ε so that now in addition to (18) we will study the implications of the shift in ε_K due to NP

$$(\varepsilon_K)^{\text{NP}} = \kappa_\varepsilon \cdot 10^{-3}, \quad 0.1 \leq \kappa_\varepsilon \leq 0.4. \quad (19)$$

The positive sign of κ_ε is motivated by the fact that if ε_K is predicted in the SM using CKM parameters extracted from B system observables, its value is found typically below the data as first emphasized in [42,58]. See also [59,60]. But it should be stressed that this depends on whether inclusive or exclusive determinations of $|V_{ub}|$ and $|V_{cb}|$ are used and with the inclusive ones SM value of ε_K agrees well with the data. But then as emphasized in [61] ΔM_s and ΔM_d are significantly above the data. Other related discussions can be found in [27,62–64].

While this possible “anomaly” is certainly not as pronounced as the ε'/ε one, it is instructive to assume that it is present at the level indicated in (19), that is at most 20%.

Step 3: In view of the uncertainty in $\kappa_{\varepsilon'}$ we set several parameters to their central values. In particular for the SM contributions to rare decays we set the CKM factors to

$$\text{Re}\lambda_t = -3.0 \cdot 10^{-4}, \quad \text{Im}\lambda_t = 1.4 \cdot 10^{-4} \quad (20)$$

which are in the ballpark of present estimates obtained by UTfit [59] and CKMfitter [60] collaborations. For this choice of CKM parameters the central value of the resulting $\varepsilon_K^{\text{SM}}$ is $1.96 \cdot 10^{-3}$. With the experimental value of ε_K in Table 1 this implies $\kappa_\varepsilon = 0.26$. But

we will still vary κ_ε while keeping the values in (20) as NP contributions do not depend on them but are sensitive functions of κ_ε .

Step 4: Having fixed the flavour violating couplings of Z or Z' in this manner, we will express NP contributions to the branching ratios for $K^+ \rightarrow \pi^+ \nu \bar{\nu}$, $K_L \rightarrow \pi^0 \nu \bar{\nu}$ and $K_L \rightarrow \mu^+ \mu^-$ and to ΔM_K in terms of $\kappa_{\varepsilon'}$ and κ_ε . This will allow us to study directly the impact of ε'/ε and ε_K anomalies in Z and Z' scenarios on these four observables. In Table 2 we indicate the dependence of a given observable on the *real* and/or the *imaginary* Z or Z' flavour violating coupling to quarks. In our strategy imaginary parts depend only on $\kappa_{\varepsilon'}$, while the real parts on both $\kappa_{\varepsilon'}$ and κ_ε . The pattern of flavour violation depends in a given NP scenario on the relative size of real and imaginary parts of couplings and we will see this explicitly later on.

	ε'/ε	ε_K	$K_L \rightarrow \pi^0 \nu \bar{\nu}$	$K^+ \rightarrow \pi^+ \nu \bar{\nu}$	$K_L \rightarrow \mu^+ \mu^-$	ΔM_K
Im Δ	*	*	*	*		*
Re Δ		*		*	*	*

Table 2: The dependence of various observables on the imaginary and/or real parts of Z and Z' flavour-violating couplings.

In the context of our presentation we will see that in Z scenarios with only left-handed or right-handed flavour violating couplings the most important constraint on the real parts of new couplings comes not from ε_K or ΔM_K but from $K_L \rightarrow \mu^+ \mu^-$. On the other hand, in all Z' scenarios and in the case of Z scenarios with left-right operators contributing to ε_K , these are always ε_K and ΔM_K and not $K_L \rightarrow \mu^+ \mu^-$ that are most important for the determination of the real parts of the new couplings after the ε'/ε constraint has been imposed.

3.2 Future

The present strategy above assumes that the progress in the evaluation of ε'/ε in the SM will be faster than experimental information on $K^+ \rightarrow \pi^+ \nu \bar{\nu}$. If in 2018 the situation will be reverse, it will be better to choose as variables κ_ε and $R_+^{\nu\bar{\nu}}$ defined in (42). In the next sections we will provide $R_+^{\nu\bar{\nu}}$ as a function of $\kappa_{\varepsilon'}$ for fixed κ_ε using the present strategy. But knowing $R_+^{\nu\bar{\nu}}$ better than ε'/ε in the SM will allow us to read off from our plots the favourite range for $\kappa_{\varepsilon'}$ in a given NP scenario for given κ_ε and the diagonal couplings of Z' . As these plots will be given for $B_6^{(1/2)} = 0.70$ and $B_8^{(3/2)} = 0.76$, the shift in ε'/ε represented by $\kappa_{\varepsilon'}$ will be given for other values of $B_6^{(1/2)}$ and $B_8^{(3/2)}$ simply by

$$\kappa_{\varepsilon'}(B_6^{(1/2)}) = \kappa_{\varepsilon'} \left[\frac{B_6^{(1/2)}}{0.70} \right], \quad \kappa_{\varepsilon'}(B_8^{(3/2)}) = \kappa_{\varepsilon'} \left[\frac{B_8^{(3/2)}}{0.76} \right], \quad (21)$$

where $\kappa_{\varepsilon'}$ without the argument is the one found in the plots. Even if going backwards will require resolution of some sign ambiguities, they should be easily resolved. Note that knowing $R_+^{\nu\bar{\nu}}$ will allow to obtain $R_0^{\nu\bar{\nu}}$, defined in (41) directly from our plots, using the value of $\kappa_{\varepsilon'}$ extracted from $R_+^{\nu\bar{\nu}}$ and κ_ε . The formulae in (21) are only relevant for

predicting ε'/ε in this manner. Clearly, when $R_0^{\nu\bar{\nu}}$ will also be known the analysis will be rather constrained.

4 Z Models

4.1 Preliminaries

The most recent analyses of ε'/ε in these models can be found in [27, 30] and some results presented below are based on these papers. In particular, the relevant renormalization group analysis in the spirit of the present paper has been performed in [27]. We summarize and slightly extend it in Appendix A.

It is straightforward to calculate the values of the Wilson coefficients entering NP part of the $K \rightarrow \pi\pi$ Hamiltonian in these models. We define these coefficients by

$$\mathcal{H}_{\text{eff}}(K \rightarrow \pi\pi)(Z) = \sum_{i=3}^{10} (C_i(\mu)Q_i + C'_i(\mu)Q'_i), \quad (22)$$

where the primed operators Q'_i are obtained from Q_i by interchanging $V - A$ and $V + A$. The operators Q_i are the ones entering the SM contribution [22]

$$\mathcal{H}_{\text{eff}}(K \rightarrow \pi\pi)(\text{SM}) = \frac{G_F}{\sqrt{2}} V_{ud} V_{us}^* \sum_{i=1}^{10} (z_i^{\text{SM}}(\mu) + \tau y_i^{\text{SM}}(\mu)) Q_i, \quad \tau = -\frac{V_{td} V_{ts}^*}{V_{ud} V_{us}^*}. \quad (23)$$

Explicit expressions for some of them have been given above and the remaining ones can be found in [22]. $Q_{1,2}$ are current-current operators, $Q_3 - Q_6$ are QCDP operators and $Q_7 - Q_{10}$ EWP operators. Note that whereas z_i and y_i are dimensionless, the coefficients in (22) carry dimension as seen explicitly below.

We define the relevant flavour violating Z couplings $\Delta_{L,R}^{sd}(Z)$ by [65]

$$i\mathcal{L}(Z) = i \left[\Delta_L^{sd}(Z) (\bar{s}\gamma^\mu P_L d) + \Delta_R^{sd}(Z) (\bar{s}\gamma^\mu P_R d) \right] Z_\mu, \quad P_{L,R} = \frac{1}{2}(1 \mp \gamma_5). \quad (24)$$

Considering then the simple tree-level Z exchange, the non-vanishing Wilson coefficients at $\mu = M_Z$ are then given at the LO as follows [27]

$$C_3(M_Z) = - \left[\frac{g_2}{6c_W} \right] \frac{\Delta_L^{sd}(Z)}{4M_Z^2}, \quad C'_5(M_Z) = - \left[\frac{g_2}{6c_W} \right] \frac{\Delta_R^{sd}(Z)}{4M_Z^2}, \quad (25)$$

$$C_7(M_Z) = - \left[\frac{4g_2 s_W^2}{6c_W} \right] \frac{\Delta_L^{sd}(Z)}{4M_Z^2}, \quad C'_9(M_Z) = - \left[\frac{4g_2 s_W^2}{6c_W} \right] \frac{\Delta_R^{sd}(Z)}{4M_Z^2}, \quad (26)$$

$$C_9(M_Z) = \left[\frac{4g_2 c_W^2}{6c_W} \right] \frac{\Delta_L^{sd}(Z)}{4M_Z^2}, \quad C'_7(M_Z) = \left[\frac{4g_2 c_W^2}{6c_W} \right] \frac{\Delta_R^{sd}(Z)}{4M_Z^2}. \quad (27)$$

We have used the known flavour conserving couplings of Z to quarks which are collected in the same notation in an appendix in [66]. The $SU(2)_L$ gauge coupling constant $g_2(M_Z) = 0.652$. We note that the values of the coefficients in front of $\Delta_{L,R}$ are in the case of C_9

and C'_7 by a factor of $c_W^2/s_W^2 \approx 3.33$ larger than for the remaining coefficients. It should also be stressed that these formulae are also valid for new Z penguins which provide one loop contributions to the couplings $\Delta_{L,R}^{sd}(Z)$.

We also notice that in contrast to the SM the contributions of current-current operators $Q_{1,2}$ are absent and they cannot be generated through renormalization group effects from penguin operators³. Moreover, whereas the QCDP operator coefficients in the SM are enhanced by more than an order of magnitude over the EWP coefficients due to the factor $\alpha_s/\alpha_{\text{em}}$, this enhancement is absent here.

In Appendix A we demonstrate that after performing the renormalization group evolution from M_Z down to m_c and considering the size of hadronic matrix elements it is sufficient to keep only contributions of Q_6 and Q'_6 generated from Q_5 and Q'_5 or contributions of Q_8 and Q'_8 , generated from Q_7 and Q'_7 , if we want to identify the sign of NP contribution to ε'/ε and do not aim for high precision. But, in Z scenarios, the known structure of flavour diagonal Z couplings to quarks implies that only EWP Q_8 and Q'_8 matter.

4.2 Left-handed Scenario (LHS)

4.2.1 ε'/ε

In this scenario only LH flavour-violating couplings are non-vanishing and the pair (Q_7, Q_8) has to be considered. Even if at $\mu = M_Z$ the Wilson coefficient of the EWP operator Q_8 vanishes in the leading order, its large mixing with Q_7 operator, its large anomalous dimension and enhanced hadronic $K \rightarrow \pi\pi$ matrix elements make it the dominant EWP operator in ε'/ε . It leaves behind the Q_7 operator whose Wilson coefficient, as seen in (26), does not vanish at $\mu = M_Z$. We find then [27]

$$\left(\frac{\varepsilon'}{\varepsilon}\right)_Z^L = \frac{1}{a} \frac{\omega_+}{|\varepsilon_K|\sqrt{2}} \frac{\text{Im}[A_2^{\text{NP}}]^L}{\text{Re}A_2} = 0.96 \times 10^9 \left[\frac{\text{Im}[A_2^{\text{NP}}]^L}{\text{GeV}} \right] \quad (28)$$

with

$$\text{Im}[A_2^{\text{NP}}]^L = \text{Im}C_8(m_c)\langle Q_8(m_c) \rangle_2 \quad (29)$$

and

$$C_8(m_c) = 0.76 C_7(M_Z) = -0.76 \left[\frac{4g_2s_W^2}{6c_W} \right] \frac{\Delta_L^{sd}(Z)}{4M_Z^2} = -2.62 \times 10^{-6} \left[\frac{\Delta_L^{sd}(Z)}{\text{GeV}^2} \right]. \quad (30)$$

Here $g_2 = g_2(M_Z) = 0.652$ is the $SU(2)_L$ gauge coupling and the factor 0.76 is the outcome of the RG evolution summarized in Appendix A. For our purposes most important is the sign in this result and that the RG factor is $\mathcal{O}(1)$. $\langle Q_8(m_c) \rangle_2$ is given in (11).

Collecting all these results we find

$$\left(\frac{\varepsilon'}{\varepsilon}\right)_Z^L = -2.64 \times 10^3 B_8^{(3/2)} \text{Im}\Delta_L^{sd}(Z). \quad (31)$$

³If new heavy charged gauge bosons are present in a given model new contributions to Wilson coefficients of current-current operators would be generated and in turn also the coefficients of penguin operators would be modified through renormalization group effects. But these effects are expected to be significantly smaller than the ones considered here.

While for our purposes this result is sufficient, in this scenario, in which the RG running starts at the electroweak scale, it is straightforward to proceed in a different manner by including NP effects through particular shifts in the functions X , Y and Z entering the analytic formula for ε'/ε in [1]. These shifts read [27]

$$\Delta X = \Delta Y = \Delta Z = c_W \frac{8\pi^2}{g_2^3} \frac{\text{Im}\Delta_L^{sd}(Z)}{\text{Im}\lambda_t} = 1.78 \times 10^6 \left[\frac{1.4 \cdot 10^{-4}}{\text{Im}\lambda_t} \right] \text{Im}\Delta_L^{sd}(Z). \quad (32)$$

In doing this we include in fact NLO QCD corrections and all operators whose Wilson coefficients are affected by NP and this allows us to confirm that only the modification in the contribution of the operator Q_8 really matters if we do not aim for high precision. Indeed, inserting these shifts into the analytic formula for ε'/ε in [1] we reproduce the result in (31) within roughly 10% and similar accuracy is expected for other estimates of NP contributions to ε'/ε below. Compared to the present uncertainty in the SM prediction for ε'/ε , this accuracy is certainly sufficient, but can be increased in the future if necessary.

The final formula for ε'/ε in LHS scenario is then given by

$$\left(\frac{\varepsilon'}{\varepsilon} \right)_{\text{LHS}} = \left(\frac{\varepsilon'}{\varepsilon} \right)_{\text{SM}} + \left(\frac{\varepsilon'}{\varepsilon} \right)_Z^L \quad (33)$$

where the second term stands for the contribution in (31) and if one aims for higher accuracy it originates in the modification related to the shifts in (32).

In order to see the implications of the ε'/ε anomaly in this NP scenario we assume that NP provides a positive shift in ε'/ε , as defined in (18), keeping $\kappa_{\varepsilon'}$ as a free *positive* definite parameter. In accordance with our strategy we set other parameters to their central values. In particular for the SM contributions to rare decays we set the CKM factors to the values in (20).

From (31) and (18) we find first

$$\text{Im}\Delta_L^{sd}(Z) = -5.0 \kappa_{\varepsilon'} \left[\frac{0.76}{B_8^{(3/2)}} \right] \cdot 10^{-7}. \quad (34)$$

The sign is fixed through the requirement of the enhancement of ε'/ε . In order to simplify the formulae below we set $B_8^{(3/2)} = 0.76$ but having (34) it is straightforward to find out what happens for or other values of $B_8^{(3/2)}$. Moreover, as seen in (14), $B_8^{(3/2)}$ is already rather precisely known.

4.2.2 ε_K , ΔM_K and $K_L \rightarrow \mu^+ \mu^-$

For $K^+ \rightarrow \pi^+ \nu \bar{\nu}$ we will also need $\text{Re}\Delta_L^{sd}(Z)$. To this end using the formulae of Appendix B we find the shifts in ε_K and ΔM_K to be

$$(\varepsilon_K)_{\text{VLL}}^Z = -4.26 \times 10^7 \text{Im}\Delta_L^{sd}(Z) \text{Re}\Delta_L^{sd}(Z) \quad (35)$$

and

$$\frac{(\Delta M_K)_{\text{VLL}}^Z}{(\Delta M_K)_{\text{exp}}} = 6.43 \times 10^7 [(\text{Re}\Delta_L^{sd}(Z))^2 - (\text{Im}\Delta_L^{sd}(Z))^2]. \quad (36)$$

From (19), (34) and (35) we determine $\text{Re}\Delta_L^{sd}(Z)$ to be

$$\text{Re}\Delta_L^{sd}(Z) = 4.7 \left[\frac{\kappa_\varepsilon}{\kappa_{\varepsilon'}} \right] \left[\frac{B_8^{(3/2)}}{0.76} \right] \cdot 10^{-5}. \quad (37)$$

However, the strongest constraint for $\text{Re}\Delta_L^{sd}(Z)$ in this scenario comes from the $K_L \rightarrow \mu^+ \mu^-$ bound in (191) which implies the allowed range

$$-1.19 \cdot 10^{-6} \leq \text{Re}\Delta_L^{sd}(Z) \leq 3.96 \cdot 10^{-6} \quad (38)$$

and consequently using (37)

$$\kappa_\varepsilon \leq 0.084 \kappa_{\varepsilon'} \left[\frac{0.76}{B_8^{(3/2)}} \right]. \quad (39)$$

Inserting the values of the couplings in (34) and (38) into (35) and (36) we find that the shift in ε_K is very small, at the level of 4% at most

$$-2.7 \kappa_{\varepsilon'} \cdot 10^{-5} \leq (\varepsilon_K)_{\text{VLL}}^Z \leq 8.4 \kappa_{\varepsilon'} \cdot 10^{-5} \quad (40)$$

with the sign following the one of $\text{Re}\Delta_L^{sd}(Z)$. The shift in ΔM_K is fully negligible.

Thus in this NP scenario SM must describe well the data on ε_K and ΔM_K unless NP generating flavour-violating Z couplings can provide significant one-loop contributions to ε_K and ΔM_K . Such a possibility is encountered in models with heavy vector-like quarks in [67], provided their masses are above 5 TeV.

4.2.3 $K^+ \rightarrow \pi^+ \nu \bar{\nu}$ and $K_L \rightarrow \pi^0 \nu \bar{\nu}$

All formulae for these decays that are relevant for us have been collected in Appendix C. In the case of $K_L \rightarrow \pi^0 \nu \bar{\nu}$ we get a unique prediction:

$$R_0^{\nu\bar{\nu}} \equiv \frac{\mathcal{B}(K_L \rightarrow \pi^0 \nu \bar{\nu})}{\mathcal{B}(K_L \rightarrow \pi^0 \nu \bar{\nu})_{\text{SM}}} = (1 - 0.6 \kappa_{\varepsilon'})^2 \quad (41)$$

which for $\kappa_{\varepsilon'} = 1.0$ amounts to a suppression of the SM prediction by a factor of 6.3.

The corresponding branching ratio for $K^+ \rightarrow \pi^+ \nu \bar{\nu}$ is suppressed through the suppression of $\text{Im}X_{\text{eff}}$ governing $K_L \rightarrow \pi^0 \nu \bar{\nu}$ and also through suppression of $\text{Re}X_{\text{eff}}$ for positive values of $\text{Re}\Delta_L^{sd}(Z)$. But for sufficiently negative values of $\text{Re}\Delta_L^{sd}(Z)$ in (38) it can be enhanced. Using the formulae in Appendix C we find then

$$R_+^{\nu\bar{\nu}} \equiv \frac{\mathcal{B}(K^+ \rightarrow \pi^+ \nu \bar{\nu})}{\mathcal{B}(K^+ \rightarrow \pi^+ \nu \bar{\nu})_{\text{SM}}} \leq 1.94. \quad (42)$$

This upper limit practically does not depend on $\kappa_{\varepsilon'}$ as the NP contribution to the dominant part of $R_+^{\nu\bar{\nu}}$ coming from the modification of $\text{Re}X_{\text{eff}}$ is independent of $\kappa_{\varepsilon'}$ and is directly bounded by $K_L \rightarrow \mu^+ \mu^-$ and not by the combination of ε'/ε and ε_K .

In Fig. 1 we show $R_0^{\nu\bar{\nu}}$ as a function of $\kappa_{\varepsilon'}$. For the chosen values of the CKM parameters in (20) one has

$$\mathcal{B}(K^+ \rightarrow \pi^+ \nu \bar{\nu})_{\text{SM}} = 7.7 \cdot 10^{-11}, \quad \mathcal{B}(K_L \rightarrow \pi^0 \nu \bar{\nu})_{\text{SM}} = 2.8 \cdot 10^{-11} \quad (43)$$

to be compared with the present SM estimates that include uncertainties in the tree-level determinations of CKM parameters [45]

$$\mathcal{B}(K^+ \rightarrow \pi^+ \nu \bar{\nu})_{\text{SM}} = (8.4 \pm 1.0) \cdot 10^{-11}, \quad \mathcal{B}(K_L \rightarrow \pi^0 \nu \bar{\nu})_{\text{SM}} = (3.4 \pm 0.6) \cdot 10^{-11}. \quad (44)$$

We will use the values in (43) in all formulae below.

4.3 Right-handed Scenario (RHS)

4.3.1 ε'/ε

In this case the operator Q'_8 dominates. But its mixing with Q'_7 is the same as the one between Q_8 and Q_7 . Only the value of $C'_7(M_Z)$ is different and the matrix element of Q'_8 differs from the one of Q_8 only by sign. Using (27) we then find

$$\left(\frac{\varepsilon'}{\varepsilon}\right)_Z^R = \frac{1}{a} \frac{\omega_+}{|\varepsilon_K| \sqrt{2}} \frac{\text{Im}[A_2^{\text{NP}}]^R}{\text{Re}A_2} = 0.96 \times 10^9 \left[\frac{\text{Im}[A_2^{\text{NP}}]^R}{\text{GeV}} \right] \quad (45)$$

with

$$\text{Im}[A_2^{\text{NP}}]^R = \text{Im}C'_8(m_c) \langle Q'_8(m_c) \rangle_2, \quad \langle Q'_8(m_c) \rangle_2 = -\langle Q_8(m_c) \rangle_2, \quad (46)$$

where

$$C'_8(m_c) = 0.76 C'_7(M_Z) = 0.76 \left[\frac{4g_2 c_W^2}{6c_W} \right] \frac{\Delta_R^{sd}(Z)}{4M_Z^2} = 8.71 \times 10^{-6} \left[\frac{\Delta_R^{sd}(Z)}{\text{GeV}^2} \right]. \quad (47)$$

Collecting all these results we find now

$$\left(\frac{\varepsilon'}{\varepsilon}\right)_Z^R = -8.79 \times 10^3 B_8^{(3/2)} \text{Im}\Delta_R^{sd}(Z) \quad (48)$$

and note that the numerical factor on the r.h.s is by a factor $c_W^2/s_W^2 = 3.33$ larger than in (31) but the sign is the same.

Thus

$$\left(\frac{\varepsilon'}{\varepsilon}\right)_{\text{RHS}} = \left(\frac{\varepsilon'}{\varepsilon}\right)_{\text{SM}} + \left(\frac{\varepsilon'}{\varepsilon}\right)_Z^R \quad (49)$$

with the last term given in (48).

From (48) and (18) we find now

$$\text{Im}\Delta_R^{sd}(Z) = -1.50 \kappa_{\varepsilon'} \left[\frac{0.76}{B_8^{(3/2)}} \right] \cdot 10^{-7}. \quad (50)$$

The sign is fixed through the requirement of the enhancement of ε'/ε . For a given $\kappa_{\varepsilon'}$ the magnitude of the required coupling can be smaller than in LHS because the relevant Wilson coefficient contains the additional factor 3.33. This also means that it is easier to enhance ε'/ε in this scenario while satisfying other constraints. This difference relative to LHS changes the implications for other observables.

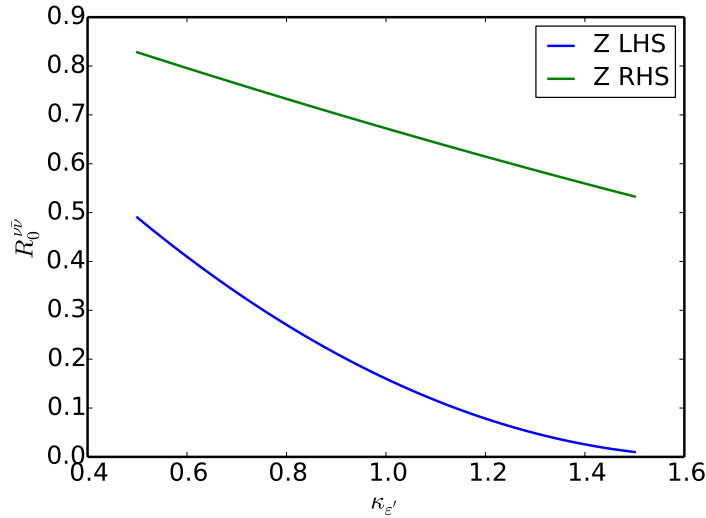


Figure 1: $R_0^{\nu\bar{\nu}}$ as a function of $\kappa_{\varepsilon'}$ for LHS and RHS Z scenarios.

4.3.2 ε_K , ΔM_K and $K_L \rightarrow \mu^+\mu^-$

The strongest constraint for $\text{Re}\Delta_L^{sd}(Z)$ in this scenario comes again from the $K_L \rightarrow \mu^+\mu^-$ bound in (191) which implies this time the allowed range

$$-3.96 \cdot 10^{-6} \leq \text{Re}\Delta_R^{sd}(Z) \leq 1.19 \cdot 10^{-6}, \quad (51)$$

simply the flip of the sign due to the flip of the sign in (194).

Using the formulae of Appendix B we find the shifts in ε_K and ΔM_K to be even smaller than in LHS. Thus also in this NP scenario SM must describe the data on ε_K and ΔM_K well unless loop contributions could be significant. On the other hand the results for $K^+ \rightarrow \pi^+\nu\bar{\nu}$ and $K_L \rightarrow \pi^0\nu\bar{\nu}$ are more interesting.

4.3.3 $K^+ \rightarrow \pi^+\nu\bar{\nu}$ and $K_L \rightarrow \pi^0\nu\bar{\nu}$

We again obtain a unique prediction:

$$R_0^{\nu\bar{\nu}} = (1 - 0.18 \kappa_{\varepsilon'})^2, \quad (52)$$

but this time the suppression of $R_0^{\nu\bar{\nu}}$ is smaller. For $\kappa_{\varepsilon'} = 1.0$ it amounts to a suppression by a factor of 1.5. In Fig. 1 we show $R_0^{\nu\bar{\nu}}$ as a function of $\kappa_{\varepsilon'}$ in this scenario.

The corresponding branching ratio for $K^+ \rightarrow \pi^+\nu\bar{\nu}$ is suppressed through the suppression of $\text{Im}X_{\text{eff}}$ and also through suppression of $\text{Re}X_{\text{eff}}$ for positive values of $\text{Re}\Delta_R^{sd}(Z)$. But for sufficiently negative values of $\text{Re}\Delta_R^{sd}(Z)$ in (51) it can be enhanced. As the allowed magnitude in the latter case is larger than in LHS, the upper bound on the branching ratio is weaker. The dependence of this upper bound on $\kappa_{\varepsilon'}$ is even weaker than in LHS as $\text{Re}X_{\text{eff}}$, which is independent of it, is dominantly responsible for the modification of the $K^+ \rightarrow \pi^+\nu\bar{\nu}$ rate. We find

$$R_+^{\nu\bar{\nu}} \leq 5.7. \quad (53)$$

Certainly such a large enhancement is very unlikely but it shows that in this scenario large enhancements of $\mathcal{B}(K^+ \rightarrow \pi^+ \nu \bar{\nu})$ are possible. The fact that in RHS the bound on $K^+ \rightarrow \pi^+ \nu \bar{\nu}$ from $K_L \rightarrow \mu^+ \mu^-$ is much weaker than in LHS has been pointed out in the context of the analysis of the Randall-Sundrum model with custodial protection, where rare decays are governed by tree-level Z exchanges with RH flavour violating couplings [68].

4.4 General Z Scenarios

4.4.1 ε'/ε

When both $\Delta_L^{sd}(Z)$ and $\Delta_R^{sd}(Z)$ are present the general formula for ε'/ε is given as follows

$$\left(\frac{\varepsilon'}{\varepsilon}\right)_Z = \left(\frac{\varepsilon'}{\varepsilon}\right)_{\text{SM}} + \left(\frac{\varepsilon'}{\varepsilon}\right)_Z^L + \left(\frac{\varepsilon'}{\varepsilon}\right)_Z^R \quad (54)$$

with the last two terms representing LHS and RHS contributions discussed above. As the operators Q_i and Q'_i do not mix under renormalization we can just add these two contributions to the SM part independently of each other.

The ε'/ε constraint now reads

$$\text{Im}\Delta_L^{sd}(Z) + 3.33 \text{Im}\Delta_R^{sd}(Z) = -5.0 \kappa_{\varepsilon'} \left[\frac{0.76}{B_8^{(3/2)}} \right] \cdot 10^{-7}. \quad (55)$$

The presence of two couplings allows now for more possibilities as we will see soon. We set $B_8^{(3/2)} = 0.76$ in what follows.

4.4.2 ε_K , ΔM_K and $K_L \rightarrow \mu^+ \mu^-$

This time also LR operators contribute to ε_K and ΔM_K and quite generally constitute by far the dominant contributions to these quantities so that we can approximate the shifts in ε_K and ΔM_K by keeping only LR contributions

$$(\varepsilon_K)^Z \approx 2.07 \cdot 10^9 [(\text{Im}\Delta_L^{sd}(Z)\text{Re}\Delta_R^{sd}(Z) + \text{Im}\Delta_R^{sd}(Z)\text{Re}\Delta_L^{sd}(Z))] \quad (56)$$

and

$$R_{\Delta M}^Z \equiv \frac{(\Delta M_K)^Z}{(\Delta M_K)_{\text{exp}}} \approx -6.21 \cdot 10^9 [(\text{Re}\Delta_L^{sd}(Z)\text{Re}\Delta_R^{sd}(Z) - \text{Im}\Delta_L^{sd}(Z)\text{Im}\Delta_R^{sd}(Z))]. \quad (57)$$

The large size of LR contribution with respect to VLL and VRR contributions is not only related to enhanced hadronic matrix elements of LR operators but also to larger Wilson coefficients at $\mu = m_c$ that are enhanced through renormalization group effects [69]. The ones of VLL and VRR operators are suppressed slightly by these effects.

The presence of LR operators has a very important consequence. While in LHS and RHS the $K_L \rightarrow \mu^+ \mu^-$ bound provided by far the strongest constraint on $\text{Re}\Delta_{L,R}^{sd}(Z)$, now also ε_K plays a role and κ_ε will enter the game. However, as we will see in the first

example below, for $\kappa_\varepsilon \geq 0.3$ and $\kappa_{\varepsilon'} \leq 0.6$ the $K_L \rightarrow \mu^+\mu^-$ will again bound the rate for $K^+ \rightarrow \pi^+\nu\bar{\nu}$.

In this context it should be remarked that in principle it is possible to eliminate LR contributions by choosing properly the real and imaginary parts of LH and RH couplings. It is also possible to use LR contributions to ΔM_K or ε_K to eliminate completely NP contributions to them by cancelling the contributions from VLL and VRR operators [27, 70]. This is only possible in the presence of suitable hierarchy between LH and RH couplings. In what follows we will assume that such fine-tuned situations do not take place.

While, the presence of LR operators is regarded often as a problem, it should be realized that in the case of possible anomalies in ε_K and ΔM_K they could be welcome in the Z case, where in LHS and RHS NP contributions to ε_K and ΔM_K turned out to be small. In order to illustrate this we will assume, as announced in Section 3, that in addition to the ε'/ε anomaly, the data show also ε_K anomaly parametrized by κ_ε in (19).

4.4.3 $K^+ \rightarrow \pi^+\nu\bar{\nu}$ and $K_L \rightarrow \pi^0\nu\bar{\nu}$

For $K^+ \rightarrow \pi^+\nu\bar{\nu}$ and $K_L \rightarrow \pi^0\nu\bar{\nu}$ the relevant expressions are collected in Appendix C. In particular (184) implies that in $K_L \rightarrow \pi^0\nu\bar{\nu}$ the enhancement of its branching ratio requires the sum of the imaginary parts of the couplings to be *positive*. This enhances also $K^+ \rightarrow \pi^+\nu\bar{\nu}$ but as seen in (183) could be compensated by the decrease of $\text{Re } X_{\text{eff}}$ unless the sum of the corresponding real parts is *negative*. For $K_L \rightarrow \mu^+\mu^-$ the relevant expressions are given in Appendix D. In particular in (194).

It is clear that with more parameters involved there are many possibilities in this NP scenario and which one is realized in nature will be only known through precise confrontation of the SM predictions for ε'/ε , $\mathcal{B}(K^+ \rightarrow \pi^+\nu\bar{\nu})$, $\mathcal{B}(K_L \rightarrow \pi^0\nu\bar{\nu})$, ε_K and ΔM_K with future data. Indeed, presently it is not excluded that NP contributes to all of these quantities so that some enhancements and/or suppressions will be required.

Now among the five quantities in question only ε'/ε and to a lesser extent ε_K exhibit some anomaly and NP models providing enhancements of both of them appear to be favoured. How much enhancement is needed in ε'/ε will strongly depend on the future value of $B_6^{(1/2)}$. In the case of ε_K this depends on the values of the CKM parameters, in particular on the value of $|V_{cb}|$.

It would also be favourable, in particular for experimentalists, if the nature required the enhancements of both $\mathcal{B}(K^+ \rightarrow \pi^+\nu\bar{\nu})$ and $\mathcal{B}(K_L \rightarrow \pi^0\nu\bar{\nu})$ relative to SM predictions, simply, because then these branching ratios would be easier to measure and one could achieve a higher experimental precision on them. But, we have seen in LHS and RHS that enhancement of ε'/ε implied automatically suppression of $\mathcal{B}(K_L \rightarrow \pi^0\nu\bar{\nu})$, while $\mathcal{B}(K^+ \rightarrow \pi^+\nu\bar{\nu})$ could be both enhanced and suppressed. NP contributions to ε_K and ΔM_K were found at the level of a few percent at most after the ε'/ε and $K_L \rightarrow \mu^+\mu^-$ constraints have been imposed. Therefore these scenarios while being in principle able to remove ε'/ε anomaly, cannot simultaneously solve possible ε_K anomaly. In fact, as already observed in [27], in these scenarios a 10 – 20% NP contribution to ε_K would give significantly larger shift in ε'/ε than it is allowed by the data.

The question then arises whether it is possible in a general Z scenario to remove the

ε'/ε anomaly through the shift in (18), enhance ε_K by a shift in (19) and simultaneously enhance $\mathcal{B}(K_L \rightarrow \pi^0 \nu \bar{\nu})$ and $\mathcal{B}(K^+ \rightarrow \pi^+ \nu \bar{\nu})$ while satisfying the $K_L \rightarrow \mu^+ \mu^-$ and ΔM_K constraints. The inspection of the formulae in Appendices B–D shows that this is indeed possible.

4.4.4 Phenomenology

In order to exhibit this possibility in explicit terms and investigate the interplay between various quantities we introduce two real parameters r_1 and r_2 through

$$\text{Im}\Delta_L^{sd}(Z) = -r_1 \text{Im}\Delta_R^{sd}(Z), \quad \text{Re}\Delta_L^{sd}(Z) = r_2 \text{Re}\Delta_R^{sd}(Z). \quad (58)$$

Using (56) we find then

$$(\varepsilon_K)^Z \approx 2.07 \cdot 10^9 (r_2 - r_1) \text{Im}\Delta_R^{sd}(Z) \text{Re}\Delta_R^{sd}(Z). \quad (59)$$

Imposing the shifts in (18) and (19) we can determine:

$$\text{Im}\Delta_R^{sd}(Z) = \frac{5.0}{(r_1 - 3.33)} \kappa_{\varepsilon'} \cdot 10^{-7}, \quad \text{Re}\Delta_R^{sd}(Z) = 0.97 \frac{(r_1 - 3.33)}{(r_2 - r_1)} \frac{\kappa_\varepsilon}{\kappa_{\varepsilon'}} \cdot 10^{-6}. \quad (60)$$

Formulae (58) and (60) inserted in the expressions in Appendices B–D allow to express the branching ratios for $K^+ \rightarrow \pi^+ \nu \bar{\nu}$, $K_L \rightarrow \pi^0 \nu \bar{\nu}$ and $K_L \rightarrow \mu^+ \mu^-$ and ΔM_K in terms of $\kappa_{\varepsilon'}$, κ_ε , r_1 and r_2 .

In particular in order to see the signs of NP effects we find first

$$\text{Re} X_{\text{eff}}(Z) = -4.44 \cdot 10^{-4} + 2.51 \cdot 10^2 (1 + r_2) \text{Re}\Delta_R^{sd}(Z), \quad (61)$$

$$\text{Im} X_{\text{eff}}(Z) = 2.07 \cdot 10^{-4} + 2.51 \cdot 10^2 (1 - r_1) \text{Im}\Delta_R^{sd}(Z), \quad (62)$$

$$\text{Re} Y_{\text{eff}}(Z) = -2.83 \cdot 10^{-4} + 2.51 \cdot 10^2 (r_2 - 1) \text{Re}\Delta_R^{sd}(Z) \quad (63)$$

and

$$R_{\Delta M}^Z \approx -6.21 \cdot 10^9 [r_2 (\text{Re}\Delta_R^{sd}(Z))^2 + r_1 (\text{Im}\Delta_R^{sd}(Z))^2]. \quad (64)$$

With $\kappa_{\varepsilon'}$ being positive we find then that ε'/ε and $\mathcal{B}(K_L \rightarrow \pi^0 \nu \bar{\nu})$, with the latter governed by $\text{Im} X_{\text{eff}}(Z)$, can be simultaneously enhanced provided

$$\text{Im}\Delta_R^{sd}(Z) < 0, \quad 1.0 < r_1 < 3.33. \quad (65)$$

If in addition ε_K and $\mathcal{B}(K^+ \rightarrow \pi^+ \nu \bar{\nu})$ should be enhanced r_2 has to satisfy⁴

$$r_2 > r_1, \quad \text{Re}\Delta_R^{sd}(Z) < 0 \quad \text{or} \quad r_2 < -1, \quad \text{Re}\Delta_R^{sd}(Z) > 0. \quad (66)$$

We illustrate the implications of these findings with two examples:

Example: 1 We fix $r_1 = 2$ and $r_2 = 3$ to get

$$\text{Im}\Delta_R^{sd}(Z) = -3.76 \kappa_{\varepsilon'} \cdot 10^{-7}, \quad \text{Re}\Delta_R^{sd}(Z) = -1.33 \frac{\kappa_\varepsilon}{\kappa_{\varepsilon'}} \cdot 10^{-6}. \quad (67)$$

⁴We assume here the enhancement of the magnitude of $\text{Re} X_{\text{eff}}$.

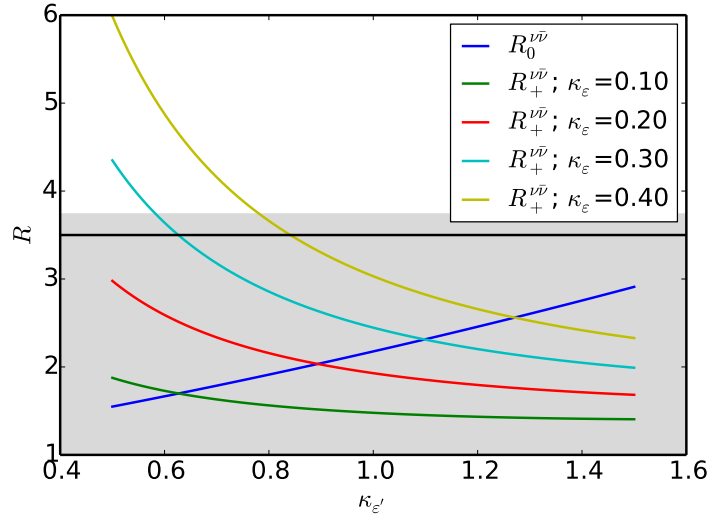


Figure 2: $R_0^{\nu\bar{\nu}}$ and $R_+^{\nu\bar{\nu}}$, as functions of $\kappa_{\varepsilon'}$ for $\kappa_{\varepsilon} = 0.1, 0.2, 0.3, 0.4$ for the example 1. The horizontal black line corresponds to the upper bound in (68). The experimental 1σ range for $R_+^{\nu\bar{\nu}}$ in (178) is displayed by the grey band.

This is in fact the case considered already in [30] but here we present it in more explicit terms. In particular we include $K^+ \rightarrow \pi^+\nu\bar{\nu}$ and $K_L \rightarrow \mu^+\mu^-$ in this discussion and not only $K_L \rightarrow \pi^0\nu\bar{\nu}$ as done in that paper. The inspection of formulae for $\text{Re } X_{\text{eff}}(Z)$ and $\text{Re } Y_{\text{eff}}(Z)$ above accompanied by numerical analysis show that in this example

$$R_+^{\nu\bar{\nu}} \approx R_L^{\mu\bar{\mu}} = \frac{\mathcal{B}(K_L \rightarrow \mu^+\mu^-)}{\mathcal{B}(K_L \rightarrow \mu^+\mu^-)_{\text{SM}}} \leq 3.5 \quad (68)$$

with the latter bound resulting from the bound in (191). On the other hand ΔM_K does not play any essential role with $|R_{\Delta M}^Z| \leq 0.04$. Here only short distance contributions to $K_L \rightarrow \mu^+\mu^-$ are involved.

In Fig. 2 we show $R_0^{\nu\bar{\nu}}$ and $R_+^{\nu\bar{\nu}}$, as functions of $\kappa_{\varepsilon'}$ for $\kappa_{\varepsilon} = 0.1, 0.2, 0.3, 0.4$ ⁵ represented in the case of $R_+^{\nu\bar{\nu}}$ by different colours

$$\kappa_{\varepsilon} = 0.1 \text{ (green)}, \quad \kappa_{\varepsilon} = 0.2 \text{ (red)}, \quad \kappa_{\varepsilon} = 0.3 \text{ (cyan)}, \quad \kappa_{\varepsilon} = 0.4 \text{ (yellow)}. \quad (69)$$

$R_0^{\nu\bar{\nu}}$ is given by blue line and the upper bound in (68) is indicated by a black horizontal line.

We observe that with increasing $\kappa_{\varepsilon'}$ the enhancement of $R_0^{\nu\bar{\nu}}$ slowly increases. On the other hand for a given κ_{ε} the ratio $R_+^{\nu\bar{\nu}}$ decreases with increasing $\kappa_{\varepsilon'}$. Both properties can easily be understood from the formulae in (61), (62) and (67). We note that for a given $\kappa_{\varepsilon'}$ the upper bound in (68) implies an upper bound on κ_{ε} which becomes weaker with increasing $\kappa_{\varepsilon'}$. Most interesting appear the values $\kappa_{\varepsilon'} \geq 1.0$ and $\kappa_{\varepsilon} \approx 0.25$ for which both ε'/ε and ε_K anomalies can be solved in agreement with the $K_L \rightarrow \mu^+\mu^-$ bound and both $K^+ \rightarrow \pi^+\nu\bar{\nu}$ and $K_L \rightarrow \pi^0\nu\bar{\nu}$ are significantly enhanced over their SM values.

⁵In principle while varying κ_{ε} we should also modify our CKM parameters as they correspond to $\kappa_{\varepsilon} = 0.26$. But the dominant dependence on CKM parameters cancels in the ratios considered and keeping CKM fixed exposes better the dependence on κ_{ε} in the plots.

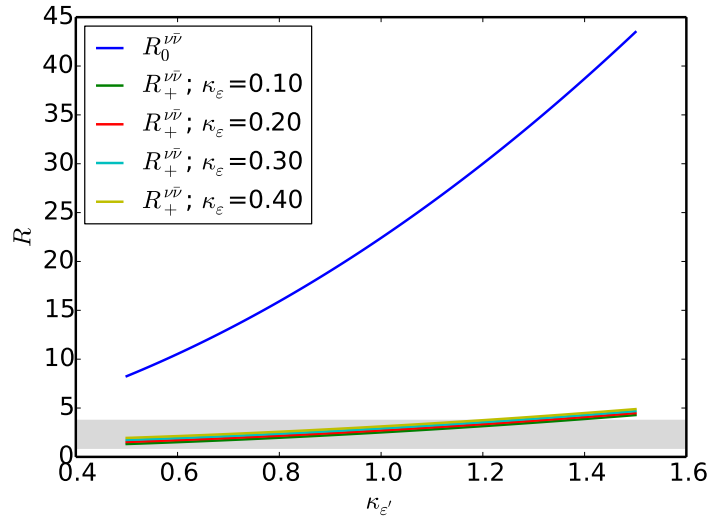


Figure 3: $R_0^{\nu\bar{\nu}}$ and $R_+^{\nu\bar{\nu}}$, as functions of $\kappa_{\epsilon'}$ for the example 2. $R_0^{\nu\bar{\nu}}$ is independent of κ_{ϵ} and the dependence of $R_+^{\nu\bar{\nu}}$ on κ_{ϵ} is negligible. The experimental 1σ range for $R_+^{\nu\bar{\nu}}$ in (178) is displayed by the grey band.

Example: 2 We fix $r_1 = 3$ and $r_2 = -2$ to get

$$\text{Im}\Delta_R^{sd}(Z) = -1.52 \kappa_{\epsilon'} \cdot 10^{-6}, \quad \text{Re}\Delta_R^{sd}(Z) = 6.6 \frac{\kappa_{\epsilon}}{\kappa_{\epsilon'}} \cdot 10^{-8}. \quad (70)$$

Note that now imaginary parts of the couplings are larger than the real parts with interesting consequences. In Fig. 3 we show for this case $R_0^{\nu\bar{\nu}}$ and $R_+^{\nu\bar{\nu}}$, as functions of $\kappa_{\epsilon'}$ again for $\kappa_{\epsilon} = 0.1, 0.2, 0.3, 0.4$. Now the relation (68) is no longer valid and the bound from $K_L \rightarrow \mu^+ \mu^-$ is irrelevant because the real parts of the couplings are much smaller than in the previous example. We observe basically no dependence of $R_+^{\nu\bar{\nu}}$ on κ_{ϵ} as this parameter affects only the real parts of the couplings which are small in this example. Again ΔM_K does not play any essential role with $|R_{\Delta M}^Z| \leq 0.05$.

We observe a very strong enhancement of *both* branching ratios which increases with increasing $\kappa_{\epsilon'}$. This should be contrasted with the previous example in which for a given κ_{ϵ} the two branching ratios were anticorrelated. This is best seen in Fig. 4 where we show in the left panel $R_0^{\nu\bar{\nu}}$ vs $R_+^{\nu\bar{\nu}}$ for the example 1 and in the right panel the corresponding plot for the example 2. A given line in the left panel, on which the ratios are anticorrelated, corresponds to a fixed value of κ_{ϵ} and the range on each line results from the variation of $\kappa_{\epsilon'}$ in the range $0.5 \leq \kappa_{\epsilon'} \leq 1.5$. We impose the constraint from $\mathcal{B}(K_L \rightarrow \mu^+ \mu^-)$. In the right panel the value of κ_{ϵ} does not matter and the range for the values of both branching ratios corresponds to $0.5 \leq \kappa_{\epsilon'} \leq 1.5$ with largest enhancements for largest $\kappa_{\epsilon'}$. Moreover, the two ratios increase in a correlated manner on the line parallel to the GN bound in (177) which expressed through the ratios $R_0^{\nu\bar{\nu}}$ and $R_+^{\nu\bar{\nu}}$ reads

$$R_0^{\nu\bar{\nu}} \leq 11.85 R_+^{\nu\bar{\nu}}. \quad (71)$$

We indicate this bound by a black line. Such a correlation between $K^+ \rightarrow \pi^+ \nu \bar{\nu}$ and $K_L \rightarrow \pi^0 \nu \bar{\nu}$ is characteristic for cases in which only imaginary parts in the new couplings

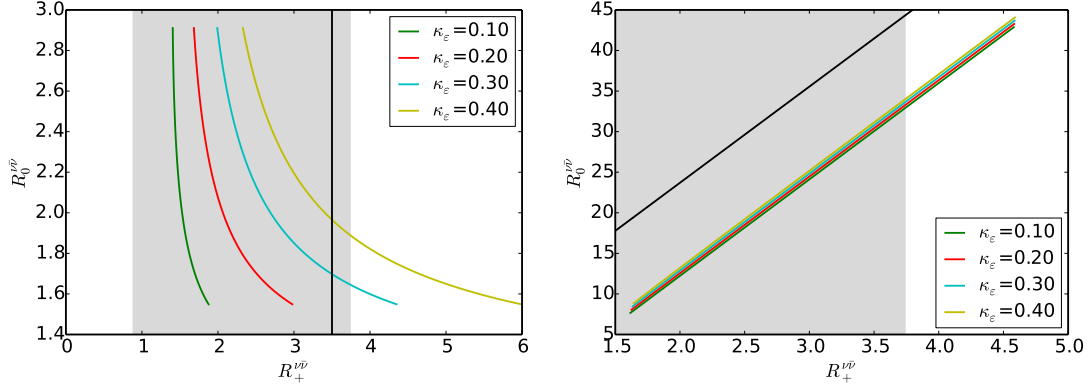


Figure 4: $R_0^{\nu\bar{\nu}}$ vs $R_+^{\nu\bar{\nu}}$ for $\kappa_\varepsilon = 0.1, 0.2, 0.3, 0.4$ for the example 1 (left panel) and the example 2 (right panel) varying $0.5 \leq \kappa_{\varepsilon'} \leq 1.5$. The vertical black line in the left panel corresponds to the upper bound in (68). The dependence on κ_ε in the right panel is negligible and the black line represents the GN bound in (71). The experimental 1σ range for $R_+^{\nu\bar{\nu}}$ in (178) is displayed by the grey band.

matter and both branching ratios are affected only by the modification of $\text{Im}X_{\text{eff}}$. For a general discussion see [71].

4.5 Summary of NP Patterns in Z Scenarios

The lessons from these four exercises are as follows:

- In the LHS, a given request for the enhancement of ε'/ε determines the coupling $\text{Im}\Delta_L^{sd}(Z)$.
- This result has direct unique implications on $K_L \rightarrow \pi^0\nu\bar{\nu}$: suppression of $\mathcal{B}(K_L \rightarrow \pi^0\nu\bar{\nu})$. This property is known from NP scenarios in which NP to $K_L \rightarrow \pi^0\nu\bar{\nu}$ and ε'/ε enters dominantly through the modification of Z -penguins.
- The imposition of the $K_L \rightarrow \mu^+\mu^-$ constraint determines the range for $\text{Re}\Delta_L^{sd}(Z)$ which with the already fixed $\text{Im}\Delta_L^{sd}(Z)$ allows to calculate the shifts in ε_K and ΔM_K . These shifts turn out to be very small for ε_K and negligible for ΔM_K . Therefore unless loop contributions from physics generating $\Delta_L^{sd}(Z)$ play significant role in both quantities, the SM predictions for ε_K and ΔM_K must agree well with data for this NP scenario to survive.
- Finally, with fixed $\text{Im}\Delta_L^{sd}(Z)$ and the allowed range for $\text{Re}\Delta_L^{sd}(Z)$, the range for $\mathcal{B}(K^+ \rightarrow \pi^+\nu\bar{\nu})$ can be obtained. But in view of uncertainties in the $K_L \rightarrow \mu^+\mu^-$ constraint both enhancements and suppressions of $\mathcal{B}(K^+ \rightarrow \pi^+\nu\bar{\nu})$ are possible and no specific pattern of correlation between $\mathcal{B}(K_L \rightarrow \pi^0\nu\bar{\nu})$ and $\mathcal{B}(K^+ \rightarrow \pi^+\nu\bar{\nu})$ is found. In the absence of a relevant ε_K constraint this is consistent with the general analysis in [71]. $\mathcal{B}(K^+ \rightarrow \pi^+\nu\bar{\nu})$ can be enhanced by a factor of 2 at most.

- Analogous pattern is found in RHS, although the numerics is different. First due the modification of the initial conditions for the Wilson coefficients the suppression of $\mathcal{B}(K_L \rightarrow \pi^0 \nu \bar{\nu})$ for a given $\kappa_{\varepsilon'}$ is smaller. Moreover, the flip of the sign in NP contribution to $K_L \rightarrow \mu^+ \mu^-$ allows for larger enhancement of $\mathcal{B}(K^+ \rightarrow \pi^+ \nu \bar{\nu})$, a property known from our previous analyses. An enhancement of $\mathcal{B}(K^+ \rightarrow \pi^+ \nu \bar{\nu})$ up to a factor of 5.7 is possible.
- In a general Z scenario the pattern of NP effects changes because of the appearance of LR operators dominating NP contributions to ε_K and ΔM_K . Consequently for large range of parameters these two quantities, in particular ε_K , provide stronger constraint on $\text{Re}\Delta_{L,R}^{sd}(Z)$ than $K_L \rightarrow \mu^+ \mu^-$. But the main virtue of the general scenario is the possibility of enhancing simultaneously ε'/ε , ε_K , $\mathcal{B}(K^+ \rightarrow \pi^+ \nu \bar{\nu})$ and $\mathcal{B}(K_L \rightarrow \pi^0 \nu \bar{\nu})$ which is not possible in LHS and RHS. Thus the presence of both LH and RH flavour-violating currents is essential for obtaining simultaneously the enhancements in question.
- We have illustrated this on two examples with the results shown in Figs. 2–4 for which as seen in Fig. 4 the correlation between branching ratios for $K^+ \rightarrow \pi^+ \nu \bar{\nu}$ and $K_L \rightarrow \pi^0 \nu \bar{\nu}$ are strikingly different. In particular in the second example in which the imaginary parts in the couplings dominate the correlation takes place along the line parallel to the line representing GN bound.

We will now turn our attention to Z' models which, as we will see, exhibit quite different pattern of NP effects in the K meson system than the LH and RH Z scenarios. In particular we will find that at the qualitative level Z' models with only LH or RH flavour-violating couplings can generate very naturally the patterns found in the two examples in Figs. 2–4 that in Z scenario required the presence of both LH and RH couplings. In fact the pattern of correlation between $K^+ \rightarrow \pi^+ \nu \bar{\nu}$ and $K_L \rightarrow \pi^0 \nu \bar{\nu}$ found in the example 1 will also be found in Z' scenario in which NP in ε'/ε is dominated by EWP operator Q_8 . On the other hand QCDP operator Q_6 generated by Z' exchange implies a pattern of correlation between $K_L \rightarrow \pi^0 \nu \bar{\nu}$ and $K^+ \rightarrow \pi^+ \nu \bar{\nu}$ found in the example 2. But the implication for NP effects in ΔM_K will turn out to be more interesting than found in the latter example.

5 Z' Models

5.1 Preliminaries

Also in this case the operators Q_8 and Q'_8 dominate NP contribution to ε'/ε in several models and we will recall some of them below. However, this time flavour diagonal Z' couplings to quarks are model dependent, which allows to construct models in which the QCDP operator Q_6 or the operator Q'_6 dominates NP contribution to ε'/ε . As this case cannot be realized in Z scenarios it is instructive to discuss this scenario first. In particular it will turn out that in this case it is much easier to reach our goal of enhancing simultaneously ε'/ε , ε_K , $K^+ \rightarrow \pi^+ \nu \bar{\nu}$ and $K_L \rightarrow \pi^0 \nu \bar{\nu}$. Moreover, the presence of flavour-violating right-handed currents is not required.

In order for Q_6 or Q'_6 to dominate the scene the diagonal RH or LH quark couplings must be flavour universal which with the normalization of Wilson coefficients in (22) implies [27]

$$C_3(M_{Z'}) = \frac{\Delta_L^{sd}(Z')\Delta_L^{qq}(Z')}{4M_{Z'}^2}, \quad C'_3(M_{Z'}) = \frac{\Delta_R^{sd}(Z')\Delta_R^{qq}(Z')}{4M_{Z'}^2}, \quad (72)$$

$$C_5(M_{Z'}) = \frac{\Delta_L^{sd}(Z')\Delta_R^{qq}(Z')}{4M_{Z'}^2}, \quad C'_5(M_{Z'}) = \frac{\Delta_R^{sd}(Z')\Delta_L^{qq}(Z')}{4M_{Z'}^2}. \quad (73)$$

The couplings $\Delta_{L,R}^{sd}(Z')$ are defined by (24) with Z replaced by Z' . $\Delta_{L,R}^{qq}(Z')$ are flavour universal quark couplings which are assumed to be real. It should be noted that EWP are absent here. Moreover, they cannot be generated from QCDP through QCD renormalization group effects so that their contributions to NP part of ε'/ε can be neglected. This should be contrasted with the SM, where they are generated by electroweak interactions from the mixing with current-current operators that have much larger Wilson coefficients than QCDP.

Now as briefly discussed in Section 7 there exist models in which only LH or RH couplings are present. In that case the Wilson coefficients $C_5(M_{Z'})$ and $C'_5(M_{Z'})$ vanish in the leading order. Non-vanishing contribution of Q_6 and Q'_6 can still be generated through their mixing with $(V \mp A) \times (V \mp A)$ operators Q_3 and Q'_3 , respectively. But this mixing is significantly smaller than between Q_6 and Q_5 and between Q'_6 and Q'_5 leading to much smaller Wilson coefficients of Q_6 and Q'_6 at $\mu = m_c$ than it is possible when the Wilson coefficients $C_5(M_{Z'})$ and $C'_5(M_{Z'})$ do not vanish. We will therefore consider only the latter case but the former case of only LH or RH couplings implies similar phenomenology to the one presented below except that NP effects in ε'/ε are significantly smaller than the ones discussed by us.

In this context we also note that without a specific model there is a considerable freedom in the values of the diagonal quark and lepton couplings of Z' , although one must make sure that they are consistent with LEP II and LHC bounds. Concerning LHC bounds, the study in [72] implies

$$|\Delta_R^{q\bar{q}}(Z')| \leq 1.0 \left[\frac{M_{Z'}}{3 \text{ TeV}} \right] \left[1 + \left(\frac{1.3 \text{ TeV}}{M_{Z'}} \right)^2 \right]. \quad (74)$$

On the other hand bounds on the leptonic Z' couplings can be extracted from the final analysis of the LEP-II data [73], although there is still a considerable freedom as the bounds are for products of electron and other lepton couplings. Therefore the allowed coupling $\Delta_L^{\nu\bar{\nu}}(Z')$ can be increased by lowering $\Delta_L^{e\bar{e}}(Z')$ coupling.

As an example for our nominal value $M_{Z'} = 3 \text{ TeV}$ the choices

$$\Delta_R^{q\bar{q}}(Z') = 1, \quad \Delta_L^{q\bar{q}}(Z') = -1, \quad \Delta_L^{\nu\bar{\nu}}(Z') = \Delta_L^{\mu\bar{\mu}}(Z') = 0.5 \quad (75)$$

are consistent with these bounds⁶. Yet, it should be kept in mind that these couplings can in principle be larger or smaller. For larger (smaller) $\Delta_L^{\nu\bar{\nu}}(Z')$ NP contributions to

⁶The relation between leptonic couplings follows from $SU(2)_L$ gauge invariance

the branching ratios for $K^+ \rightarrow \pi^+ \nu \bar{\nu}$ and $K_L \rightarrow \pi^0 \nu \bar{\nu}$ will be larger (smaller), but in a correlated manner. The implications of the change of the couplings $\Delta_{L,R}^{q\bar{q}}(Z')$ are more profound as we will see in the context of our presentation. But, for the time being we will assume that $\Delta_{L,R}^{q\bar{q}}(Z')$ are $\mathcal{O}(1)$.

5.2 Z' with QCD Penguin Dominance (LHS)

5.2.1 ε'/ε

We begin with NP scenario with purely LH flavour-violating quark couplings and flavour universal RH flavour diagonal couplings. In this case the operator Q_6 is dominant. It mixes with the operator Q_5 and the LO RG analysis gives [27] (see Appendix A)

$$C_6(m_c) = 1.13 \frac{\Delta_L^{sd}(Z') \Delta_R^{qq}(Z')}{4M_{Z'}^2} = 3.14 \times 10^{-8} \left[\frac{\Delta_L^{sd}(Z') \Delta_R^{qq}(Z')}{\text{GeV}^2} \right] \left[\frac{3 \text{ TeV}}{M_{Z'}} \right]^2 \quad (76)$$

with 1.13 resulting from RG evolution from $M_{Z'} = 3 \text{ TeV}$ down to $\mu = m_c$. With increasing $M_{Z'}$ this factor increases logarithmically but $C_6(m_c)$ decreases much faster because of the last factor. Still as we will discuss later if the flavour structure of a given model is such that the suppression by Z' propagator is compensated by the increase of flavour-violating couplings, for $M_{Z'} \geq 10 \text{ TeV}$ the RG effects above $M_{Z'} = 3 \text{ TeV}$ begin to play some role implying additional enhancements of both QCDDP and EWP contributions to ε'/ε . The contribution of Q_5 can be neglected because of its strongly colour suppressed matrix element. Moreover, relative importance of Q_5 decreases with increasing $M_{Z'}$ again due to RG effects. See Appendix A for details.

We then find

$$\left(\frac{\varepsilon'}{\varepsilon} \right)_{Z'}^L = - \frac{\text{Im}[A_0^{\text{NP}}]^L}{\text{Re}A_0} \left[\frac{\omega_+}{|\varepsilon_K| \sqrt{2}} \right] (1 - \hat{\Omega}_{\text{eff}}) = -3.69 \times 10^7 \left[\frac{\text{Im}[A_0^{\text{NP}}]^L}{\text{GeV}} \right] \quad (77)$$

where we set all relevant quantities at their central values and

$$[A_0^{\text{NP}}]^L = C_6(m_c) \langle Q_6(m_c) \rangle_0 \quad (78)$$

with $\langle Q_6(\mu) \rangle_0$ given in (10).

Collecting all these results we find

$$\left(\frac{\varepsilon'}{\varepsilon} \right)_{Z'}^L = 0.67 B_6^{(1/2)} \left[\frac{3 \text{ TeV}}{M_{Z'}} \right]^2 \text{Im}(\Delta_L^{sd}(Z') \Delta_R^{qq}(Z')). \quad (79)$$

It should be noted that due to a large value of $M_{Z'}$ and the suppression factors of the Q_6 contribution to ε'/ε mentioned before, the overall numerical factor in this result is for $\Delta_R^{qq}(Z') = \mathcal{O}(1)$ by more than three orders of magnitude smaller than in the case of the corresponding Z scenario. See (31).

We next request the enhancement of ε'/ε as given in (18) and set the values of CKM factors to the ones in (20). Setting $B_6^{(1/2)} = 0.7$, a typical value consistent with lattice and large N results, we find from (79) and (18)

$$\text{Im} \Delta_L^{sd}(Z') = 2.1 \left[\frac{\kappa_{\varepsilon'}}{\Delta_R^{q\bar{q}}(Z')} \right] \left[\frac{0.70}{B_6^{(1/2)}} \right] \left[\frac{M_{Z'}}{3 \text{ TeV}} \right]^2 \cdot 10^{-3}. \quad (80)$$

The sign is fixed through the requirement of the enhancement of ε'/ε in (18) and the sign of $\Delta_R^{q\bar{q}}(Z')$ in (75). The large difference between the values in (34) and (80) is striking. The strong suppression of NP contribution to ε'/ε by a large Z' mass, suppressed matrix element of Q_6 relative to the one of Q_8 and the inverse “ $\Delta I = 1/2$ ” factor in (4) have to be compensated by increasing $\text{Im}\Delta_L^{sd}(Z')$. This will have interesting consequences.

5.2.2 ε_K , ΔM_K and $K_L \rightarrow \mu^+\mu^-$

Because of the increased value of $\text{Im}\Delta_L^{sd}(Z')$, not $K_L \rightarrow \mu^+\mu^-$ bound (191), as in the corresponding Z scenario, but ε_K and ΔM_K put the strongest constraints on $\text{Re}\Delta_L^{sd}(Z')$.

Using the instructions at the end of Appendix B we find

$$(\varepsilon_K)_{\text{VLL}}^{Z'} = -3.51 \times 10^4 \left[\frac{3 \text{ TeV}}{M_{Z'}} \right]^2 \text{Im}\Delta_L^{sd}(Z') \text{Re}\Delta_L^{sd}(Z') \quad (81)$$

and

$$R_{\Delta M}^{Z'} = \frac{(\Delta M_K)_{\text{VLL}}^{Z'}}{(\Delta M_K)_{\text{exp}}} = 5.29 \times 10^4 \left[\frac{3 \text{ TeV}}{M_{Z'}} \right]^2 [(\text{Re}\Delta_L^{sd}(Z'))^2 - (\text{Im}\Delta_L^{sd}(Z'))^2] \quad (82)$$

Requiring the enhancement of ε_K as in (19) and using (80) we find

$$\text{Re}\Delta_L^{sd}(Z') = -1.4 \kappa_\varepsilon \left[\frac{\Delta_R^{q\bar{q}}(Z')}{\kappa_{\varepsilon'}} \right] \left[\frac{B_6^{(1/2)}}{0.70} \right] \cdot 10^{-5}. \quad (83)$$

It should be noted that this result is independent of the value of $M_{Z'}$. Moreover, there is again a striking difference from the Z case as now $\text{Re}\Delta_L^{sd}(Z')$ is much smaller than $\text{Im}\Delta_L^{sd}(Z')$ making the coupling $\Delta_L^{sd}(Z')$ to an excellent approximation imaginary with two first interesting consequences:

- The $K_L \rightarrow \mu^+\mu^-$ constraint is easily satisfied.
- ΔM_K is uniquely *suppressed* with the suppression increasing with increasing $\kappa_{\varepsilon'}$ and $M_{Z'}$:

$$R_{\Delta M}^{Z'}(\text{QCDP}) \equiv \frac{(\Delta M_K)_{\text{VLL}}^{Z'}}{(\Delta M_K)_{\text{exp}}} = -0.23 \left[\frac{\kappa_{\varepsilon'}}{\Delta_R^{q\bar{q}}(Z')} \right]^2 \left[\frac{M_{Z'}}{3 \text{ TeV}} \right]^2 \left[\frac{0.70}{B_6^{(1/2)}} \right]^2. \quad (84)$$

Whether this suppression is consistent with the data cannot be answered at present because of large uncertainties in the evaluation of ΔM_K within the SM.

Indeed the present SM estimate without the inclusion of long distance effects reads [74]

$$R_{\Delta M}^{\text{SM}} = 0.89 \pm 0.34. \quad (85)$$

Large N approach [16] indicates that long distance contributions enhance this ratio by roughly 20%. First lattice calculations [75] are still subject to large uncertainties and also the large error in (85) precludes any definite conclusions at present whether NP should enhance or suppress this ratio.

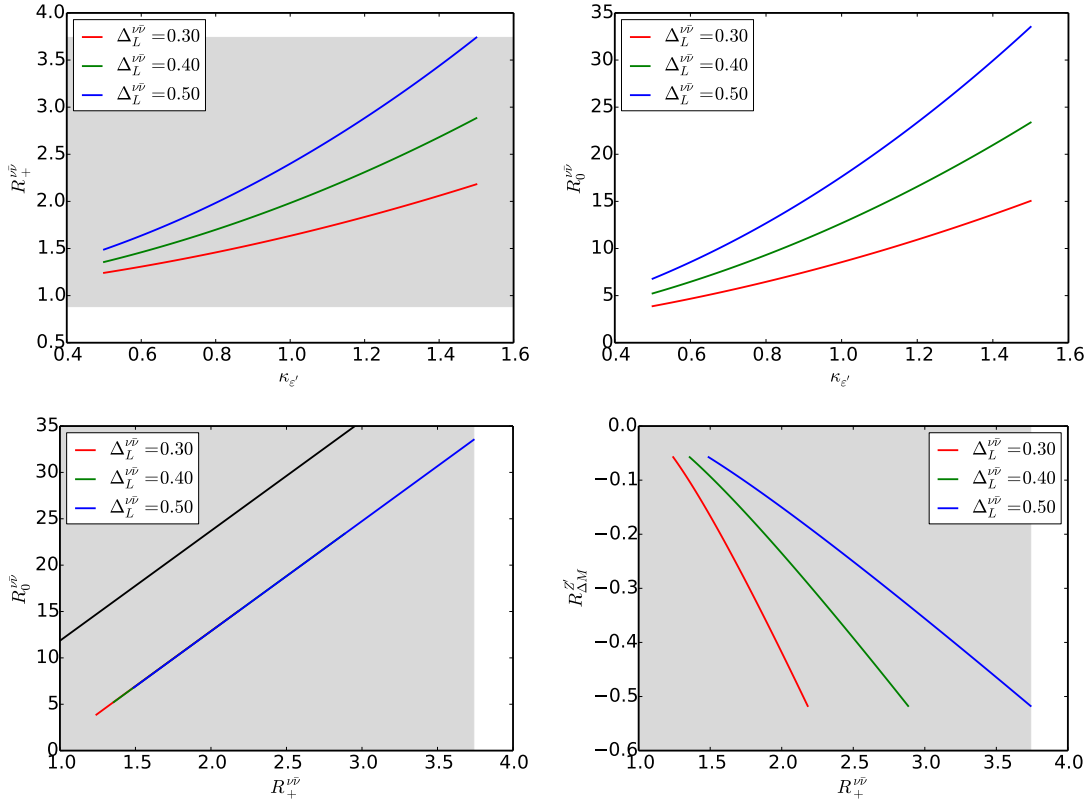


Figure 5: $R_+^{\nu\bar{\nu}}$ and $R_0^{\nu\bar{\nu}}$, as functions of $\kappa_{\varepsilon'}$ for $\Delta_L^{\nu\bar{\nu}}(Z') = 0.3, 0.4, 0.5$ for QCDP scenario. $M_{Z'} = 3$ TeV. The dependence on κ_ε is negligible. The upper black line in the lower left panel is the GN bound. In the fourth panel correlation of $R_{\Delta M}^{Z'}$ with $R_+^{\nu\bar{\nu}}$ is given. The experimental 1σ range for $R_+^{\nu\bar{\nu}}$ in (178) is displayed by the grey band.

5.2.3 $K^+ \rightarrow \pi^+\nu\bar{\nu}$ and $K_L \rightarrow \pi^0\nu\bar{\nu}$

But the most interesting implications of the ε'/ε anomaly in this scenario are the ones for $K^+ \rightarrow \pi^+\nu\bar{\nu}$ and $K_L \rightarrow \pi^0\nu\bar{\nu}$. Inserting the couplings in (80) and (83) into (186) and (187) we find that the branching ratios $\mathcal{B}(K_L \rightarrow \pi^0\nu\bar{\nu})$ and $\mathcal{B}(K^+ \rightarrow \pi^+\nu\bar{\nu})$ are to an excellent approximation affected only through the shift in $\text{Im} X_{\text{eff}}$. Therefore, there is a strict correlation between $\mathcal{B}(K_L \rightarrow \pi^0\nu\bar{\nu})$ and $\mathcal{B}(K^+ \rightarrow \pi^+\nu\bar{\nu})$ which in the plane of these two branching ratios takes place on the branch parallel to the Grossman-Nir bound [76] in (71). This is a very striking difference from Z scenarios LHS and RHS which to our knowledge has not been noticed before. On the other hand there are some similarities to the example 2 in the general Z scenario in which the imaginary parts of the couplings dominate and the value of the parameter κ_ε does not play any role for $K^+ \rightarrow \pi^+\nu\bar{\nu}$ and $K_L \rightarrow \pi^0\nu\bar{\nu}$.

In Fig. 5 we show $R_0^{\nu\bar{\nu}}$ and $R_+^{\nu\bar{\nu}}$ as functions of $\kappa_{\varepsilon'}$ and different values of $\Delta_L^{\nu\bar{\nu}}(Z')$ with the colour coding:

$$\Delta_L^{\nu\bar{\nu}}(Z') = 0.3 \text{ (red)}, \quad \Delta_L^{\nu\bar{\nu}}(Z') = 0.4 \text{ (green)}, \quad \Delta_L^{\nu\bar{\nu}}(Z') = 0.5 \text{ (blue)}. \quad (86)$$

We keep the diagonal quark coupling $\Delta_R^{q\bar{q}}(Z') = 1$ but as seen in (80) the results depend

only on the ratio $\kappa_{\varepsilon'}/\Delta_R^{q\bar{q}}(Z')$ and it is straightforward to find out what happens for other values of $\Delta_R^{q\bar{q}}(Z')$. As the real parts of flavour violating couplings are small the parameter κ_ε has no impact on this plot. In the third panel we show $R_0^{\nu\bar{\nu}}$ vs $R_+^{\nu\bar{\nu}}$ with the lower straight line representing the strict correlation between both ratios mentioned before and the upper line is the GN upper bound. In the fourth panel we show the correlation of $R_{\Delta M}^{Z'}$ with $R_+^{\nu\bar{\nu}}$ for different values of $\Delta_L^{\nu\bar{\nu}}(Z')$.

We observe that for $\Delta_L^{\nu\bar{\nu}}(Z') = 0.5$ and $\kappa_{\varepsilon'} = 1.0$ the branching ratio $\mathcal{B}(K_L \rightarrow \pi^0 \nu \bar{\nu})$ is enhanced by a factor of 17.6 and $\mathcal{B}(K^+ \rightarrow \pi^+ \nu \bar{\nu})$ by a factor of 2.4 with respect to the SM values. Moreover ΔM_K is suppressed by roughly 25%. These results are for $M_{Z'} = 3 \text{ TeV}$. Larger values of $M_{Z'}$ will be considered in Section 5.8.

The NP effects for largest $\kappa_{\varepsilon'}$ are spectacular but probably unrealistic. There are various means to decrease them as can be deduced from the plots in Fig. 5. We give two examples

- $\kappa_{\varepsilon'}$ in (18) could turn out to be moderate, say $\kappa_{\varepsilon'} = 0.5$, so that $\text{Im}\Delta_L^{sd}(Z')$ is smaller by a factor of two relative to the $\kappa_{\varepsilon'} = 1.0$ case. The enhancements of $\mathcal{B}(K_L \rightarrow \pi^0 \nu \bar{\nu})$ and $\mathcal{B}(K^+ \rightarrow \pi^+ \nu \bar{\nu})$ will then decrease approximately to 6.8 and 1.5, respectively. Moreover the suppression of ΔM_K will only be by 6%. The enhancement of ε_K in (19) can still be kept by increasing $\text{Re}\Delta_L^{sd}(Z')$ by a factor of 2 without any visible consequences for other observables.
- The enhancements of $\mathcal{B}(K_L \rightarrow \pi^0 \nu \bar{\nu})$ and $\mathcal{B}(K^+ \rightarrow \pi^+ \nu \bar{\nu})$ can be decreased by making $\Delta_L^{\nu\bar{\nu}}(Z')$ smaller. In fact this will be the only option if $\kappa_{\varepsilon'}$ will be required to be close to unity. Note, however, that modifying $\Delta_L^{\nu\bar{\nu}}(Z')$ will affect the two branching ratios in a correlated manner.

It should also be kept in mind that an increase of $\Delta_R^{q\bar{q}}(Z')$ to obtain larger enhancement of ε'/ε and smaller $\text{Im}\Delta_L^{sd}(Z')$ is bounded by the LHC data in (74).

Clearly, the result that the branching ratios $\mathcal{B}(K_L \rightarrow \pi^0 \nu \bar{\nu})$ and $\mathcal{B}(K^+ \rightarrow \pi^+ \nu \bar{\nu})$ are enhanced because ε'/ε is enhanced is related to the choice of the signs of flavour diagonal quark and neutrino couplings in (75). If the sign of one of these couplings is reversed but still the enhancement of ε'/ε is required, both branching ratios are suppressed along the branch parallel to the GN bound. But ΔM_K being governed by the square of the imaginary couplings is always suppressed. We summarize all cases in Table 3. It should also be noticed that this pattern would not change if it turned out that ε_K should be suppressed ($\kappa_\varepsilon < 0$), which would reverse the sign of $\text{Re}\Delta_L^{sd}(Z')$. Simply, because $\text{Re}\Delta_L^{sd}(Z')$ is so much smaller than $\text{Im}\Delta_L^{sd}(Z')$ that its sign does not matter.

In summary the two striking predictions of this scenario is the simultaneous enhancement or simultaneous suppression of the branching ratios for $K^+ \rightarrow \pi^+ \nu \bar{\nu}$ and $K_L \rightarrow \pi^0 \nu \bar{\nu}$ accompanied always by the suppression of ΔM_K . Finding the enhancement of $K^+ \rightarrow \pi^+ \nu \bar{\nu}$ and suppression of $K_L \rightarrow \pi^0 \nu \bar{\nu}$ or vice versa at NA62 and KOPIO experiments and/or the need for an enhancement of ΔM_K by NP would rule out this scenario independently of what will happen with ε_K .

$\Delta_R^{qq}(Z')$	$\Delta_L^{\nu\bar{\nu}}(Z')$	ε'/ε	$\mathcal{B}(K_L \rightarrow \pi^0 \nu \bar{\nu})$	$\mathcal{B}(K^+ \rightarrow \pi^+ \nu \bar{\nu})$	ΔM_K
+	+	+	+	+	-
-	+	+	-	-	-
+	-	+	-	-	-
-	-	+	+	+	-

Table 3: Pattern of correlated enhancements (+) and suppressions (-) in Z' scenarios in which NP in ε'/ε is dominated by QCDP operator Q_6 .

5.3 Z' with QCD Penguin Dominance (RHS)

In the case of LHS the flavour symmetry on all diagonal RH quark couplings has to be imposed. But in the RHS the flavour diagonal couplings are left-handed and the ones in an $SU(2)_L$ doublet must be equal to each other due to $SU(2)_L$ gauge symmetry which is still unbroken for Z' masses larger than few TeV. Thus it is more natural in this case to generate only QCDP operators than in LHS.

We find this time

$$C'_6(m_c) = 1.13 \frac{\Delta_R^{sd}(Z') \Delta_L^{qq}(Z')}{4M_{Z'}^2} = 3.14 \times 10^{-8} \left[\frac{\Delta_R^{sd}(Z') \Delta_L^{qq}(Z')}{\text{GeV}^2} \right] \left[\frac{3 \text{ TeV}}{M_{Z'}} \right]^2 \quad (87)$$

ε'/ε is again given by (77) but this time

$$[A_0^{\text{NP}}]^R = C'_6(\mu) \langle Q'_6(\mu) \rangle_0, \quad \langle Q'_6(\mu) \rangle_0 = -\langle Q_6(\mu) \rangle_0 \quad (88)$$

Collecting all these results we find

$$\left(\frac{\varepsilon'}{\varepsilon} \right)_{Z'}^R = -0.67 B_6^{(1/2)} \left[\frac{3 \text{ TeV}}{M_{Z'}} \right]^2 \text{Im}(\Delta_R^{sd}(Z') \Delta_L^{qq}(Z')). \quad (89)$$

The difference in sign from (89) is only relevant in a model in which the flavour diagonal couplings are known or can be measured somewhere. With the choice of the quark flavour diagonal couplings in (75) there is no change in the values of flavour violating couplings except that now these are right-handed couplings instead of left-handed ones. Even if NP contribution to $K_L \rightarrow \mu^+ \mu^-$ changes sign, this change is too small to be relevant because the real parts of NP couplings are small. For other choices of signs of flavour diagonal couplings a DNA-Table analogous to Table 3 can be constructed by just reversing the signs of $\Delta_R^{q\bar{q}}(Z')$ and replacing it by $\Delta_L^{q\bar{q}}(Z')$.

5.4 Z' with QCD Penguin Dominance (General)

5.4.1 ε'/ε

We will next consider scenario in which both LH and RH flavour violating Z' couplings are present. From (79) and (89) we find

$$\left(\frac{\varepsilon'}{\varepsilon} \right)_{Z'} = 0.67 B_6^{(1/2)} \left[\frac{3 \text{ TeV}}{M_{Z'}} \right]^2 \left[\text{Im}(\Delta_L^{sd}(Z') \Delta_R^{qq}(Z')) - \text{Im}(\Delta_R^{sd}(Z') \Delta_L^{qq}(Z')) \right]. \quad (90)$$

This result is interesting in itself. If Z' couplings to quarks are left-right symmetric there is, similar to $K_L \rightarrow \mu^+ \mu^-$, no NP contribution to ε'/ε . In view of strong indication for $\kappa_{\varepsilon'} \neq 0$ left-right symmetry in the Z' couplings to quarks has to be broken.

But there is still another reason that such a situation cannot be realized as either the coupling $\Delta_L^{qq}(Z')$ or the coupling $\Delta_R^{qq}(Z')$ can be flavour universal. They cannot be both flavour universal as then it would not be possible to generate large flavour violating couplings in the mass eigenstate basis for any of the terms in (90). But one could consider e.g. $\Delta_R^{qq}(Z')$ to be flavour universal to a high degree still allowing for a strongly suppressed but non-vanishing coupling $\Delta_R^{sd}(Z')$. In any case for these reasons only one term in (90) will be important allowing in principle the solution to the ε'/ε anomaly. But the presence of both LH and RH flavour-violating couplings, even if one is much smaller than the other, changes the ε_K and ΔM_K constraints through LR operators, as we have seen in the general Z case. While in the latter scenario this allowed us to obtain interesting results for rare decays, in Z' scenarios the requirement of much larger couplings than in the Z case for solving the ε'/ε anomaly makes the ε_K and ΔM_K constraints problematic as we will discuss briefly now.

5.4.2 ε_K and ΔM_K

We have now

$$(\varepsilon_K)^{\text{NP}} = (\varepsilon_K)_{\text{VLL}}^{Z'} + (\varepsilon_K)_{\text{VRR}}^{Z'} + (\varepsilon_K)_{\text{LR}}^{Z'} \quad (91)$$

where

$$(\varepsilon_K)_{\text{LR}}^{Z'} = -3.39 \times 10^6 \left[\frac{3 \text{ TeV}}{M_{Z'}} \right]^2 \text{Im} [\Delta_L^{sd}(Z') \Delta_R^{sd}(Z')]^* \quad (92)$$

and

$$R_{\Delta M}^{Z'} = \frac{(\Delta M_K)_{\text{VLL}}^{Z'}}{(\Delta M_K)_{\text{exp}}} + \frac{(\Delta M_K)_{\text{VRR}}^{Z'}}{(\Delta M_K)_{\text{exp}}} + \frac{(\Delta M_K)_{\text{LR}}^{Z'}}{(\Delta M_K)_{\text{exp}}} \quad (93)$$

with

$$\frac{(\Delta M_K)_{\text{LR}}^{Z'}}{(\Delta M_K)_{\text{exp}}} = -1.02 \times 10^7 \left[\frac{3 \text{ TeV}}{M_{Z'}} \right]^2 \text{Re} [\Delta_L^{sd}(Z') \Delta_R^{sd}(Z')]^* . \quad (94)$$

5.4.3 Implications

In view of the large coupling $\text{Im} \Delta_L^{sd}(Z')$ or $\text{Im} \Delta_R^{sd}(Z')$ required to solve the ε'/ε anomaly, NP contributions to ε_K and ΔM_K in the presence of both LH and RH currents are very large. The only solution would be a very fine-tuned scenario in which the four couplings $\text{Im} \Delta_{L,R}^{sd}(Z')$ and $\text{Re} \Delta_{L,R}^{sd}(Z')$ take very particular values. But eventually in order to get significant shift in ε'/ε and satisfy ΔM_K and ε_K constraints either RH or LH couplings would have to be very small bringing us back to the LHS or RHS scenario, respectively.

We conclude therefore that the solution to the ε'/ε anomaly in Z' scenarios through the QCDP is only possible in the LHS or RHS if one wants to avoid fine-tuning of couplings. Then also the branching ratios for $K^+ \rightarrow \pi^+ \nu \bar{\nu}$ and $K_L \rightarrow \pi^0 \nu \bar{\nu}$ can be enhanced in a correlated manner and ε_K enhanced as favoured by the data.

This is different from the Z case, where the four enhancements in question could only be simultaneously obtained in the presence of LH and RH couplings without fine-tuning of parameters.

5.5 A heavy G'

We have just seen that the removal of ε'/ε anomaly in Q_6 scenario implies for $\Delta_L^{\nu\bar{\nu}}(Z') = \mathcal{O}(1)$ large NP effects in $K^+ \rightarrow \pi^+\nu\bar{\nu}$ and $K_L \rightarrow \pi^0\nu\bar{\nu}$. It is possible that the ε'/ε anomaly will remain but no NP will be found in $K^+ \rightarrow \pi^+\nu\bar{\nu}$ and $K_L \rightarrow \pi^0\nu\bar{\nu}$. The simplest solution would be to set $\Delta_L^{\nu\bar{\nu}}(Z') = 0$. But another possibility would be the presence of a heavy G' which does not couple to neutrinos. One of the prominent examples of this type are Kaluza-Klein gluons in Randall-Sundrum scenarios that belong to the adjoint representation of the colour $SU(3)_c$. But here we want to consider a simplified scenario that has been considered in the context of NP contribution to the $\Delta I = 1/2$ rule in [27] and some of the results obtained there can be used in the case of ε'/ε here.

Following [27] we will then assume that these gauge bosons carry a common mass $M_{G'}$ and being in the octet representation of $SU(3)_c$ couple to fermions in the same manner as gluons do. However, we will allow for different values of their left-handed and right-handed couplings. Therefore up to the colour matrix t^a , the couplings to quarks will be again parametrized by:

$$\Delta_L^{sd}(G'), \quad \Delta_R^{sd}(G'), \quad \Delta_L^{qq}(G'), \quad \Delta_R^{qq}(G'). \quad (95)$$

As G' carries colour, the RG analysis is modified through the change of the initial conditions at $\mu = M_{G'}$ that read now [27]

$$C_3(M_{G'}) = \left[-\frac{1}{6}\right] \frac{\Delta_L^{sd}(G')\Delta_L^{qq}(G')}{4M_{G'}^2}, \quad C'_3(M_{G'}) = \left[-\frac{1}{6}\right] \frac{\Delta_R^{sd}(G')\Delta_R^{qq}(G')}{4M_{G'}^2}, \quad (96)$$

$$C_4(M_{G'}) = \left[\frac{1}{2}\right] \frac{\Delta_L^{sd}(G')\Delta_L^{qq}(G')}{4M_{G'}^2}, \quad C'_4(M_{G'}) = \left[\frac{1}{2}\right] \frac{\Delta_R^{sd}(G')\Delta_R^{qq}(G')}{4M_{G'}^2}, \quad (97)$$

$$C_5(M_{G'}) = \left[-\frac{1}{6}\right] \frac{\Delta_L^{sd}(G')\Delta_R^{qq}(G')}{4M_{G'}^2}, \quad C'_5(M_{G'}) = \left[-\frac{1}{6}\right] \frac{\Delta_R^{sd}(G')\Delta_L^{qq}(G')}{4M_{G'}^2}, \quad (98)$$

$$C_6(M_{G'}) = \left[\frac{1}{2}\right] \frac{\Delta_L^{sd}(G')\Delta_R^{qq}(G')}{4M_{G'}^2}, \quad C'_6(M_{G'}) = \left[\frac{1}{2}\right] \frac{\Delta_R^{sd}(G')\Delta_L^{qq}(G')}{4M_{G'}^2}. \quad (99)$$

In the LHS scenario the contributions of primed operators are absent. Moreover, due the non-vanishing value of $C_6(M_{G'})$ the dominance of the operator Q_6 is this time even more pronounced than in the case of a colourless Z' . See Appendix A. One finds then in the LHS [27]

$$C_6(m_c) = 1.61 \frac{\Delta_L^{sd}(G')\Delta_R^{qq}(G')}{4M_{G'}^2} \quad (100)$$

with 1.61 resulting from RG evolution from $M_{G'} = 3.0$ TeV down to m_c .

We find then

$$\left(\frac{\varepsilon'}{\varepsilon}\right)_{G'}^L = 0.70 B_6^{(1/2)} \left[\frac{3.5 \text{ TeV}}{M_{G'}}\right]^2 \text{Im}(\Delta_L^{sd}(G'))\Delta_R^{qq}(G'), \quad (101)$$

where the difference in the RG factor for $M_{G'} = 3.0$ TeV and $M_{G'} = 3.5$ TeV can be neglected.

Now the upper bound on $\Delta_R^{qq}(G')$ from LHC reads [72]

$$|\Delta_R^{q\bar{q}}(G')| \leq 2.0 \left[\frac{M_{G'}}{3.5 \text{ TeV}} \right] \left[1 + \left(\frac{1.4 \text{ TeV}}{M_{G'}} \right)^2 \right]. \quad (102)$$

Taking $B_6^{(1/2)} = 0.7$, $\Delta_R^{qq}(G') = 2.0$ and $M_{G'} = 3.5 \text{ TeV}$ we find then

$$\left(\frac{\varepsilon'}{\varepsilon} \right)_{G'}^L = 0.98 \text{Im} \Delta_L^{sd}(G') \quad (103)$$

and consequently the removal of ε'/ε anomaly requires now

$$\text{Im} \Delta_L^{sd}(G') = 1.02 \kappa_{\varepsilon'} \left[\frac{2.0}{\Delta_R^{q\bar{q}}(G')} \right] 10^{-3}, \quad (104)$$

which is by a factor of two lower than in the case of Z' .

As shown in [27] NP contributions to ε_K and ΔM_K are for $M_{G'} = M_{Z'}$ suppressed by a colour factor of three relative to Z' case, but also in this case the removal of the ε_K tension together with (104) implies that the coupling $\Delta_L^{sd}(G')$ is nearly imaginary. Therefore, also in this case the unique prediction is the suppression of ΔM_K below its SM value. Yet, this suppression is smaller relative to Z' case by roughly a factor of 17 due to smaller value of $\text{Im} \Delta_L^{sd}(G')$, the colour factor $1/3$ in NP contribution to ΔM_K and the higher mass of G' . Thus in contrast to the Z' case, NP effects in ΔM_K are fully negligible in this scenario.

While, this scenario of NP is not very exciting, we cannot exclude it at present. It should also be remarked that NP contributions to ΔM_K could be obtained also with G' by making $\Delta_R^{sd}(G')$ non-vanishing.

5.6 Z' with Electroweak Penguin Dominance

5.6.1 The case of $\Delta_R^{qq}(Z') = \mathcal{O}(1)$

We will next consider the case of a Z' model of the LHS type in which NP contribution to ε'/ε is governed by the Q_8 operator. The 331 models discussed briefly in Section 7.5 are specific models belonging to this class of models. It should be noted that as far as $K^+ \rightarrow \pi^+ \nu \bar{\nu}$, $K_L \rightarrow \pi^0 \nu \bar{\nu}$, ε_K , ΔM_K and $K_L \rightarrow \mu^+ \mu^-$ are concerned the formulae of the LH scenario in which Q_6 dominated NP in ε'/ε remain unchanged. On the other hand the formula for ε'/ε is modified in a very significant matter which will imply striking differences from QCDP scenario.

Generalizing the analysis of 331 models in [77] to a Z' model with arbitrary diagonal couplings we find

$$C_8(m_c) = 1.35 C_7(M_{Z'}) = 1.35 \frac{\Delta_L^{sd}(Z') \Delta_R^{qq}(Z')}{4M_{Z'}^2} \quad (105)$$

with 1.35 resulting from RG evolution from $M_{Z'} = 3.0 \text{ TeV}$ down to m_c . Here, in order to simplify the notation we denoted the RH flavour diagonal quark coupling simply by $\Delta_R^{qq}(Z')$ ⁷.

⁷In reality it is a proper linear combination of diagonal up-quark and down-quark couplings that enters the Q_7 and Q_8 penguin operators. We denote this combination simply by $\Delta_R^{qq}(Z')$.

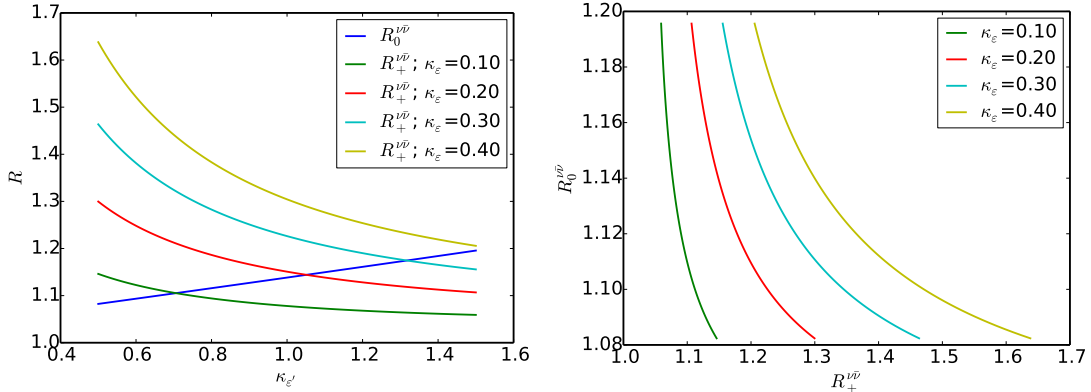


Figure 6: $R_0^{\nu\bar{\nu}}$ and $R_+^{\nu\bar{\nu}}$, as functions of $\kappa_{\epsilon'}$ for $\kappa_{\epsilon} = 0.1, 0.2, 0.3, 0.4$ for EWP scenario.

Proceeding as in LHS Z scenario in Section 4.2 and replacing $C_8(m_c)$ in (30) by (105) we find instead of (79)

$$\left(\frac{\epsilon'}{\epsilon}\right)_{Z'}^L = 38.0 B_8^{(3/2)} \left[\frac{3 \text{ TeV}}{M_{Z'}}\right]^2 \text{Im}(\Delta_L^{sd}(Z')) \Delta_R^{q\bar{q}}(Z'). \quad (106)$$

Compared to (79) the larger overall coefficient implies a smaller $\text{Im}\Delta_L^{sd}(Z')$ required to solve the ϵ'/ϵ anomaly. On the other hand compared to (31) in the LHS Z scenario, the sign of the model dependent $\Delta_R^{q\bar{q}}(Z')$ can be chosen in such a manner that one can enhance simultaneously ϵ'/ϵ and $\mathcal{B}(K_L \rightarrow \pi^0 \nu \bar{\nu})$. This was not possible in the LH Z scenario in which the diagonal quark couplings were fixed.

Setting $B_8^{(3/2)} = 0.76$ we find the required couplings for the solution of ϵ'/ϵ and ϵ_K anomalies through the shifts in (18) and (19) to be:

$$\text{Im}\Delta_L^{sd}(Z') = 3.5 \left[\frac{\kappa_{\epsilon'}}{\Delta_R^{q\bar{q}}(Z')}\right] \left[\frac{0.76}{B_8^{(3/2)}}\right] \left[\frac{M_{Z'}}{3 \text{ TeV}}\right]^2 \cdot 10^{-5}, \quad (107)$$

$$\text{Re}\Delta_L^{sd}(Z') = -8.2 \kappa_{\epsilon} \left[\frac{\Delta_R^{q\bar{q}}(Z')}{\kappa_{\epsilon'}}\right] \left[\frac{B_8^{(3/2)}}{0.76}\right] \cdot 10^{-4} \quad (108)$$

which in view of a large $M_{Z'}$ can be made consistent with the $K_L \rightarrow \mu^+ \mu^-$ bound for $\Delta_A^{\mu\bar{\mu}}(Z') = \mathcal{O}(1)$. Note that $\text{Re}\Delta_L^{sd}(Z')$ is independent of $M_{Z'}$.

We observe that the signs in (107) and (108) are the same as in (80) and (83), respectively implying that also now $\mathcal{B}(K_L \rightarrow \pi^0 \nu \bar{\nu})$ and $\mathcal{B}(K^+ \rightarrow \pi^+ \nu \bar{\nu})$ will be enhanced over their SM values but the correlation between these enhancements is different due to the fact that the real part of $\Delta_L^{sd}(Z')$ is larger than its imaginary part. Moreover NP effects implied in these decays by the ϵ'/ϵ and ϵ_K anomalies turn out to be significantly smaller than in the QCDP scenario.

In the first panel in Fig. 6 we show $R_0^{\nu\bar{\nu}}$ and $R_+^{\nu\bar{\nu}}$ as functions of $\kappa_{\epsilon'}$ and different values of κ_{ϵ} with the colour coding in (69). $R_0^{\nu\bar{\nu}}$ is given by the blue line. Due to smaller values of imaginary parts required for a given $\kappa_{\epsilon'}$ to fit the data on ϵ'/ϵ the implied NP

effects in both ratios are smaller than in the QCDP case and therefore we set this time $\Delta_L^{\nu\bar{\nu}}(Z') = 0.5$. On the other hand in contrast to QCDP case, where there is no dependence on κ_ε , the enhancement of $\mathcal{B}(K^+ \rightarrow \pi^+\nu\bar{\nu})$ in EWP scenario strongly depends on the ratio $\kappa_\varepsilon/\kappa_{\varepsilon'}$. This is also seen in the second panel in which we present the results of the first panel as $R_0^{\nu\bar{\nu}}$ vs $R_+^{\nu\bar{\nu}}$. This result has a pattern similar to the first Z example in Fig. 4 but NP effects are now much smaller.

$\Delta_R^{q\bar{q}}(Z')$	$\Delta_L^{\nu\bar{\nu}}(Z')$	ε'/ε	$ \varepsilon_K $	$\mathcal{B}(K_L \rightarrow \pi^0\nu\bar{\nu})$	$\mathcal{B}(K^+ \rightarrow \pi^+\nu\bar{\nu})$	ΔM_K
+	+	+	+	+	+	+
+	+	+	-	+	-	+
-	+	+	+	-	-	+
-	+	+	-	-	+	+
+	-	+	+	-	-	+
+	-	+	-	-	+	+
-	-	+	+	+	+	+
-	-	+	-	+	-	+

Table 4: Pattern of correlated enhancements (+) and suppressions (-) in Z' scenarios in which NP in ε'/ε is dominated by EWP operator Q_8 .

Interestingly, we find that ΔM_K is exclusively *enhanced* as opposed to its suppression in QCDP scenario as seen in (84). This time we have

$$R_{\Delta M}^{Z'}(\text{EWP}) \equiv \frac{(\Delta M_K)_{\text{VLL}}^{Z'}}{(\Delta M_K)_{\text{exp}}} = 3.6 \cdot 10^{-2} \kappa_\varepsilon^2 \left[\frac{\Delta_R^{q\bar{q}}(Z')}{\kappa_{\varepsilon'}} \right]^2 \left[\frac{0.76}{B_8^{(3/2)}} \right]^2 \left[\frac{3 \text{ TeV}}{M_{Z'}} \right]^2. \quad (109)$$

We note that dependence on $\kappa_{\varepsilon'}$ and $\Delta_R^{q\bar{q}}(Z')$ is different than in (84) and the enhancement depends on κ_ε . But the striking difference is in the size of the effect and its $M_{Z'}$ dependence. NP contribution to ΔM_K is now in the ballpark of a few percent only and decreases with increasing $M_{Z'}$ as opposed to the QCD penguin case, where it is sizable and increases with increasing $M_{Z'}$ thereby significantly suppressing ΔM_K . See Fig. 5.

Clearly, similar to the case of the Q_6 dominance, the result that the branching ratios $\mathcal{B}(K_L \rightarrow \pi^0\nu\bar{\nu})$ and $\mathcal{B}(K^+ \rightarrow \pi^+\nu\bar{\nu})$ are enhanced because ε'/ε is enhanced is related to the choice of the signs of flavour diagonal quark and neutrino couplings in (75). If the sign of one of these couplings is reversed but still the enhancement of ε'/ε is required, both branching ratios are suppressed. But if in addition we require that ε_K is suppressed then $K^+ \rightarrow \pi^+\nu\bar{\nu}$ is enhanced again but $K_L \rightarrow \pi^0\nu\bar{\nu}$ suppressed. We show various possibilities in Table 4. This table differs from Table 3 because the flip of the sign of $\text{Re}\Delta_L^{sd}(Z')$, caused by the flip of the sign of NP contribution to ε_K , now matters as $\text{Re}\Delta_L^{sd}(Z')$ is much larger than in the QCDP case. This has no impact on $K_L \rightarrow \pi^0\nu\bar{\nu}$ but changes enhancement of $K^+ \rightarrow \pi^+\nu\bar{\nu}$ into its suppression and vice versa. On the other hand ΔM_K being governed this time by the square of the real couplings is always enhanced as opposed to the QCDP case.

The striking prediction of this scenario is also the prediction that in the case of a negative shift of ε_K by NP one of the branching ratios must be enhanced with respect to the SM and the other suppressed, a feature which is not possible in the QCDP scenario.

In view of these rather different results it should be possible to distinguish the QCDDP and EWP mechanisms in Z' scenarios when the situation with ε'/ε and ε_K anomalies will be clarified and the data on $\mathcal{B}(K_L \rightarrow \pi^0 \nu \bar{\nu})$ and $\mathcal{B}(K^+ \rightarrow \pi^+ \nu \bar{\nu})$ will be available. The improved knowledge of ΔM_K will be important in this distinction due to the different signs and sizes of NP contributions to ΔM_K in these two scenarios.

5.6.2 The case of $\Delta_R^{qq}(Z') \ll 1$

The pattern just discussed is modified if $\Delta_R^{qq}(Z')$ is strongly suppressed for some dynamical reason. For instance choosing $\Delta_R^{qq}(Z') = 0.01$ we find

$$\text{Im}\Delta_L^{sd}(Z') = 3.5 \kappa_{\varepsilon'} 10^{-3}, \quad \text{Re}\Delta_L^{sd}(Z') = -8.2 \frac{\kappa_{\varepsilon}}{\kappa_{\varepsilon'}} 10^{-6} \quad (110)$$

which as seen in (80) and (83) is rather similar to the case of the QCDDP so that enhancements of $K^+ \rightarrow \pi^+ \nu \bar{\nu}$ and $K_L \rightarrow \pi^0 \nu \bar{\nu}$ are correlated on a branch parallel to the GN bound. Yet, it should be emphasized that in the EWP case this can only be obtained by choosing the coupling $\Delta_R^{qq}(Z')$ to be very small, while in the case of QCDDP one obtains this result automatically as in order to satisfy all flavour bounds while solving the ε'/ε anomaly $\Delta_R^{qq}(Z')$ must be $\mathcal{O}(1)$.

We will not consider the cases of RHS and of a general scenario. Due to the arbitrary values of diagonal couplings not much new can be learned relative to the cases already considered. But such scenarios could be of interest in specific models.

5.7 The Impact of $Z - Z'$ mixing

Generally, in a Z' scenario, the $Z - Z'$ mixing will generate in the process of electroweak symmetry breaking flavour-violating tree-level Z contributions. As an example a non-vanishing coupling

$$\Delta_L^{sd}(Z) = \sin \xi \Delta_L^{sd}(Z') \quad (111)$$

will be generated with ξ being the mixing angle. This mixing is bounded by LEP data to be $\mathcal{O}(10^{-3})$ and has the structure

$$\sin \xi = c_{\text{mix}} \frac{M_Z^2}{M_{Z'}^2} \quad (112)$$

with c_{mix} being a model dependent factor. Inserting (111) into (26) and performing RG evolution from M_Z to m_c we find the Z contribution to C_8 generated by this mixing:

$$C_8(m_c) = -0.76 c_{\text{mix}} \left[\frac{4g_2 s_W^2}{6c_W} \right] \frac{\Delta_L^{sd}(Z')}{4M_{Z'}^2}. \quad (113)$$

Comparing with (105) we observe that Z contribution has eventually the same dependence on $M_{Z'}$ as Z' contribution. Which of these contributions is larger depends on the model dependent values of c_{mix} and $\Delta_R^{q\bar{q}}$ which govern Z' contribution to ε'/ε .

A simple class of models that illustrates these effects are 331 models in which c_{mix} and $\Delta_R^{q\bar{q}}$ are given in terms of fundamental parameters of these models. A detailed analysis of

the impact of $Z - Z'$ mixing on flavour observables in 331 models, including ε'/ε , can be found in [77] and in a recent update in [78]. One finds after taking electroweak precision constraints into account, that in most of these models for a large range of parameters Z' contributions dominate but if one aims for precision the effects of Z contributions cannot be neglected. A brief summary of the analysis in [78] is given in Section 7.5.

5.8 Z' Outside the Reach of the LHC

5.8.1 QCD Penguin Dominance

Our discussion in Section 5.2 has revealed interesting $M_{Z'}$ dependence of flavour observables when the ε'/ε and ε_K constraints in (18) and (19) are imposed. They originate in the fact that these constraints taken together require the following $M_{Z'}$ dependence of the Z' couplings

- $\text{Im}\Delta_L^{sd}(Z')$ must increase as $M_{Z'}^2$,
- $\text{Re}\Delta_L^{sd}(Z')$ must be independent of $M_{Z'}$.

Therefore the increase of $M_{Z'}$ assures the dominance of imaginary couplings. This should be no surprise as both quantities are CP-violating and the imaginary couplings have to be larger in order to explain the anomalies in ε'/ε and ε_K at larger $M_{Z'}$.

As a consequence of this $M_{Z'}$ dependence

- $\mathcal{B}(K_L \rightarrow \pi^0 \nu \bar{\nu})$ is independent of $M_{Z'}$ because $\text{Im}X_{\text{eff}}$ is independent of it. The suppression by $1/M_{Z'}^2$ is cancelled by the increase of $\text{Im}\Delta_L^{sd}(Z')$.
- But $\text{Re}X_{\text{eff}}$ decreases with increasing $M_{Z'}$ and consequently in principle $\mathcal{B}(K^+ \rightarrow \pi^+ \nu \bar{\nu})$ will decrease. But this effect is so small in QCDP scenario that similar to $\mathcal{B}(K_L \rightarrow \pi^0 \nu \bar{\nu})$ also this branching ratio will be independent of $M_{Z'}$ with NP contributing only through $\text{Im}X_{\text{eff}}$.
- On the other hand the branching ratio for $K_L \rightarrow \mu^+ \mu^-$ decreases with increasing $M_{Z'}$ as it depends only on real parts of the couplings.

As a result of this pattern the correlation between $\mathcal{B}(K_L \rightarrow \pi^0 \nu \bar{\nu})$ and $\mathcal{B}(K^+ \rightarrow \pi^+ \nu \bar{\nu})$ will be confined to the line parallel to the GN bound. But what is interesting is that this correlation will depend only on $\kappa_{\varepsilon'}$ and is independent of $M_{Z'}$. Comparing (80) with (83) we find that the real parts are comparable with imaginary ones only for $M_{Z'} < 500$ GeV which is clearly excluded by the LHC. Therefore, for fixed $\kappa_{\varepsilon'}$ and κ_{ε} nothing will change as far as $K^+ \rightarrow \pi^+ \nu \bar{\nu}$ and $K_L \rightarrow \pi^0 \nu \bar{\nu}$ are concerned when $M_{Z'}$ is increased but the constraint from $K_L \rightarrow \mu^+ \mu^-$ will be weaker.

Yet, these *scaling laws* cannot be true forever as for sufficiently large $M_{Z'}$ the couplings will enter non-perturbative regime and our calculations will no longer apply. Moreover, these *scaling laws* did not yet take into account the bound on NP contributions to ΔM_K . Indeed as seen in (84) this contribution increases in QCDP scenario with increasing $M_{Z'}$ and suppresses ΔM_K that is positive in the SM. At some value of $M_{Z'}$ this NP effect will be too large for the theory to agree with experiment. The rescue could come from

increased value of $\Delta_R^{q\bar{q}}(Z')$ or decreased value of $\kappa_{\varepsilon'}$. This simply means that when ΔM_K constraint is taken into account there is an upper bound on $\kappa_{\varepsilon'}$ which becomes stronger with increasing $M_{Z'}$. Or in other words at sufficiently high values of $M_{Z'}$ it will not be possible to explain the anomalies in question and with further increase of $M_{Z'}$ NP will decouple.

At this stage one should emphasize that for more precise calculations, when going to much higher values of $M_{Z'}$, well above the LHC scales, RG effects represented by numerical factors like 1.13, 1.61 and 1.35 for QCDP, G' and EWP contributions to ε'/ε valid for $M_{Z'} = 3 \text{ TeV}$ have to be modified as collected in Table 5 in Appendix A. For $M_{Z'} = 100 \text{ TeV}$ they are increased typically by a factor of 1.3–1.5 relative to $M_{Z'} = 3 \text{ TeV}$.

Formula (84) generalized to include RG corrections for $M_{Z'} \geq 3 \text{ TeV}$ reads

$$R_{\Delta M}^{Z'}(\text{QCDP}) = -0.23 \left[\frac{1.13}{r_{65}(M_{Z'})} \right]^2 \left[\frac{\kappa_{\varepsilon'}}{\Delta_R^{q\bar{q}}(Z')} \right]^2 \left[\frac{M_{Z'}}{3 \text{ TeV}} \right]^2 \left[\frac{0.70}{B_6^{(1/2)}} \right]^2, \quad (114)$$

with $r_{65}(M_{Z'})$ given in Table 5. In Fig 7 we show $R_{\Delta M}^{Z'}(\text{QCDP})$ as a function of $M_{Z'}$ for different values of the ratio

$$\bar{\kappa}_{\varepsilon'} \equiv \frac{\kappa_{\varepsilon'}}{\Delta_R^{q\bar{q}}(Z')}. \quad (115)$$

We observe that already for $M_{Z'} = 6 \text{ TeV}$ the shift in ΔM_K is large unless $\kappa_{\varepsilon'}$ is at most 0.5 or $\Delta_R^{q\bar{q}}(Z') > 1.0$. As seen in (74) for $M_{Z'} = 6 \text{ TeV}$ the choice $\Delta_R^{q\bar{q}}(Z') = 2.0$ is still consistent with LHC bounds.

The bound on ΔM_K in question can be avoided to some extent by going to the general Z' scenario which contains also $\Delta_R^{sd}(Z')$. This allows, as suggested in [27], to weaken with some fine-tuning ΔM_K constraint while solving ε'/ε anomaly. But, in order to perform a meaningful analysis the value of ΔM_K in the SM must be known significantly better than it is the case now. In particular if suppressions of ΔM_K are not allowed one will have to abandon this scenario. Then, as we will discuss soon, the EWP scenario would be favoured.

It should also be emphasized that in a concrete model additional constraints could come from other observables, in particular from observables like the $B_{s,d}^0 - \bar{B}_{s,d}^0$ mass differences $\Delta M_{s,d}$ and CP asymmetries $S_{\psi K_S}$ and $S_{\psi\phi}$ which could further change the scaling laws. We refer to [78] for scaling laws found in the context of 331 models.

5.8.2 Electroweak Penguin Dominance

The main difference in this scenario is the finding that for $\Delta_R^{q\bar{q}} = \mathcal{O}(1)$ and $M_{Z'} = 3 \text{ TeV}$

$$\text{Re}\Delta_R^{sd}(Z') \gg \text{Im}\Delta_R^{sd}(Z'). \quad (116)$$

With increasing $M_{Z'}$ this hierarchy becomes for fixed $(\kappa_{\varepsilon'}, \kappa_{\varepsilon})$ smaller as $\text{Im}\Delta_R^{sd}(Z')$ increases with $M_{Z'}$ and $\text{Re}\Delta_R^{sd}(Z')$ is independent of it. By comparing (107) and (108) we learn that the magnitudes of both couplings are equal for

$$M_{Z'} = 14.5 \sqrt{\kappa_{\varepsilon}} \left[\frac{\Delta_R^{qq}}{\kappa_{\varepsilon'}} \right] \text{ TeV} \quad (117)$$

But even for these values of $M_{Z'}$

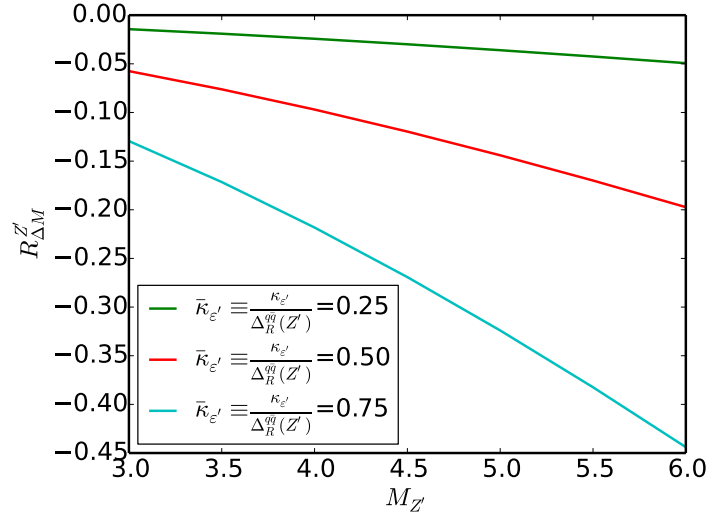


Figure 7: $R_{\Delta M}^{Z'}(\text{QCDP})$ as a function of $M_{Z'}$ for different values of $\bar{\kappa}_{\epsilon'}$.

- The correlation between $K^+ \rightarrow \pi^+ \nu \bar{\nu}$ and $K_L \rightarrow \pi^0 \nu \bar{\nu}$ is away from the branch parallel to the GN bound.
- NP contribution to ΔM_K has opposite sign to the one in QCDP scenario and ΔM_K is enhanced and not suppressed relative to its SM value. Moreover this enhancement is at the level of a few percent only and decreases with increasing $M_{Z'}$ so that possible problems with ΔM_K constraint encountered in QCDP scenario are absent here unless future precise estimates of ΔM_K in the SM will require sizable contribution from NP.

Clearly a precise value of ΔM_K in the SM will be crucial in order to see whether the enhancement of ΔM_K predicted here is consistent with the data. In particular if an enhancement of ΔM_K is not allowed, one will have to abandon this scenario.

5.9 Summary of NP Patterns in Z' Scenarios

The striking difference from Z scenarios, known already from our previous studies, is the increased importance of the constraints from $\Delta F = 2$ observables. This has two virtues in the presence of the ϵ'/ϵ constraint:

- The real parts of the couplings are determined for not too a large κ_ϵ from the ϵ_K constraint, which is theoretically cleaner than the $K_L \rightarrow \mu^+ \mu^-$ constraint that was more important in LHS and RHS Z scenarios.
- There is a large hierarchy between real and imaginary parts of the flavour violating couplings implied by anomalies in both Q_6 and Q_8 scenarios. But as seen in (80) and (83) in the case of Q_6 and in (107) and (108) in the case of Q_8 this hierarchy is different unless the ϵ_K anomaly is absent.

Because of a significant difference in the manner QCDP and electroweak penguins enter ε'/ε , there are striking differences in the implications for the correlation between $K^+ \rightarrow \pi^+\nu\bar{\nu}$ and $K_L \rightarrow \pi^0\nu\bar{\nu}$ in these two NP scenarios if significant NP contributions to ε'/ε are required:

- In the case of QCDP scenario the correlation between $\mathcal{B}(K_L \rightarrow \pi^0\nu\bar{\nu})$ and $\mathcal{B}(K^+ \rightarrow \pi^+\nu\bar{\nu})$ takes place along the branch parallel to the GN bound. Moreover, this feature is independent of $M_{Z'}$.
- In the EWP scenario this correlation proceeds away from this branch for diagonal couplings $\mathcal{O}(1)$ if NP in ε_K is present with the departure from this branch increasing with the increased NP effect in ε_K . But with increasing $M_{Z'}$ this branch will be approached although it is reached for $M_{Z'}$ well beyond the LHC scales unless κ_ε is very small. See (117).
- For fixed values of the neutrino and diagonal quark couplings the predicted enhancements of $\mathcal{B}(K_L \rightarrow \pi^0\nu\bar{\nu})$ and $\mathcal{B}(K^+ \rightarrow \pi^+\nu\bar{\nu})$ are much larger when NP in QCDP is required to remove the ε'/ε anomaly. This is simply related to the fact that QCDP operators are less effective in enhancing ε'/ε than EWP operators and consequently the imaginary parts of the flavour violating couplings are required to be larger.
- Finally, a striking difference is the manner in which NP affects ΔM_K in these two scenarios. In QCDP scenario ΔM_K is *suppressed* and this effect increases with increasing $M_{Z'}$ whereas in the EWP scenario ΔM_K is *enhanced* and this effect decreases with increasing $M_{Z'}$ as long as real couplings dominate. Already on the basis of this property one could differentiate between these two scenarios when the SM prediction for ΔM_K improves.

The plots in Figs. 5 and 6 show clearly the differences between QCDP and EWP scenarios.

6 Hybrid Scenarios: Z and Z'

Similar to flavour non-universal Z' couplings to quarks in the flavour basis, leading to flavour-violating Z' couplings to quarks in the mass eigenstate basis, also flavour-violating Z couplings can be generated. As an example in Randall-Sundrum scenario such couplings result from the breakdown of flavour universality of Z couplings to quarks in the flavour basis. But such couplings are also generated in the presence of new heavy fermions with different transformation properties under the SM gauge group than the ordinary quarks and leptons. The mixing of these new fermions with the ordinary fermions generates flavour-violating Z couplings in the mass eigenstate basis. In order to avoid anomalies the most natural here are vector-like fermions.

In the presence of both Z and Z' contributions, independently of the dynamics behind their origin, the formulae for all observables discussed by us can be straightforwardly generalized using the formulae of previous sections. We find then

$$\left(\frac{\varepsilon'}{\varepsilon}\right)_{\text{NP}} = \left(\frac{\varepsilon'}{\varepsilon}\right)_Z + \left(\frac{\varepsilon'}{\varepsilon}\right)_{Z'}. \quad (118)$$

Z contribution is given in the case of the LHS in (31). Z' contribution in the QCDP scenario is given in (79) and the one for EWP in (106).

Similar we have

$$(\varepsilon_K)_{\text{VLL}}^{\text{NP}} = (\varepsilon_K)_{\text{VLL}}^Z + (\varepsilon_K)_{\text{VLL}}^{Z'} \quad (119)$$

with the two contributions given in (35) and (81), respectively. Next

$$\frac{(\Delta M_K)_{\text{VLL}}^{\text{NP}}}{(\Delta M_K)_{\text{exp}}} = \frac{(\Delta M_K)_{\text{VLL}}^Z}{(\Delta M_K)_{\text{exp}}} + \frac{(\Delta M_K)_{\text{VLL}}^{Z'}}{(\Delta M_K)_{\text{exp}}} \quad (120)$$

with Z and Z' contributions given in (36) and (82), respectively.

In the case of $K^+ \rightarrow \pi^+ \nu \bar{\nu}$ and $K_L \rightarrow \pi^0 \nu \bar{\nu}$ we simply have

$$\text{Re } X_{\text{eff}}^{\text{NP}} = \text{Re } X_{\text{eff}}(Z) + \text{Re } X_{\text{eff}}(Z') \quad (121)$$

and

$$\text{Im } X_{\text{eff}}^{\text{NP}} = \text{Im } X_{\text{eff}}(Z) + \text{Im } X_{\text{eff}}(Z'), \quad (122)$$

where different contributions can be found in (183), (184), (186) and (187).

In order to get a rough idea about the relative size of Z and Z' contributions to different observables we assume first that their contributions to ε'/ε and ε_K are related as follows

$$\left(\frac{\varepsilon'}{\varepsilon} \right)_Z = a \left(\frac{\varepsilon'}{\varepsilon} \right)_{Z'}, \quad (\varepsilon_K)_{\text{VLL}}^Z = b (\varepsilon_K)_{\text{VLL}}^{Z'} \quad (123)$$

with a and b being real, positive and $\mathcal{O}(1)$.

Proceeding as in the previous sections we find for Z couplings now

$$\text{Im} \Delta_L^{sd}(Z) = -5.0 \frac{a}{(1+a)} \kappa_{\varepsilon'} \left[\frac{0.76}{B_8^{(3/2)}} \right] \cdot 10^{-7} \quad (124)$$

and

$$\text{Re} \Delta_L^{sd}(Z) = 4.7 \frac{b(1+a)}{a(1+b)} \left[\frac{\kappa_\varepsilon}{\kappa_{\varepsilon'}} \right] \left[\frac{B_8^{(3/2)}}{0.76} \right] \cdot 10^{-5}, \quad (125)$$

which for $a \gg 1$ and $b \gg 1$ reduce to (34) and (37), respectively.

For Z' scenario with QCDP dominance in ε'/ε we find

$$\text{Im} \Delta_L^{sd}(Z') = \frac{2.1}{(1+a)} \left[\frac{\kappa_{\varepsilon'}}{\Delta_R^{q\bar{q}}(Z')} \right] \left[\frac{0.70}{B_6^{(1/2)}} \right] \left[\frac{M_{Z'}}{3 \text{ TeV}} \right]^2 \cdot 10^{-3} \quad (126)$$

and

$$\text{Re} \Delta_L^{sd}(Z') = -1.4 \frac{(1+a)}{(1+b)} \kappa_\varepsilon \left[\frac{\Delta_R^{q\bar{q}}(Z')}{\kappa_{\varepsilon'}} \right] \left[\frac{B_6^{(1/2)}}{0.70} \right] \cdot 10^{-5}, \quad (127)$$

which for $a = b = 0$ reduce to (80) and (83), respectively.

Correspondingly for Z' scenario with EWP dominance in ε'/ε we find

$$\text{Im}\Delta_L^{sd}(Z') = \frac{3.5}{(1+a)} \left[\frac{\kappa_{\varepsilon'}}{\Delta_R^{q\bar{q}}(Z')} \right] \left[\frac{0.76}{B_8^{(3/2)}} \right] \left[\frac{M_{Z'}}{3 \text{ TeV}} \right]^2 \cdot 10^{-5}, \quad (128)$$

$$\text{Re}\Delta_L^{sd}(Z') = -8.2 \frac{(1+a)}{(1+b)} \kappa_\varepsilon \left[\frac{\Delta_R^{q\bar{q}}(Z')}{\kappa_{\varepsilon'}} \right] \left[\frac{B_8^{(3/2)}}{0.76} \right] \cdot 10^{-4}, \quad (129)$$

which reduce for $a = b = 0$ to (107) and (129), respectively.

The comparison of (125) with (38) tells us that b cannot be $\mathcal{O}(1)$ but rather $b \leq 0.05$. We conclude therefore that

- Z' dominates the contribution of NP to ε_K which is consistent with previous general analysis [65].

On the other hand assuming that $a = \mathcal{O}(1)$ the inspection of the formulae for the quantities in (120)-(122) implies the following pattern of Z and Z' contributions.

In the QCDDP scenario:

- NP contribution to ΔM_K is dominated by Z' .
- $\text{Re} X_{\text{eff}}^{\text{NP}}$ is dominated by Z
- $\text{Im} X_{\text{eff}}^{\text{NP}}$ is dominated by Z' .

In the EWP scenario:

- Z and Z' contributions to ΔM_K are of the same order.
- Contributions from Z and Z' to $\text{Re} X_{\text{eff}}^{\text{NP}}$ are of the same order but as they have opposite signs for $\Delta_R^{q\bar{q}}(Z')\Delta_L^{\nu\bar{\nu}}(Z') > 0$ the branching ratio for $K^+ \rightarrow \pi^+\nu\bar{\nu}$ can be enhanced or suppressed if necessary, dependently on the values of parameters involved.
- $\text{Im} X_{\text{eff}}^{\text{NP}}$ is dominated by Z .

Now, in many model constructions the full Z' and Z flavour-violating couplings, both real and imaginary parts, are related by a common real factor so that the ratio of real couplings of Z' and Z equals the ratio of imaginary ones. Imposing this on the couplings obtained above we find the relations between the parameters a and b and knowing already that $b \ll 1$ we can find out the size of a in different scenarios. In the case of QCDDP scenario we obtain

$$a^2 = b \frac{1.4}{(\Delta_R^{q\bar{q}}(Z'))^2} \cdot 10^4 \left[\frac{M_{Z'}}{3 \text{ TeV}} \right]^2 \left[\frac{0.70}{B_6^{(1/2)}} \right]^2 \left[\frac{B_8^{(3/2)}}{0.76} \right]^2, \quad (\text{QCDDP}) \quad (130)$$

and for EWP one

$$a^2 = b \frac{4.0}{(\Delta_R^{q\bar{q}}(Z'))^2} \left[\frac{M_{Z'}}{3 \text{ TeV}} \right]^2. \quad (\text{EWP}) \quad (131)$$

For $b \leq 0.05$ one has then in the QCDDP scenario for Z'

$$a \leq \frac{26.5}{\Delta_R^{q\bar{q}}(Z')} \left[\frac{M_{Z'}}{3 \text{ TeV}} \right], \quad (\text{QCDDP}), \quad (132)$$

where we neglected the difference between $B_6^{(1/2)}$ and $B_8^{(3/2)}$. Evidently, unless the contribution of Z to ε_K is totally negligible, Z generally dominates NP contribution to ε'/ε and therefore Q_8 operator wins over Q_6 as expected already from arguments given at the beginning of our paper. This also implies that now, as opposed to the case of $a = \mathcal{O}(1)$ discussed above, contributions from Z and Z' to $\text{Im } X_{\text{eff}}^{\text{NP}}$ can be for sufficiently large a of the same order. But, as they have opposite signs for $\Delta_L^{\nu\bar{\nu}}(Z') > 0$, the branching ratio for $K_L \rightarrow \pi^0 \nu\bar{\nu}$ can be enhanced or suppressed if necessary, dependently on the values of parameters involved.

On the other hand in EWP scenario both contributions are dominated by Q_8 operator. We find then

$$a \leq \frac{0.45}{\Delta_R^{q\bar{q}}(Z')} \left[\frac{M_{Z'}}{3 \text{ TeV}} \right], \quad (\text{EWP}), \quad (133)$$

so that in this case $a = \mathcal{O}(1)$ and Z contribution to ε'/ε can be comparable to the Z' one. Consequently the pattern of NP effects listed for EWP above applies. Only for very suppressed $\Delta_R^{q\bar{q}}(Z')$ and large $M_{Z'}$ the contribution from Z can again dominate as in QCDDP scenario.

Without a specific model it is not possible to make more concrete predictions but it is clear that the structure of NP contributions is more involved than in previous scenarios. One should also keep in mind that in certain models contributions from loop diagrams could play some role, in particular in models in which vector-like quarks and new heavy scalars are present.

7 Selected Models

7.1 Preliminaries

Here we will briefly describe results in specific models as presented already in the literature. Some of these analyses have to be updated but the pattern of NP effects in the described NP scenarios is known and consistent with pattern found in previous sections.

7.2 Models with Minimal Flavour Violation

The recent analysis of simplified models, in particular those with minimal flavour violation and those with $U(2)^3$ symmetry shows that one should not expect a solution to ε'/ε anomaly from such models [30]. This is also the case of the MSSM with MFV as already analyzed in [79] and NP effects in this scenario must be presently even smaller due to the increase of the supersymmetry scale.

7.3 A Model with a Universal Extra Dimension

In this model NP contribution to ε'/ε depends on only one new parameter: the compactification radius. One finds ε'/ε to be smaller than its SM value independently of the compactification radius [80]. Consequently this model is disfavoured by ε'/ε and there is no need to discuss its implications for other observables.

7.4 Littlest Higgs Model with T-Parity

In this model NP contributions to $K^+ \rightarrow \pi^+\nu\bar{\nu}$, $K_L \rightarrow \pi^0\nu\bar{\nu}$ and ε'/ε are governed by EWP and in particular the ones in ε'/ε by the operator Q_8 . The model has the same operator structure as the SM and FCNC processes appear first at one loop level. But effectively for these three observables the model has the structure of Z LH scenario with the coupling $\Delta_L^{sd}(Z)$ resulting from one-loop contributions involving new fermions and gauge bosons. Moreover NP contributions to ε_K are governed by new box diagrams. Consequently the correlation with between $K^+ \rightarrow \pi^+\nu\bar{\nu}$, $K_L \rightarrow \pi^0\nu\bar{\nu}$, ε'/ε is more involved than in simple models discussed by us. But the anticorrelation between ε'/ε and $K_L \rightarrow \pi^0\nu\bar{\nu}$ is also valid here.

The most recent analysis in [31] shows that

- The LHT model agrees well with the data on $\Delta F = 2$ observables and is capable of removing some slight tensions between the SM predictions and the data. In particular ε_K can be enhanced.
- If ε'/ε constraint is ignored the most interesting departures from SM predictions can be found for $K^+ \rightarrow \pi^+\nu\bar{\nu}$ and $K_L \rightarrow \pi^0\nu\bar{\nu}$ decays. An enhancement of the branching ratio for $K^+ \rightarrow \pi^+\nu\bar{\nu}$ by a factor of two relative to the SM prediction is still possible. An even larger enhancement in the case of $K_L \rightarrow \pi^0\nu\bar{\nu}$ is allowed. But as expected from the properties of Z LH scenario of Section 4.2, when the ε'/ε constraint is taken into account the necessary enhancement of ε'/ε requires rather strong suppression of $K_L \rightarrow \pi^0\nu\bar{\nu}$. On the other hand significant shifts of $K^+ \rightarrow \pi^+\nu\bar{\nu}$ with respect to SM are then no longer allowed. Figs. 6 and 7 in [31] show this behaviour in a spectacular manner.

7.5 331 Models

The 331 models are based on the gauge group $SU(3)_C \times SU(3)_L \times U(1)_X$. In these models new contributions to ε'/ε and other flavour observables are dominated by tree-level exchanges of a Z' with non-negligible contributions from tree-level Z exchanges generated through the $Z - Z'$ mixing. The size of these NP effects depends not only on $M_{Z'}$ but in particular on a parameter β , which distinguishes between various 331 models, on fermion representations under the gauge group and a parameter $\tan\bar{\beta}$ present in the $Z - Z'$ mixing [77]. The ranges of these parameters are restricted by electroweak precision tests and flavour data, in particular from B physics. A recent updated analysis has been presented in [78].

The model belongs to the class of Z' models with LH flavour-violating couplings with only a small effect from $Z - Z'$ mixing in ε'/ε that is dominated by the operator Q_8 . But,

in contrast to the general case analyzed in Section 5.6, the diagonal couplings are known in a given 331 model as functions of β . The new analysis in [78] shows that the impact of a required enhancement of ε'/ε on other flavour observables is significant. The main findings of [78] for $M_{Z'} = 3 \text{ TeV}$ are as follows:

- Among seven 331 models singled out in [77] through electroweak precision study only three can provide significant shift of ε'/ε but for $M_{Z'} = 3 \text{ TeV}$ not larger than 6×10^{-4} , that is $\kappa_{\varepsilon'} \leq 0.6$.
- Two of them can simultaneously suppress $B_s \rightarrow \mu^+ \mu^-$ but do not offer the explanation of the suppression of the Wilson coefficient C_9 in $B \rightarrow K^* \mu^+ \mu^-$ (the so-called LHCb anomaly).
- On the contrary the third model offers partial explanation of this anomaly simultaneously enhancing ε'/ε but does not provide suppression of $B_s \rightarrow \mu^+ \mu^-$ which could be required when the data improves and the inclusive value of $|V_{cb}|$ will be favoured.
- NP effects in $K^+ \rightarrow \pi^+ \nu \bar{\nu}$, $K_L \rightarrow \pi^0 \nu \bar{\nu}$ and $B \rightarrow K(K^*) \nu \bar{\nu}$ are found to be small. This could be challenged by NA62, KOPIO and Belle II experiments in this decade.

Interestingly, the special flavour structure of 331 models implies that even for $M_{Z'} = 30 \text{ TeV}$ a shift of ε'/ε up to 8×10^{-4} and a significant shift in ε_K can be obtained, while the effects in other flavour observables are small. This makes these models appealing in view of the possibility of accessing masses of $M_{Z'}$ far beyond the LHC reach. The increase in the maximal shift in ε'/ε is caused by RG effects summarized in Table 5. But for $M_{Z'} > 30 \text{ TeV}$ the ΔM_K constraint becomes important and NP effects in ε'/ε decrease as $1/M_{Z'}$.

7.6 More Complicated Models

Clearly there are other possibilities involving new operators. In particular it has been pointed out that in general supersymmetric models ε'/ε can receive important contributions from chromomagnetic penguin operators [81, 82]. In fact in 1999 this contribution could alone be responsible for experimental value of ε'/ε subject to very large uncertainties of the relevant hadronic matrix element. This assumed the masses of squarks and gluinos in the ballpark of 500 GeV. With the present lower bounds on these masses in the ballpark of few TeV, it is unlikely that these operators can still provide a significant contribution to ε'/ε when all constraints from other observables are taken into account. Similar comments apply to other models like the one in [83], Randall-Sundrum models [84] and left-right symmetric models [85], where in the past ε'/ε could receive important contributions from chromomagnetic penguins. It would be interesting to update such analyses, in particular when the value of $B_6^{(1/2)}$ and the hadronic matrix elements of chromomagnetic penguins will be better known.

8 New Physics in $\text{Re}A_0$ and $\text{Re}A_2$

The calculations of $K \rightarrow \pi\pi$ isospin amplitudes $\text{Re}A_0$ and $\text{Re}A_2$ within the SM, related to the $\Delta I = 1/2$ rule in (4) have been the subject of many efforts in the last 40 years. Some aspects of these efforts have been recalled in [16]. Here we only note that both the dual approach to QCD [16] and lattice approach [3] obtain satisfactory results for the amplitude $\text{Re}A_2$ within the SM leaving there only small room for NP contributions.

On the other hand, whereas in the large N approach one finds [16]

$$\left(\frac{\text{Re}A_0}{\text{Re}A_2}\right)_{\text{dual QCD}} = 16.0 \pm 1.5, \quad (134)$$

the most recent result from the RBC-UKQCD collaboration reads [4]

$$\left(\frac{\text{Re}A_0}{\text{Re}A_2}\right)_{\text{lattice QCD}} = 31.0 \pm 6.6. \quad (135)$$

Due to large error in the lattice result, both results are compatible with each other and both signal that this rule follows dominantly from the QCD dynamics related to current-current operators. In addition both leave room for sizable NP contributions. But, from the present perspective only lattice simulations can provide precise value of $\text{Re}A_0$ one day, so that we will know whether some part of this rule at the level of (20–30)%, as signalled by the result in (134), originates in NP contributions.

This issue has been addressed in [27], where it has been demonstrated that a QCDP generated by a heavy Z' and in particular a heavy G' in the reach of the LHC could be responsible for the missing piece in $\text{Re}A_0$ in (134) but this requires a very large fine-tuning of parameters in order to satisfy the experimental bounds from ΔM_K and ε_K even in the absence of the ε'/ε anomaly, which was unknown at the time of the publication in [27].

The point is that a sizable contribution of Q_6 operator to $\text{Re}A_0$ requires $\text{Re}\Delta_L^{sd}(Z') = \mathcal{O}(1)$ which as stressed in [27] violates ΔM_K by many orders of magnitude if only LH flavour-violating currents are considered. In the presence of ε'/ε anomaly, which requires $\text{Im}\Delta_L^{sd}(Z') = \mathcal{O}(10^{-3})$ the results of previous sections show that also ε_K constraint is then violated by several orders of magnitude.

The only possible solution is the introduction of both LH and RH flavour violating currents with real and imaginary parts of both currents properly chosen so that both ΔM_K and ε_K constraints are satisfied and significant contribution to $\text{Re}A_0$ is obtained. The ε'/ε anomaly provides additional constraint but as seen in Fig. 4 of [27] in the case of Z' scenario and in Section 6 of that paper in the case of G' scenario, satisfactory results for $\text{Re}A_0$, ε'/ε , ε_K and ΔM_K can be obtained. But it should be kept in mind that such a solution requires very high fine-tuning of parameters and on the basis of the analysis in [27] the central value of lattice result in (135) is too far away from the data that one could attribute this difference to any NP.

In summary, the future precise lattice calculations will hopefully tell us whether there is some NP contributing significantly to $\text{Re}A_0$. This would enrich the present analysis as one would have, together with $\text{Re}A_2$, two additional constraints. But on the basis of [27] it is rather unlikely that this NP is represented by heavy Z' or G' unless the nature allows for very high fine-tunings.

9 2018 Visions

With all these results at hand we can dream about the discovery of NP in $K^+ \rightarrow \pi^+ \nu \bar{\nu}$ by the NA62 experiment:

$$\mathcal{B}(K^+ \rightarrow \pi^+ \nu \bar{\nu}) = (18.0 \pm 2.0) \cdot 10^{-11}, \quad (\text{NA62, 2018}). \quad (136)$$

Indeed, looking at the grey bands in several figures presented by us, such a result would be truly tantalizing with a big impact on our field.

We will next assume that the lattice values of $B_6^{(1/2)}$ and $B_8^{(3/2)}$ will be close to our central values

$$B_6^{(1/2)} \approx 0.70, \quad B_8^{(3/2)} \approx 0.76, \quad (137)$$

and that the CKM parameters are such that $\kappa_{\varepsilon'} \approx 1.0$ will be required.

Concerning ε_K we will consider two scenarios, one with $\kappa_\varepsilon = 0.4$ and the other with $\kappa_\varepsilon = 0$, that is no ε_K anomaly.

9.1 $\kappa_{\varepsilon'} = 1.0$ and $\kappa_\varepsilon = 0.4$

Inspecting the results of previous sections, we conclude the following

- Z scenarios with only LH and RH couplings will be ruled out as they cannot accommodate ε_K anomaly with $\kappa_\varepsilon = 0.4$ unless at one loop level in the presence of new heavy fermions or scalars significant contributions to ε_K would be generated. Then in principle the rates for $K^+ \rightarrow \pi^+ \nu \bar{\nu}$ in LHS and RHS could be made consistent with the result in (136).
- It is clearly much easier to reproduce the data in the general Z scenario. In fact as seen in Fig. 4 both examples presented by us could accommodate the result in (136), explain simultaneously ε'/ε and ε_K anomalies and predict an enhancement of $\mathcal{B}(K_L \rightarrow \pi^0 \nu \bar{\nu})$ by a factor of two to three in the first example and by an order of magnitude in the second example.
- As seen in Fig. 5 the QCDP generated by Z' can reproduce the result in (136) for $\Delta_L^{\nu \bar{\nu}}(Z') = 0.5$ and $\kappa_{\varepsilon'} = 1.0$. This then implies the enhancement of the rate for $K_L \rightarrow \pi^0 \nu \bar{\nu}$ by a factor of 15 – 20: good news for KOPIO. Moreover, ε_K can be made consistent with the data independently of $\kappa_{\varepsilon'}$.
- Interestingly, as seen in Fig. 6, EWP generated by Z' will not be able to explain the result in (136) unless the coupling $\Delta_R^{q\bar{q}}(Z')$ is very strongly suppressed below unity. Also NP effects in $K_L \rightarrow \pi^0 \nu \bar{\nu}$ are predicted to be small.

9.2 $\kappa_{\varepsilon'} = 1.0$ and $\kappa_\varepsilon = 0.0$

If ε_K can be explained within the SM the main modification relative to the case of $\kappa_\varepsilon \neq 0$ is that in all scenarios the correlation between $K_L \rightarrow \pi^0 \nu \bar{\nu}$ and $K^+ \rightarrow \pi^+ \nu \bar{\nu}$ takes place on the branch parallel to GN bound in strict correlation with ε'/ε or equivalently $\kappa_{\varepsilon'}$. Yet, there are differences between various scenarios:

- Z scenarios with only LH or RH currents and EWP(Z') scenario with $\Delta_R^{q\bar{q}} = \mathcal{O}(1)$ imply SM-like values for $\mathcal{B}(K^+ \rightarrow \pi^+\nu\bar{\nu})$, far below the result in (136).
- For QCDP(Z') nothing changes relative to the previous case and interesting results for both rare decay branching ratios can be obtained. Also the general Z case can work in view of sufficient number of free parameters. EWP scenario can also work provided $\Delta_R^{q\bar{q}}(Z')$ is very strongly suppressed below unity.

In summary we observe that a NA62 measurement of $\mathcal{B}(K^+ \rightarrow \pi^+\nu\bar{\nu})$ in the ballpark of the result in (136) will be able to make reduction of possibilities with the simplest scenario being QCDP generated through a tree-level Z' exchange. But then the crucial question will be what is the value of ΔM_K in the SM.

10 Outlook and Open Questions

Our general analysis of ε'/ε and ε_K in models with tree-level flavour-violating Z and Z' exchanges shows that such dynamics could be responsible for the observed ε'/ε anomaly with interesting implications for other flavour observables in the K meson system. In particular it could shed some light on NP in ε_K and ΔM_K . Our results are summarized in numerous plots and two tables which show that the inclusion of other observables can clearly distinguish between various possibilities.

Except for the case of Z scenarios with only left-handed (LHS) and right-handed (RHS) flavour violating currents, where $K_L \rightarrow \mu^+\mu^-$ bound was the most important constraint on the real parts of flavour violating couplings, in the remaining scenarios the pattern of flavour violation was governed in the large part of the parameter space entirely by CP-violating quantities: ε'/ε and ε_K . NP effects in them were described by two parameters $\kappa_{\varepsilon'}$ and κ_{ε} as defined in (18) and (19).

In LH and RH Z' scenarios the role of ε'/ε was to determine imaginary parts of flavour violating Z' couplings. Having them, the role of ε_K was to determine the real parts of these couplings. These then had clear implications for other observables, in particular for the branching ratios for $K^+ \rightarrow \pi^+\nu\bar{\nu}$ and $K_L \rightarrow \pi^0\nu\bar{\nu}$ and for ΔM_K . The case of general scenarios with LH and RH couplings is more involved but also here we could get a picture what is going on.

From our point of view the most interesting results of this work are as follows:

- In LH and RH Z scenarios the enhancement of ε'/ε implies uniquely suppression of $K_L \rightarrow \pi^0\nu\bar{\nu}$. Moreover, NP effects in ε_K and ΔM_K are very small.
- Simultaneous enhancements of ε'/ε , ε_K and of the branching ratios for $K^+ \rightarrow \pi^+\nu\bar{\nu}$ and $K_L \rightarrow \pi^0\nu\bar{\nu}$ in Z scenarios are only possible in the presence of both LH and RH flavour violating couplings. As far as ε'/ε and $K_L \rightarrow \pi^0\nu\bar{\nu}$ are concerned this finding has already been reported in [30] but our new analysis summarized in Figs. 2-4 extended this case significantly.
- If the enhancement of ε'/ε in Z' scenarios is governed by QCDP operator Q_6 , the branching ratios for $K_L \rightarrow \pi^0\nu\bar{\nu}$ and $K^+ \rightarrow \pi^+\nu\bar{\nu}$ are strictly correlated, as seen in Fig. 5, along the branch parallel to the GN bound. They can be both enhanced

or suppressed dependently on the signs of diagonal quark and neutrino couplings that are relevant for ε'/ε and these rare decays, respectively. Various possibilities are summarized in Table 3. There we see that in these scenarios ΔM_K is uniquely *suppressed* relative to its SM value. This is directly related to the dominance of *imaginary* parts of flavour violating couplings necessary to provide sufficient enhancement of ε'/ε . The suppression of ΔM_K could turn out to be a challenge for this scenario implying possibly an upper bound on $\kappa_{\varepsilon'}$ as we stressed in Section 5.8 and illustrated in Fig. 5 and in particular in Fig. 7. On the other hand the role of ε_K is smaller, even if solution to possible tensions there are offered.

- But two messages on QCDP scenario from our analysis are clear. If $\mathcal{B}(K^+ \rightarrow \pi^+ \nu \bar{\nu})$ will turn out one day to be enhanced by NP relative to the SM prediction and $\mathcal{B}(K_L \rightarrow \pi^0 \nu \bar{\nu})$ suppressed or vice versa, the QCDP scenario will not be able to describe it. This is also the case when ΔM_K in the SM will be found below its experimental value.
- Rather different pattern of the implications of the ε'/ε anomaly are found in Z' scenarios in which the enhancement of ε'/ε is governed by EWP operator Q_8 . In particular the correlation between $K^+ \rightarrow \pi^+ \nu \bar{\nu}$ and $K_L \rightarrow \pi^0 \nu \bar{\nu}$ depends on the size and the sign of NP contribution to ε_K which was not the case of QCDP scenario. Moreover, as seen in Fig. 6, the structure of this correlation is very different from the one in Fig. 5, although also in this case, for $\kappa_\varepsilon > 0$, both branching ratios are enhanced with respect their SM values. They can also be simultaneously suppressed for different signs of diagonal quark and neutrino couplings. Various possibilities are summarized in Table 4.
- But as we emphasized and shown in this table, for $\kappa_\varepsilon < 0$ in the EWP scenario, the enhancement of $K^+ \rightarrow \pi^+ \nu \bar{\nu}$ implies simultaneous suppression of $K_L \rightarrow \pi^0 \nu \bar{\nu}$ or vice versa which is not possible in the QCDP scenario. Moreover, in this scenario ΔM_K is uniquely *enhanced* relative to its SM value. This is directly related to the dominance of the *real* parts of flavour violating couplings necessary to provide sufficient contribution to ε_K in the presence of an enhancement of ε'/ε . But, as opposed to the QCDP case, this NP effect is small.

These results show that a good knowledge of ΔM_K within the SM would help a lot in distinguishing between QCDP and EWP scenarios. Presently the uncertainties in ΔM_K from both perturbative contributions [74] and long distance calculations both within large N approach [16] and lattice simulations [75] are too large to be able to conclude whether positive or negative shift, if any, in ΔM_K from NP is favoured.

The dominant part of our Z' study concerned $M_{Z'}$ in the reach of the LHC but as we demonstrated in Section 5.8, ε'/ε will give us an insight into short distance dynamics even if Z' cannot be seen by ATLAS and CMS experiments. We also restricted our study to the K meson system. In concrete models there are correlations between observables in K meson system and other meson systems. An example are models with minimal flavour violation. But as shown in [30], in such models NP effects in ε'/ε , ε_K , $K^+ \rightarrow \pi^+ \nu \bar{\nu}$ and $K_L \rightarrow \pi^0 \nu \bar{\nu}$ are small. Larger effects can be obtained in LHT and 331 models for which the most recent analyses can be found in [31] and [78], respectively.

There is no doubt that in the coming years K meson physics will strike back, in particular through improved estimates of SM predictions for ε'/ε , ε_K , ΔM_K and $K_L \rightarrow \mu^+\mu^-$ and through crucial measurements of the branching ratios for $K^+ \rightarrow \pi^+\nu\bar{\nu}$ and $K_L \rightarrow \pi^0\nu\bar{\nu}$. Correlations with other meson systems, lepton flavour physics, electric dipole moments and other rare processes should allow us to identify NP at very short distance scales [28] and we should hope that this physics will also be directly seen at the LHC.

Let us then end our paper by listing most pressing questions for the coming years. On the theoretical side we have:

- **What is the value of $\kappa_{\varepsilon'}$?** Here the answer will come not only from lattice QCD but also through improved values of the CKM parameters, NNLO QCD corrections and an improved understanding of FSI and isospin breaking effects. The NNLO QCD corrections should be available soon. The recent analysis in the large N approach in [17] indicates that FSI are likely to be important for the $\Delta I = 1/2$ rule in agreement with previous studies [10–15], but much less relevant for ε'/ε .
- **What is the value of κ_ε ?** Here the reduction of CKM uncertainties is most important. But the most recent analysis in [61] indicates that if no NP is present in ε_K , it is expected to be found in $\Delta M_{s,d}$.
- **What is the value of ΔM_K in the SM?** Here lattice QCD should provide useful answers.
- **What are the precise values of $\text{Re}A_2$ and $\text{Re}A_0$?** Again lattice QCD will play the crucial role here.

On the experimental side we have:

- **What is $\mathcal{B}(K^+ \rightarrow \pi^+\nu\bar{\nu})$ from NA62?** We should know it in 2018.
- **What is $\mathcal{B}(K_L \rightarrow \pi^0\nu\bar{\nu})$ from KOPIO?** We should know it around the year 2020.
- **Do Z' , G' or other new particles with masses in the reach of the LHC exist?** We could know it already this year.

Definitely there are exciting times ahead of us!

Acknowledgements

First of all I would like to thank Robert Buras-Schnell for a very careful and critical reading of the manuscript and decisive help in numerical calculations, in particular for constructing all the plots present in this paper. I thank Jean-Marc Gérard for illuminating discussions. The collaboration with Fulvia De Fazio on ε'/ε in the context of 331 models and brief discussions with Christoph Bobeth are also highly appreciated. This research was done and financed in the context of the ERC Advanced Grant project “FLAVOUR” (267104) and was partially supported by the DFG cluster of excellence “Origin and Structure of the Universe”.

A More Information on Renormalization Group Evolution

A.1 QCD Penguins

We follow here [27] and consider first the case of Z' with flavour universal diagonal quark couplings. In this case the QCDP Q_5 and Q_6 have to be considered. The mixing with other operators is neglected and we work in LO approximation.

Denoting then by $\vec{C}(M_{Z'})$ the column vector with components given by the Wilson coefficients C_5 and C_6 at $\mu = M_{Z'}$ we find their values at $\mu = m_c$ by means of

$$\vec{C}(m_c) = \hat{U}(m_c, M_{Z'})\vec{C}(M_{Z'}) \quad (138)$$

where

$$\hat{U}(m_c, M_{Z'}) = \hat{U}^{(f=4)}(m_c, m_b)\hat{U}^{(f=5)}(m_b, m_t)\hat{U}^{(f=6)}(m_t, M_{Z'}) \quad (139)$$

and [86]

$$\hat{U}^{(f)}(\mu_1, \mu_2) = \hat{V} \left(\begin{bmatrix} \alpha_s(\mu_2) \\ \alpha_s(\mu_1) \end{bmatrix}^{\frac{\bar{\gamma}^{(0)}}{2\beta_0}} \right) \hat{V}^{-1}. \quad (140)$$

The relevant 2×2 one-loop anomalous dimension matrix in the basis (Q_5, Q_6) can be extracted from the known 6×6 matrix [87] and is given as follows

$$\hat{\gamma}_s(\alpha_s) = \hat{\gamma}_s^{(0)} \frac{\alpha_s}{4\pi}, \quad \hat{\gamma}_s^{(0)} = \begin{pmatrix} 2 & -6 \\ -f\frac{2}{9} & -16 + f\frac{2}{3} \end{pmatrix} \quad (141)$$

with f being the number of quark flavours.

The matrix \hat{V} diagonalizes $\hat{\gamma}^{(0)T}$

$$\hat{\gamma}_D^{(0)} = \hat{V}^{-1}\hat{\gamma}^{(0)T}\hat{V}, \quad (142)$$

$\bar{\gamma}^{(0)}$ is the vector containing the diagonal elements of the diagonal matrix :

$$\hat{\gamma}_D^{(0)} = \begin{pmatrix} \gamma_+^{(0)} & 0 \\ 0 & \gamma_-^{(0)} \end{pmatrix} \quad (143)$$

and

$$\beta_0 = \frac{33 - 2f}{3}. \quad (144)$$

For $\alpha_s(M_Z) = 0.1185$, $m_c = 1.3 \text{ GeV}$ and $M_{Z'} = 3 \text{ TeV}$ we have

$$\begin{bmatrix} C_5(m_c) \\ C_6(m_c) \end{bmatrix} = \begin{bmatrix} 0.86 & 0.19 \\ 1.13 & 3.60 \end{bmatrix} \begin{bmatrix} 1 \\ 0 \end{bmatrix} \frac{\Delta_L^{sd}(Z')\Delta_R^{qq}(Z')}{4M_{Z'}^2}. \quad (145)$$

Consequently

$$C_5(m_c) = 0.86 \frac{\Delta_L^{sd}(Z')\Delta_R^{qq}(Z')}{4M_{Z'}^2}, \quad C_6(m_c) = 1.13 \frac{\Delta_L^{sd}(Z')\Delta_R^{qq}(Z')}{4M_{Z'}^2}. \quad (146)$$

Due to the large element (1, 2) in the matrix (141) and the large anomalous dimension of the Q_6 operator represented by the (2, 2) element of this matrix, $C_6(m_c)$ is by a factor of 1.3 larger than $C_5(m_c)$ even if $C_6(M_{Z'})$ vanishes at LO. Moreover the matrix element $\langle Q_5 \rangle_0$ is strongly colour suppressed [9] which is not the case of $\langle Q_6 \rangle_0$ and within a good approximation we can neglect the contribution of Q_5 . In the case of (Q'_5, Q'_6) the formulae remain unchanged except that the value of $C'_5(M_{Z'})$ differs from $C_5(M_{Z'})$.

In the case of G' the initial conditions for the Wilson coefficients C_5 and C_6 at $\mu = M_{G'}$ are modified and given in (98) and (99). One finds then

$$\begin{bmatrix} C_5(m_c) \\ C_6(m_c) \end{bmatrix} = \begin{bmatrix} 0.86 & 0.19 \\ 1.13 & 3.60 \end{bmatrix} \begin{bmatrix} -1/6 \\ 1/2 \end{bmatrix} \frac{\Delta_L^{sd}(G') \Delta_R^{qq}(G')}{4M_{G'}^2}. \quad (147)$$

Consequently instead of (146) one has

$$C_5(m_c) = -0.05 \frac{\Delta_L^{sd}(G') \Delta_R^{qq}(G')}{4M_{G'}^2}, \quad C_6(m_c) = 1.61 \frac{\Delta_L^{sd}(G') \Delta_R^{qq}(G')}{4M_{G'}^2} \quad (148)$$

so that now Q_6 operator is even more dominant over Q_5 than in the Z' scenario.

A.2 Electroweak Penguins

The basic equation for the RG evolution can also be used for Z models except that

$$\vec{C}(m_c) = \hat{U}(m_c, M_Z) \vec{C}(M_Z) \quad (149)$$

where

$$\hat{U}(m_c, M_Z) = \hat{U}^{(f=4)}(m_c, m_b) \hat{U}^{(f=5)}(m_b, M_Z) \quad (150)$$

and the relevant one-loop anomalous dimension matrix in the (Q_7, Q_8) basis is very similar to the one in (141)

$$\hat{\gamma}_s^{(0)} = \begin{pmatrix} 2 & -6 \\ 0 & -16 \end{pmatrix}. \quad (151)$$

Performing the renormalization group evolution from M_Z to $m_c = 1.3 \text{ GeV}$ we find [27]

$$C_7(m_c) = 0.87 C_7(M_Z) \quad C_8(m_c) = 0.76 C_7(M_Z). \quad (152)$$

Due to the large element (1, 2) in the matrix (151) and the large anomalous dimension of the Q_8 operator represented by the (2, 2) element in (151), the two coefficients are comparable in size. But the matrix element $\langle Q_7 \rangle_2$ is colour suppressed which is not the case of $\langle Q_8 \rangle_2$ and within a good approximation we can neglect the contributions of Q_7 . In the case of (Q'_7, Q'_8) the formulae remain unchanged except that the value of $C'_7(M_Z)$ differs from $C_7(M_Z)$.

If a Z' model has such flavour diagonal couplings that at the end only the operators (Q_7, Q_8) or (Q'_7, Q'_8) have to be considered, additional evolution from M_Z to $M_{Z'}$ has to be performed as in (139) but the anomalous dimension matrix is as given in (151). One finds then for $\alpha_s(M_Z) = 0.1185$, $m_c = 1.3 \text{ GeV}$ and $M_{Z'} = 3 \text{ TeV}$ [77]

$$C_8(m_c) = 1.35 C_7(M_{Z'}) \quad (153)$$

with 1.35 being RG factor. The longer RG evolution than in the case of Z made this factor larger.

A.3 Beyond the LHC Scales

In the case of Z' we define for arbitrary $M_{Z'}$ the factors r_{65} and r_{87} by

$$C_6(m_c) = r_{65} C_5(M_{Z'}), \quad C_8(m_c) = r_{87} C_7(M_{Z'}). \quad (154)$$

In the case of G' we define the corresponding factor through

$$C_6(m_c) = r_{G'} \frac{\Delta_L^{sd}(G') \Delta_R^{qq}(G')}{4M_{G'}^2}. \quad (155)$$

All these factors increase with increasing $M_{Z'}$. We show this dependence in Table 5⁸.

$M_{Z'}$	3 TeV	6 TeV	10 TeV	20 TeV	50 TeV	100 TeV
r_{65}	1.13	1.22	1.28	1.37	1.48	1.56
r_{87}	1.35	1.48	1.56	1.69	1.85	1.97
$r_{G'}$	1.61	1.70	1.77	1.85	1.96	2.05

Table 5: The $M_{Z'}(M_{G'})$ dependence of the RG factors r_{65} , r_{87} and $r_{G'}$ at LO with two-loop running of α_s .

B ε_K and ΔM_K

B.1 General Formulae

For the CP-violating parameter ε_K and ΔM_K we have respectively

$$\varepsilon_K = \frac{\tilde{\kappa}_\varepsilon e^{i\varphi_\varepsilon}}{\sqrt{2}(\Delta M_K)_{\text{exp}}} [\text{Im}(M_{12}^K)] \equiv e^{i\varphi_\varepsilon} [\varepsilon_K^{\text{SM}} + \varepsilon_K^{\text{NP}}], \quad (156)$$

$$\Delta M_K = 2\text{Re}(M_{12}^K) = (\Delta M_K)^{\text{SM}} + (\Delta M_K)^{\text{NP}} \quad (157)$$

where $\varphi_\varepsilon = (43.51 \pm 0.05)^\circ$ and $\tilde{\kappa}_\varepsilon = 0.94 \pm 0.02$ [42, 43] takes into account that $\varphi_\varepsilon \neq \frac{\pi}{4}$ and includes long distance effects in $\text{Im}(\Gamma_{12})$ and $\text{Im}(M_{12})$. We have separated the overall phase factor so that $\varepsilon_K^{\text{SM}}$ and $\varepsilon_K^{\text{NP}}$ are real quantities with $\varepsilon_K^{\text{NP}}$ representing NP contributions.

Generally we can write

$$M_{12}^K = [M_{12}^K]_{\text{SM}} + [M_{12}^K]_{\text{NP}}, \quad (158)$$

where the first term is the SM contribution for which the explicit expression can be found e.g. in [28]. We decompose the NP part as follows

$$[M_{12}^K]_{\text{NP}} = [M_{12}^K]_{\text{VLL}} + [M_{12}^K]_{\text{VRR}} + [M_{12}^K]_{\text{LR}}. \quad (159)$$

The first two contributions come from the operators

$$Q_1^{\text{VLL}} = (\bar{s}\gamma_\mu P_L d) (\bar{s}\gamma^\mu P_L d), \quad Q_1^{\text{VRR}} = (\bar{s}\gamma_\mu P_R d) (\bar{s}\gamma^\mu P_R d) \quad (160)$$

and the last one from

$$Q_1^{\text{LR}} = (\bar{s}\gamma_\mu P_L d) (\bar{s}\gamma^\mu P_R d), \quad Q_2^{\text{LR}} = (\bar{s}P_L d) (\bar{s}P_R d). \quad (161)$$

⁸We thank Christoph Bobeth for checking this table.

B.2 Z and Z' Cases

Using formulae in [65] we find then in the case of tree-level Z contribution

$$[M_{12}^{K1*}]_{\text{VLL}} = \frac{1}{6} F_K^2 \hat{B}_K m_K \eta_2 \tilde{r} \left[\frac{\Delta_L^{sd}(Z)}{M_Z} \right]^2 \quad (162)$$

where

$$\eta_2 = 0.576, \quad \tilde{r} \approx 1.068, \quad \hat{B}_K \approx 0.75. \quad (163)$$

For VRR one should just replace L by R. We emphasize the complex conjugation in this formula.

For the LR contribution we simply have

$$[M_{12}^{K1*}]_{\text{LR}} = \frac{\Delta_L^{sd}(Z) \Delta_R^{sd}(Z)}{M_Z^2} \langle \hat{Q}_1^{\text{LR}}(M_Z) \rangle^{sd} \quad (164)$$

where using the technology of [69, 88] we have expressed the amplitude in terms of the renormalisation scheme independent matrix element

$$\langle \hat{Q}_1^{\text{LR}}(M_Z) \rangle^{sd} = \langle Q_1^{\text{LR}}(M_Z) \rangle^{sd} \left(1 - \frac{1}{6} \frac{\alpha_s(M_Z)}{4\pi} \right) - \frac{\alpha_s(M_Z)}{4\pi} \langle Q_2^{\text{LR}}(M_Z) \rangle^{sd}. \quad (165)$$

On the basis of [89–91] one finds for M_Z and $M_{Z'} = 3 \text{ TeV}$

$$\langle \hat{Q}_1^{\text{LR}}(M_Z) \rangle^{sd} \approx -0.09 \text{ GeV}^3, \quad \langle \hat{Q}_1^{\text{LR}}(M_{Z'}) \rangle^{sd} \approx -0.16 \text{ GeV}^3. \quad (166)$$

This matrix element increases with increasing $M_{Z'}$. See Table 5 in [70].

For ε_K and ΔM_K , inserting relevant contributions to M_{12} into (156) and (157), we get then in the case of Z

$$\varepsilon_K^{\text{NP}} = -4.26 \cdot 10^7 [\text{Im} \Delta_L^{sd}(Z) \text{Re} \Delta_L^{sd}(Z) + \text{Im} \Delta_R^{sd}(Z) \text{Re} \Delta_R^{sd}(Z)] + (\varepsilon_K)_{\text{LR}}^Z \quad (167)$$

with

$$(\varepsilon_K)_{\text{LR}}^Z = 2.07 \cdot 10^9 [\text{Im} \Delta_L^{sd}(Z) \text{Re} \Delta_R^{sd}(Z) + \text{Im} \Delta_R^{sd}(Z) \text{Re} \Delta_L^{sd}(Z)] \quad (168)$$

and

$$\frac{(\Delta M_K)_{\text{LR}}^{\text{NP}}}{(\Delta M_K)_{\text{exp}}} = 6.43 \cdot 10^7 \sum_{P=L,R} [(\text{Re} \Delta_P^{sd}(Z))^2 - (\text{Im} \Delta_P^{sd}(Z))^2] + \frac{(\Delta M_K)_{\text{LR}}^Z}{(\Delta M_K)_{\text{exp}}} \quad (169)$$

with

$$\frac{(\Delta M_K)_{\text{LR}}^Z}{(\Delta M_K)_{\text{exp}}} = -6.21 \cdot 10^9 [\text{Re} \Delta_L^{sd}(Z) \text{Re} \Delta_R^{sd}(Z) - \text{Im} \Delta_L^{sd}(Z) \text{Im} \Delta_R^{sd}(Z)]. \quad (170)$$

The fact that the LR contributions in these expressions have opposite sign to the ones from VLL and VRR operators is related to the opposite signs in the relevant hadronic matrix elements.

For the Z' tree-level exchanges, M_Z should be replaced by $M_{Z'}$, in VLL and VRR contributions $\tilde{r} = 0.95$ should be used and in LR contribution the value of the matrix element $\langle \hat{Q}_1^{\text{LR}} \rangle$ in (166). See Section 5 for explicit formulae.

C $K^+ \rightarrow \pi^+ \nu \bar{\nu}$ and $K_L \rightarrow \pi^0 \nu \bar{\nu}$

C.1 General Formulae

The branching ratios for $K^+ \rightarrow \pi^+ \nu \bar{\nu}$ and $K_L \rightarrow \pi^0 \nu \bar{\nu}$ in any extension of the SM in which light neutrinos couple only to left-handed currents are given as follows

$$\mathcal{B}(K^+ \rightarrow \pi^+ \nu \bar{\nu}) = \kappa_+ \cdot \left[\left(\frac{\text{Im } X_{\text{eff}}}{\lambda^5} \right)^2 + \left(\frac{\text{Re } \lambda_c}{\lambda} P_c(X) + \frac{\text{Re } X_{\text{eff}}}{\lambda^5} \right)^2 \right], \quad (171)$$

$$\mathcal{B}(K_L \rightarrow \pi^0 \nu \bar{\nu}) = \kappa_L \cdot \left(\frac{\text{Im } X_{\text{eff}}}{\lambda^5} \right)^2, \quad (172)$$

where $\lambda = |V_{us}|$ and [92]

$$\kappa_+ = (5.173 \pm 0.025) \cdot 10^{-11} \left[\frac{\lambda}{0.225} \right]^8, \quad \kappa_L = (2.231 \pm 0.013) \cdot 10^{-10} \left[\frac{\lambda}{0.225} \right]^8. \quad (173)$$

For the charm contribution, represented by $P_c(X)$, the calculations in [92–96] imply [45]

$$P_c(X) = 0.404 \pm 0.024, \quad (174)$$

where the error is dominated by the long distance uncertainty estimated in [96]. Next

$$X_{\text{eff}} = V_{ts}^* V_{td} [X_L + X_R], \quad (175)$$

where the functions X_L and X_R summarise the contributions from left-handed and right-handed quark currents, respectively. $\lambda_i = V_{is}^* V_{id}$ are the CKM factors. In what follows we will set these factors to

$$\text{Re } \lambda_t = -3.0 \cdot 10^{-4}, \quad \text{Im } \lambda_t = 1.4 \cdot 10^{-4} \quad (176)$$

which are in the ballpark of present best estimates [59, 60]. The Grossman-Nir (GN) bound on $\mathcal{B}(K_L \rightarrow \pi^0 \nu \bar{\nu})$ reads [76]

$$\mathcal{B}(K_L \rightarrow \pi^0 \nu \bar{\nu}) \leq \frac{\kappa_L}{\kappa_+} \mathcal{B}(K^+ \rightarrow \pi^+ \nu \bar{\nu}) = 4.31 \mathcal{B}(K^+ \rightarrow \pi^+ \nu \bar{\nu}), \quad (177)$$

where we have shown only the central value as it is never reached in the models considered by us. See Figs. 4 and 5.

Experimentally we have [97]

$$\mathcal{B}(K^+ \rightarrow \pi^+ \nu \bar{\nu})_{\text{exp}} = (17.3_{-10.5}^{+11.5}) \cdot 10^{-11}, \quad (178)$$

and the 90% C.L. upper bound [98]

$$\mathcal{B}(K_L \rightarrow \pi^0 \nu \bar{\nu})_{\text{exp}} \leq 2.6 \cdot 10^{-8}. \quad (179)$$

C.2 Z and Z' Cases

In what follows we will give the expressions for X_{eff} in Z and Z' models which inserted into (171) and (172) give the branching ratios for $K^+ \rightarrow \pi^+ \nu \bar{\nu}$ and $K_L \rightarrow \pi^0 \nu \bar{\nu}$. It should be noted that the particular values of the CKM factors in (176) enter only in the SM contributions and in their interferences with NP contributions.

In the case of tree-level Z exchanges we have [65]

$$X_L = X_L^{\text{SM}} + \frac{\Delta_L^{\nu\bar{\nu}}(Z) \Delta_L^{sd}(Z)}{g_{\text{SM}}^2 M_Z^2 V_{ts}^* V_{td}}, \quad X_R = \frac{\Delta_L^{\nu\bar{\nu}}(Z) \Delta_R^{sd}(Z)}{g_{\text{SM}}^2 M_Z^2 V_{ts}^* V_{td}} \quad (180)$$

where

$$g_{\text{SM}}^2 = 4 \frac{M_W^2 G_F^2}{2\pi^2} = 1.78137 \times 10^{-7} \text{ GeV}^{-2}. \quad (181)$$

In the SM only X_L is non-vanishing and is given by [99–102]

$$X_L^{\text{SM}} = 1.481 \pm 0.009 \quad (182)$$

as extracted in [45] from original papers. With the known coupling $\Delta_L^{\nu\bar{\nu}}(Z) = 0.372$ and the CKM factors in (176) we have then

$$\text{Re } X_{\text{eff}}(Z) = -4.44 \cdot 10^{-4} + 2.51 \cdot 10^2 [\text{Re} \Delta_L^{sd}(Z) + \text{Re} \Delta_R^{sd}(Z)], \quad (183)$$

$$\text{Im } X_{\text{eff}}(Z) = 2.07 \cdot 10^{-4} + 2.51 \cdot 10^2 [\text{Im} \Delta_L^{sd}(Z) + \text{Im} \Delta_R^{sd}(Z)], \quad (184)$$

where the first terms on the r.h.s are SM contributions for CKM factors in (176). Note that in $K_L \rightarrow \pi^0 \nu \bar{\nu}$ the enhancement of its branching ratio requires the sum of the imaginary parts of the couplings to be *positive*. This enhances also $K^+ \rightarrow \pi^+ \nu \bar{\nu}$ but could be compensated by the decrease of $\text{Re } X_{\text{eff}}$ unless the sum of the corresponding real parts is *negative*.

In the case of tree-level Z' exchanges one should just replace everywhere the index Z by Z' , in particular M_Z by $M_{Z'}$, and use $\Delta_L^{\nu\bar{\nu}}(Z')$.

The numerical factors in the NP parts in (183) and (184) above should then be multiplied by

$$R = \left[\frac{M_Z}{M_{Z'}} \right]^2 \frac{\Delta_L^{\nu\bar{\nu}}(Z')}{0.372} = 2.48 \times 10^{-3} \left[\frac{3 \text{ TeV}}{M_{Z'}} \right]^2 \Delta_L^{\nu\bar{\nu}}(Z'). \quad (185)$$

Thus we get

$$\text{Re } X_{\text{eff}}(Z') = -4.44 \cdot 10^{-4} + 0.62 \left[\frac{3 \text{ TeV}}{M_{Z'}} \right]^2 [\text{Re} \Delta_L^{sd}(Z') + \text{Re} \Delta_R^{sd}(Z')] \Delta_L^{\nu\bar{\nu}}(Z'), \quad (186)$$

$$\text{Im } X_{\text{eff}}(Z') = 2.07 \cdot 10^{-4} + 0.62 \left[\frac{3 \text{ TeV}}{M_{Z'}} \right]^2 [\text{Im} \Delta_L^{sd}(Z') + \text{Im} \Delta_R^{sd}(Z')] \Delta_L^{\nu\bar{\nu}}(Z'). \quad (187)$$

D $K_L \rightarrow \mu^+ \mu^-$

D.1 General Formulae

Only the so-called short distance (SD) part of a dispersive contribution to $K_L \rightarrow \mu^+ \mu^-$ can be reliably calculated. It is given generally as follows ($\lambda = 0.2252$)

$$\mathcal{B}(K_L \rightarrow \mu^+ \mu^-)_{\text{SD}} = 2.01 \cdot 10^{-9} \left(\frac{\text{Re } Y_{\text{eff}}}{\lambda^5} + \frac{\text{Re } \lambda_c}{\lambda} P_c(Y) \right)^2, \quad (188)$$

where at NNLO [103]

$$P_c(Y) = 0.115 \pm 0.017. \quad (189)$$

The short distance contributions are described by

$$Y_{\text{eff}} = V_{ts}^* V_{td} [Y_L(K) - Y_R(K)], \quad (190)$$

where the functions Y_L and Y_R summarise the contributions from left-handed and right-handed quark currents, respectively. Notice the minus sign in front of Y_R , as opposed to X_R in (175), that results from the fact that only the axial-vector current contributes. This difference allows to be sensitive to right-handed couplings, which is not possible in the case of $K \rightarrow \pi \nu \bar{\nu}$ decays.

The extraction of the short distance part from the data is subject to considerable uncertainties. The most recent estimate gives [104]

$$\mathcal{B}(K_L \rightarrow \mu^+ \mu^-)_{\text{SD}} \leq 2.5 \cdot 10^{-9}, \quad (191)$$

to be compared with $(0.8 \pm 0.1) \cdot 10^{-9}$ in the SM. With our choice of CKM parameters we find $0.72 \cdot 10^{-9}$. It is important to improve this estimate as this would further increase the role of this decay in bounding NP contributions not only in Z scenarios.

D.2 Z and Z' Cases

In the case of tree-level Z exchanges we have [65]

$$Y_L(K) = Y_L^{\text{SM}}(K) + \frac{\Delta_A^{\mu\bar{\mu}}(Z) \Delta_L^{sd}(Z)}{g_{\text{SM}}^2 M_Z^2 V_{ts}^* V_{td}}, \quad Y_R(K) = \frac{\Delta_A^{\mu\bar{\mu}}(Z) \Delta_R^{sd}(Z)}{g_{\text{SM}}^2 M_Z^2 V_{ts}^* V_{td}}, \quad (192)$$

where [105]

$$Y_L^{\text{SM}}(K) = 0.942. \quad (193)$$

With the known coupling $\Delta_A^{\mu\bar{\mu}}(Z) = 0.372$ and the CKM factors in (176) we have then

$$\text{Re } Y_{\text{eff}}(Z) = -2.83 \cdot 10^{-4} + 2.51 \cdot 10^2 [\text{Re} \Delta_L^{sd}(Z) - \text{Re} \Delta_R^{sd}(Z)]. \quad (194)$$

In the case of tree-level Z' exchanges one should just replace everywhere the index Z by Z' , in particular M_Z by $M_{Z'}$, and use $\Delta_A^{\mu\bar{\mu}}(Z')$. As $\Delta_A^{\mu\bar{\mu}}(Z) = \Delta_L^{\nu\bar{\nu}}(Z)$ also the same numerical factor in (185) should multiply NP part in (194). Thus we have

$$\text{Re } Y_{\text{eff}}(Z') = -2.83 \cdot 10^{-4} + 0.62 \left[\frac{3 \text{ TeV}}{M_{Z'}} \right]^2 [\text{Re} \Delta_L^{sd}(Z') - \text{Re} \Delta_R^{sd}(Z')] \Delta_A^{\mu\bar{\mu}}(Z'). \quad (195)$$

E $K_L \rightarrow \pi^0 \ell^+ \ell^-$

The rare decays $K_L \rightarrow \pi^0 e^+ e^-$ and $K_L \rightarrow \pi^0 \mu^+ \mu^-$ are dominated by CP-violating contributions. The indirect CP-violating contributions are determined by the measured decays $K_S \rightarrow \pi^0 \ell^+ \ell^-$ and the parameter ε_K in a model independent manner. It is the dominant contribution within the SM with both branching being $\mathcal{O}(10^{-11})$ [106] and by one order of magnitude smaller than the present experimental bounds

$$\mathcal{B}(K_L \rightarrow \pi^0 e^+ e^-)_{\text{exp}} < 28 \cdot 10^{-11} \quad [107], \quad \mathcal{B}(K_L \rightarrow \pi^0 \mu^+ \mu^-)_{\text{exp}} < 38 \cdot 10^{-11} \quad [108], \quad (196)$$

leaving thereby large room for NP contributions. In the models analyzed by us these bounds have no impact on $K^+ \rightarrow \pi^+ \nu \bar{\nu}$ and $K_L \rightarrow \pi^0 \nu \bar{\nu}$ decays but the present data on $K^+ \rightarrow \pi^+ \nu \bar{\nu}$ do not allow to reach the above bounds in the $Z'(Z)$ scenarios considered.

To our knowledge, there are no definite plans to measure these decays in the near future and we will not analyze them here. They are similar to $B \rightarrow K \ell^+ \ell^-$ decays except that the dipole operator contributions turn out to be small in the SM and in many NP scenarios. NP contributions shift the values of the coefficients C_{7V} and C_{7A} which are sensitive to $\Delta_V^{\mu\bar{\mu}}(Z')$ and $\Delta_A^{\mu\bar{\mu}}(Z')$, respectively. Similar for Z . In the presence of right-handed flavour violating currents also C'_{7V} and C'_{7A} are generated. This is the case of RS scenario with custodial protection [68]. There are also recent efforts to improve SM prediction by means of lattice QCD [109]. The importance of testing NP scenarios, in particular those involving right-handed currents, by means of these decays has been stressed in [106]. Moreover, the measurement of both decays could disentangle the scalar/pseudoscalar from vector/axialvector contributions. But from present perspective such tests will eventually become realistic only in the next decade. References to reach literature can be found in [106] and the analysis of these decays within general Z and Z' models can be found in [65]. As seen in Figs. 12 and 33 of that paper there is a strong correlation between these decays and $K_L \rightarrow \pi^0 \nu \bar{\nu}$ in Z and Z' scenarios so that the increase of $\mathcal{B}(K_L \rightarrow \pi^0 \nu \bar{\nu})$ increases also the branching ratios for $K_L \rightarrow \pi^0 \ell^+ \ell^-$. But the presence of the indirect CP-violating contributions in the latter decays, that are negligible in $K_L \rightarrow \pi^0 \nu \bar{\nu}$, shadows NP effects in them. Only when $\mathcal{B}(K_L \rightarrow \pi^0 \nu \bar{\nu})$ is enhanced by an order of magnitude sizable enhancements of $\mathcal{B}(K_L \rightarrow \pi^0 \ell^+ \ell^-)$ are possible. Similar correlations are found in the LHT model [110] and RSc [68].

In Z scenarios due to the smallness of $\Delta_V^{\mu\bar{\mu}}(Z)$ NP enters these decays predominantly through C_{7A} and C'_{7A} . More interesting is the NP pattern in Z' scenarios due to the $SU(2)_L$ relation

$$\Delta_L^{\nu\bar{\nu}}(Z') = \frac{\Delta_V^{\mu\bar{\mu}}(Z') - \Delta_A^{\mu\bar{\mu}}(Z')}{2}. \quad (197)$$

This relation implies correlations between Z' contributions to $K^+ \rightarrow \pi^+ \nu \bar{\nu}$, $K_L \rightarrow \pi^0 \nu \bar{\nu}$, $K_L \rightarrow \mu^+ \mu^-$ and $K_L \rightarrow \pi^0 \ell^+ \ell^-$ analogous to the ones between $B \rightarrow K(K^*) \nu \bar{\nu}$, $B_d \rightarrow K(K^*) \mu^+ \mu^-$ and $B_s \rightarrow \mu^+ \mu^-$ that have been analyzed in detail in [111]. In order for such relations to become vital in the K -meson system theoretical uncertainties in $K_L \rightarrow \mu^+ \mu^-$ and $K_L \rightarrow \pi^0 \ell^+ \ell^-$ have to be decreased by much. For the most recent analysis of $K_{L,S} \rightarrow \pi^0 \ell^+ \ell^-$ and $K^+ \rightarrow \pi^+ \ell^+ \ell^-$ decays including correlations with LHCb anomalies see [112].

References

- [1] A. J. Buras, M. Gorbahn, S. Jäger, and M. Jamin, *Improved anatomy of ε'/ε in the Standard Model*, *JHEP* **11** (2015) 202, [[arXiv:1507.06345](#)].
- [2] A. J. Buras, *Kaon Theory News*, in *Proceedings, 2015 European Physical Society Conference on High Energy Physics (EPS-HEP 2015)*, 2015. [arXiv:1510.00128](#).
- [3] T. Blum et al., *$K \rightarrow \pi\pi$ $\Delta I = 3/2$ decay amplitude in the continuum limit*, *Phys. Rev.* **D91** (2015), no. 7 074502, [[arXiv:1502.00263](#)].
- [4] **RBC, UKQCD** Collaboration, Z. Bai et al., *Standard Model Prediction for Direct CP Violation in K Decay*, *Phys. Rev. Lett.* **115** (2015), no. 21 212001, [[arXiv:1505.07863](#)].
- [5] N. Garron, *CP violation and Kaon weak matrix elements from Lattice QCD*, in *8th International Workshop on Chiral Dynamics (CD 2015) Pisa, Italy, June 29-July 3, 2015*, 2015. [arXiv:1512.02440](#).
- [6] **NA48** Collaboration, J. Batley et al., *A Precision measurement of direct CP violation in the decay of neutral kaons into two pions*, *Phys. Lett.* **B544** (2002) 97–112, [[hep-ex/0208009](#)].
- [7] **KTeV** Collaboration, A. Alavi-Harati et al., *Measurements of direct CP violation, CPT symmetry, and other parameters in the neutral kaon system*, *Phys. Rev.* **D67** (2003) 012005, [[hep-ex/0208007](#)].
- [8] **KTeV** Collaboration, E. Abouzaid et al., *Precise Measurements of Direct CP Violation, CPT Symmetry, and Other Parameters in the Neutral Kaon System*, *Phys. Rev.* **D83** (2011) 092001, [[arXiv:1011.0127](#)].
- [9] A. J. Buras and J.-M. Gerard, *Upper Bounds on ε'/ε Parameters $B_6^{(1/2)}$ and $B_8^{(3/2)}$ from Large N QCD and other News*, *JHEP* **12** (2015) 008, [[arXiv:1507.06326](#)].
- [10] E. Pallante and A. Pich, *Strong enhancement of ε'/ε through final state interactions*, *Phys. Rev. Lett.* **84** (2000) 2568–2571, [[hep-ph/9911233](#)].
- [11] E. Pallante and A. Pich, *Final state interactions in kaon decays*, *Nucl. Phys.* **B592** (2001) 294–320, [[hep-ph/0007208](#)].
- [12] A. J. Buras et al., *Final state interactions and ε'/ε : A critical look*, *Phys. Lett.* **B480** (2000) 80–86, [[hep-ph/0002116](#)].
- [13] M. Buchler, G. Colangelo, J. Kambor, and F. Orellana, *A Note on the dispersive treatment of $K \rightarrow \pi\pi$ with the kaon off-shell*, *Phys. Lett.* **B521** (2001) 29–32, [[hep-ph/0102289](#)].
- [14] M. Buchler, G. Colangelo, J. Kambor, and F. Orellana, *Dispersion relations and soft pion theorems for $K \rightarrow \pi\pi$* , *Phys. Lett.* **B521** (2001) 22–28, [[hep-ph/0102287](#)].

- [15] E. Pallante, A. Pich, and I. Scimemi, *The Standard model prediction for ε'/ε* , *Nucl. Phys.* **B617** (2001) 441–474, [[hep-ph/0105011](#)].
- [16] A. J. Buras, J.-M. Gérard, and W. A. Bardeen, *Large- N Approach to Kaon Decays and Mixing 28 Years Later: $\Delta I = 1/2$ Rule, \hat{B}_K and ΔM_K* , *Eur. Phys. J.* **C74** (2014), no. 5 2871, [[arXiv:1401.1385](#)].
- [17] A. J. Buras and J.-M. Gerard, *Final State Interactions in $K \rightarrow \pi\pi$ Decays: $\Delta I = 1/2$ Rule vs. ε'/ε* , [arXiv:1603.05686](#).
- [18] A. J. Buras, M. Jamin, M. Lautenbacher, and P. H. Weisz, *Effective Hamiltonians for $\Delta S = 1$ and $\Delta B = 1$ non-leptonic decays beyond the leading logarithmic approximation*, *Nucl. Phys.* **B370** (1992) 69–104.
- [19] A. J. Buras, M. Jamin, M. E. Lautenbacher, and P. H. Weisz, *Two loop anomalous dimension matrix for $\Delta S = 1$ weak non-leptonic decays. 1. $\mathcal{O}(\alpha_s^2)$* , *Nucl. Phys.* **B400** (1993) 37–74, [[hep-ph/9211304](#)].
- [20] A. J. Buras, M. Jamin, and M. E. Lautenbacher, *Two-loop anomalous dimension matrix for $\Delta S = 1$ weak non-leptonic decays. 2. $\mathcal{O}(\alpha\alpha_s)$* , *Nucl. Phys.* **B400** (1993) 75–102, [[hep-ph/9211321](#)].
- [21] M. Ciuchini, E. Franco, G. Martinelli, and L. Reina, *ε'/ε at the next-to-leading order in QCD and QED*, *Phys. Lett.* **B301** (1993) 263–271, [[hep-ph/9212203](#)].
- [22] A. J. Buras, M. Jamin, and M. E. Lautenbacher, *The anatomy of ε'/ε beyond leading logarithms with improved hadronic matrix elements*, *Nucl. Phys.* **B408** (1993) 209–285, [[hep-ph/9303284](#)].
- [23] M. Ciuchini, E. Franco, G. Martinelli, and L. Reina, *The $\Delta S = 1$ effective Hamiltonian including next-to-leading order QCD and QED corrections*, *Nucl. Phys.* **B415** (1994) 403–462, [[hep-ph/9304257](#)].
- [24] A. J. Buras, P. Gambino, and U. A. Haisch, *Electroweak penguin contributions to non-leptonic $\Delta F = 1$ decays at NNLO*, *Nucl. Phys.* **B570** (2000) 117–154, [[hep-ph/9911250](#)].
- [25] M. Gorbahn and U. Haisch, *Effective Hamiltonian for non-leptonic $|\Delta F| = 1$ decays at NNLO in QCD*, *Nucl. Phys.* **B713** (2005) 291–332, [[hep-ph/0411071](#)].
- [26] J. Brod and M. Gorbahn, *ϵ_K at Next-to-Next-to-Leading Order: The Charm-Top-Quark Contribution*, *Phys. Rev.* **D82** (2010) 094026, [[arXiv:1007.0684](#)].
- [27] A. J. Buras, F. De Fazio, and J. Girrbach, *$\Delta I = 1/2$ rule, ε'/ε and $K \rightarrow \pi\nu\bar{\nu}$ in $Z'(Z)$ and G' models with FCNC quark couplings*, *Eur. Phys. J.* **C74** (2014) 2950, [[arXiv:1404.3824](#)].

- [28] A. J. Buras and J. Girrbach, *Towards the Identification of New Physics through Quark Flavour Violating Processes*, *Rept. Prog. Phys.* **77** (2014) 086201, [arXiv:1306.3775].
- [29] C. Lehner, E. Lunghi, and A. Soni, *Emerging lattice approach to the K -Unitarity Triangle*, arXiv:1508.01801.
- [30] A. J. Buras, D. Buttazzo, and R. Knegjens, *$K \rightarrow \pi\nu\bar{\nu}$ and ϵ'/ϵ in Simplified New Physics Models*, *JHEP* **11** (2015) 166, [arXiv:1507.08672].
- [31] M. Blanke, A. J. Buras, and S. Recksiegel, *Quark flavour observables in the Littlest Higgs model with T -parity after LHC Run 1*, arXiv:1507.06316.
- [32] G. A. Rinella, R. Aliberti, F. Ambrosino, B. Angelucci, A. Antonelli, et al., *Prospects for $K^+ \rightarrow \pi^+\nu\bar{\nu}$ at CERN in NA62*, arXiv:1411.0109.
- [33] A. Romano, *The $K^+ \rightarrow \pi^+\nu\bar{\nu}$ decay in the NA62 experiment at CERN*, arXiv:1411.6546.
- [34] **for the KOTO collaboration** Collaboration, K. Shiomi, *$K_L^0 \rightarrow \pi^0\nu\bar{\nu}$ at KOTO*, arXiv:1411.4250.
- [35] V. Cirigliano, A. Pich, G. Ecker, and H. Neufeld, *Isospin violation in ϵ'* , *Phys. Rev. Lett.* **91** (2003) 162001, [hep-ph/0307030].
- [36] V. Cirigliano, G. Ecker, H. Neufeld, and A. Pich, *Isospin breaking in $K \rightarrow \pi\pi$ decays*, *Eur. Phys. J.* **C33** (2004) 369–396, [hep-ph/0310351].
- [37] J. Bijnens and F. Borg, *Isospin breaking in $K \rightarrow 3\pi$ decays III: Bremsstrahlung and fit to experiment*, *Eur. Phys. J.* **C40** (2005) 383–394, [hep-ph/0501163].
- [38] **Particle Data Group** Collaboration, K. Olive et al., *Review of Particle Physics*, *Chin.Phys.* **C38** (2014) 090001. Updates available on <http://pdg.lbl.gov>.
- [39] S. Aoki, Y. Aoki, C. Bernard, T. Blum, G. Colangelo, et al., *Review of lattice results concerning low-energy particle physics*, *Eur. Phys. J.* **C74** (2014), no. 9 2890, [arXiv:1310.8555].
- [40] **Particle Data Group** Collaboration, J. Beringer et al., *Review of Particle Physics (RPP)*, *Phys.Rev.* **D86** (2012) 010001.
- [41] **Heavy Flavor Averaging Group** Collaboration, Y. Amhis et al., *Averages of B -Hadron, C -Hadron, and tau-lepton properties as of early 2012*, arXiv:1207.1158. <http://www.slac.stanford.edu/xorg/hfag>.
- [42] A. J. Buras and D. Guadagnoli, *Correlations among new CP violating effects in $\Delta F = 2$ observables*, *Phys. Rev.* **D78** (2008) 033005, [arXiv:0805.3887].
- [43] A. J. Buras, D. Guadagnoli, and G. Isidori, *On ϵ_K beyond lowest order in the Operator Product Expansion*, *Phys.Lett.* **B688** (2010) 309–313, [arXiv:1002.3612].

- [44] A. J. Buras, M. Jamin, and P. H. Weisz, *Leading and next-to-leading QCD corrections to ε parameter and $B^0 - \bar{B}^0$ mixing in the presence of a heavy top quark*, *Nucl. Phys.* **B347** (1990) 491–536.
- [45] A. J. Buras, D. Buttazzo, J. Girrbach-Noe, and R. Knegjens, *$K^+ \rightarrow \pi^+ \nu \bar{\nu}$ and $K_L \rightarrow \pi^0 \nu \bar{\nu}$ in the Standard Model: status and perspectives*, *JHEP* **11** (2015) 033, [[arXiv:1503.02693](#)].
- [46] A. J. Buras and J.-M. Gérard, *$1/N$ Expansion for Kaons*, *Nucl.Phys.* **B264** (1986) 371.
- [47] W. A. Bardeen, A. J. Buras, and J.-M. Gérard, *The $\Delta I = 1/2$ Rule in the Large N Limit*, *Phys. Lett.* **B180** (1986) 133.
- [48] A. J. Buras and J. M. Gerard, *Isospin Breaking Contributions to ε'/ε* , *Phys. Lett.* **B192** (1987) 156.
- [49] J. Bijnens and J. Prades, *ε'/ε in the chiral limit*, *JHEP* **06** (2000) 035, [[hep-ph/0005189](#)].
- [50] T. Hambye, S. Peris, and E. de Rafael, *Delta $I = 1/2$ and epsilon-prime / epsilon in large $N(c)$ QCD*, *JHEP* **05** (2003) 027, [[hep-ph/0305104](#)].
- [51] J. Bijnens, E. Gamiz, and J. Prades, *Matching the electroweak penguins Q_7 , Q_8 and spectral correlators*, *JHEP* **10** (2001) 009, [[hep-ph/0108240](#)].
- [52] V. Cirigliano, J. F. Donoghue, E. Golowich, and K. Maltman, *Determination of $\langle(\pi\pi)I=2|Q_{7,8}|K^0\rangle$ in the chiral limit*, *Phys. Lett.* **B522** (2001) 245–256, [[hep-ph/0109113](#)].
- [53] V. Cirigliano, J. F. Donoghue, E. Golowich, and K. Maltman, *Improved determination of the electroweak penguin contribution to ε'/ε in the chiral limit*, *Phys. Lett.* **B555** (2003) 71–82, [[hep-ph/0211420](#)].
- [54] M. Ciuchini, E. Franco, G. Martinelli, L. Reina, and L. Silvestrini, *An Upgraded analysis of ε'/ε at the next-to-leading order*, *Z. Phys.* **C68** (1995) 239–256, [[hep-ph/9501265](#)].
- [55] S. Bosch et al., *Standard model confronting new results for ε'/ε* , *Nucl. Phys.* **B565** (2000) 3–37, [[hep-ph/9904408](#)].
- [56] A. J. Buras and M. Jamin, *ε'/ε at the NLO: 10 years later*, *JHEP* **01** (2004) 048, [[hep-ph/0306217](#)].
- [57] S. Bertolini, M. Fabbrichesi, and J. O. Eeg, *Theory of the CP violating parameter ε'/ε* , *Rev. Mod. Phys.* **72** (2000) 65–93, [[hep-ph/9802405](#)].
- [58] E. Lunghi and A. Soni, *Possible Indications of New Physics in B_d -mixing and in $\sin(2\beta)$ Determinations*, *Phys. Lett.* **B666** (2008) 162–165, [[arXiv:0803.4340](#)].

- [59] **UTfit Collaboration** Collaboration, M. Bona et al., *The Unitarity Triangle Fit in the Standard Model and Hadronic Parameters from Lattice QCD: A Reappraisal after the Measurements of Delta $m(s)$ and $BR(B \rightarrow \tau\nu_\tau)$* , *JHEP* **0610** (2006) 081, [[hep-ph/0606167](http://arxiv.org/abs/hep-ph/0606167)]. Updates on <http://www.utfit.org>.
- [60] J. Charles, O. Deschamps, S. Descotes-Genon, H. Lacker, A. Menzel, et al., *Current status of the Standard Model CKM fit and constraints on $\Delta F = 2$ New Physics*, [arXiv:1501.05013](http://arxiv.org/abs/1501.05013). Updates on <http://ckmfitter.in2p3.fr>.
- [61] M. Blanke and A. J. Buras, *Universal Unitarity Triangle 2016 and the Tension Between $\Delta M_{s,d}$ and ε_K in CMFV Models*, [arXiv:1602.04020](http://arxiv.org/abs/1602.04020).
- [62] A. J. Buras and J. Girrbach, *Stringent Tests of Constrained Minimal Flavour Violation through $\Delta F = 2$ Transitions*, *The European Physical Journal C* **9** (73) 2013, [[arXiv:1304.6835](http://arxiv.org/abs/1304.6835)].
- [63] J. A. Bailey, Y.-C. Jang, W. Lee, and S. Park, *Determination of ε_K using lattice QCD inputs*, *PoS LATTICE2015* (2015) 348, [[arXiv:1511.00969](http://arxiv.org/abs/1511.00969)].
- [64] A. Bazavov et al., *$B_{(s)}^0$ -mixing matrix elements from lattice QCD for the Standard Model and beyond*, [arXiv:1602.03560](http://arxiv.org/abs/1602.03560).
- [65] A. J. Buras, F. De Fazio, and J. Girrbach, *The Anatomy of Z' and Z with Flavour Changing Neutral Currents in the Flavour Precision Era*, *JHEP* **1302** (2013) 116, [[arXiv:1211.1896](http://arxiv.org/abs/1211.1896)].
- [66] A. J. Buras, F. De Fazio, and J. Girrbach, *331 models facing new $b \rightarrow s\mu^+\mu^-$ data*, *JHEP* **1402** (2014) 112, [[arXiv:1311.6729](http://arxiv.org/abs/1311.6729)].
- [67] K. Ishiwata, Z. Ligeti, and M. B. Wise, *New Vector-Like Fermions and Flavor Physics*, *JHEP* **10** (2015) 027, [[arXiv:1506.03484](http://arxiv.org/abs/1506.03484)].
- [68] M. Blanke, A. J. Buras, B. Duling, K. Gemmler, and S. Gori, *Rare K and B Decays in a Warped Extra Dimension with Custodial Protection*, *JHEP* **03** (2009) 108, [[arXiv:0812.3803](http://arxiv.org/abs/0812.3803)].
- [69] A. J. Buras, S. Jager, and J. Urban, *Master formulae for $\Delta F = 2$ NLO QCD factors in the standard model and beyond*, *Nucl.Phys.* **B605** (2001) 600–624, [[hep-ph/0102316](http://arxiv.org/abs/hep-ph/0102316)].
- [70] A. J. Buras, D. Buttazzo, J. Girrbach-Noe, and R. Knegjens, *Can we reach the Zeptouniverse with rare K and $B_{s,d}$ decays?*, *JHEP* **1411** (2014) 121, [[arXiv:1408.0728](http://arxiv.org/abs/1408.0728)].
- [71] M. Blanke, *Insights from the Interplay of $K \rightarrow \pi\nu\bar{\nu}$ and ε_K on the New Physics Flavour Structure*, *Acta Phys.Polon.* **B41** (2010) 127, [[arXiv:0904.2528](http://arxiv.org/abs/0904.2528)].
- [72] M. de Vries, *Four-quark effective operators at hadron colliders*, *JHEP* **03** (2015) 095, [[arXiv:1409.4657](http://arxiv.org/abs/1409.4657)].

- [73] **ALEPH Collaboration, DELPHI Collaboration, L3 Collaboration, OPAL Collaboration, LEP Electroweak Working Group Collaboration**, S. Schael et al., *Electroweak Measurements in Electron-Positron Collisions at W-Boson-Pair Energies at LEP*, arXiv:1302.3415.
- [74] J. Brod and M. Gorbahn, *Next-to-Next-to-Leading-Order Charm-Quark Contribution to the CP Violation Parameter ε_K and ΔM_K* , *Phys.Rev.Lett.* **108** (2012) 121801, [arXiv:1108.2036].
- [75] Z. Bai, N. H. Christ, T. Izubuchi, C. T. Sachrajda, A. Soni, and J. Yu, *$K_L - K_S$ Mass Difference from Lattice QCD*, *Phys. Rev. Lett.* **113** (2014) 112003, [arXiv:1406.0916].
- [76] Y. Grossman and Y. Nir, *$K_L \rightarrow \pi^0 \nu \bar{\nu}$ beyond the standard model*, *Phys. Lett.* **B398** (1997) 163–168, [hep-ph/9701313].
- [77] A. J. Buras, F. De Fazio, and J. Girrbach-Noe, *Z-Z' mixing and Z-mediated FCNCs in $SU(3)_C \times SU(3)_L \times U(1)_X$ Models*, *JHEP* **1408** (2014) 039, [arXiv:1405.3850].
- [78] A. J. Buras and F. De Fazio, *ε'/ε in 331 Models*, *JHEP* **03** (2016) 010, [arXiv:1512.02869].
- [79] A. J. Buras, P. Gambino, M. Gorbahn, S. Jager, and L. Silvestrini, *ε'/ε and rare k and b decays in the mssm*, *Nucl. Phys.* **B592** (2001) 55–91, [hep-ph/0007313].
- [80] A. J. Buras, A. Poschenrieder, M. Spranger, and A. Weiler, *The impact of universal extra dimensions on $b \rightarrow x_s \gamma$, $b \rightarrow x_s \text{gluon}$, $b \rightarrow x_s \mu^+ \mu^-$, $k_l \rightarrow \pi^0 e^+ e^-$, and ε'/ε* , *Nucl. Phys.* **B678** (2004) 455–490, [hep-ph/0306158].
- [81] A. Masiero and H. Murayama, *Can ε'/ε be supersymmetric?*, *Phys. Rev. Lett.* **83** (1999) 907–910, [hep-ph/9903363].
- [82] A. J. Buras, G. Colangelo, G. Isidori, A. Romanino, and L. Silvestrini, *Connections between ε'/ε and rare kaon decays in supersymmetry*, *Nucl. Phys.* **B566** (2000) 3–32, [hep-ph/9908371].
- [83] S. Davidson, G. Isidori, and S. Uhlig, *Solving the flavour problem with hierarchical fermion wave functions*, *Phys. Lett.* **B663** (2008) 73–79, [arXiv:0711.3376].
- [84] O. Gedalia, G. Isidori, and G. Perez, *Combining Direct and Indirect Kaon CP Violation to Constrain the Warped KK Scale*, *Phys.Lett.* **B682** (2009) 200–206, [arXiv:0905.3264].
- [85] S. Bertolini, J. O. Eeg, A. Maiezza, and F. Nesti, *New physics in ε' from gluomagnetic contributions and limits on Left-Right symmetry*, *Phys. Rev.* **D86** (2012) 095013, [arXiv:1206.0668].

- [86] A. J. Buras, *Weak Hamiltonian, CP violation and rare decays*, hep-ph/9806471. In 'Probing the Standard Model of Particle Interactions', F. David and R. Gupta, eds., 1998, Elsevier Science B.V.
- [87] F. J. Gilman and M. B. Wise, *Effective Hamiltonian for $\Delta s = 1$ Weak Nonleptonic Decays in the Six Quark Model*, *Phys. Rev.* **D20** (1979) 2392.
- [88] A. J. Buras and J. Girrbach, *Complete NLO QCD Corrections for Tree Level Delta F = 2 FCNC Processes*, *JHEP* **1203** (2012) 052, [arXiv:1201.1302].
- [89] **RBC and UKQCD** Collaboration, P. Boyle, N. Garron, and R. Hudspith, *Neutral kaon mixing beyond the standard model with $n_f = 2 + 1$ chiral fermions*, *Phys. Rev.* **D86** (2012) 054028, [arXiv:1206.5737].
- [90] **ETM** Collaboration, V. Bertone et al., *Kaon Mixing Beyond the SM from $N_f=2$ tmQCD and model independent constraints from the UTA*, *JHEP* **1303** (2013) 089, [arXiv:1207.1287].
- [91] **SWME** Collaboration, B. J. Choi et al., *Kaon BSM B-parameters using improved staggered fermions from $N_f = 2 + 1$ unquenched QCD*, *Phys. Rev.* **D93** (2016), no. 1 014511, [arXiv:1509.00592].
- [92] F. Mescia and C. Smith, *Improved estimates of rare K decay matrix-elements from $K_{\ell 3}$ decays*, *Phys. Rev.* **D76** (2007) 034017, [arXiv:0705.2025].
- [93] A. J. Buras, M. Gorbahn, U. Haisch, and U. Nierste, *The rare decay $K^+ \rightarrow \pi^+ \nu \bar{\nu}$ at the next-to-next-to-leading order in QCD*, *Phys. Rev. Lett.* **95** (2005) 261805, [hep-ph/0508165].
- [94] A. J. Buras, M. Gorbahn, U. Haisch, and U. Nierste, *Charm quark contribution to $K^+ \rightarrow \pi^+ \nu \bar{\nu}$ at next-to-next-to-leading order*, *JHEP* **11** (2006) 002, [hep-ph/0603079].
- [95] J. Brod and M. Gorbahn, *Electroweak Corrections to the Charm Quark Contribution to $K^+ \rightarrow \pi^+ \nu \bar{\nu}$* , *Phys. Rev.* **D78** (2008) 034006, [arXiv:0805.4119].
- [96] G. Isidori, F. Mescia, and C. Smith, *Light-quark loops in $K \rightarrow \pi \nu \bar{\nu}$* , *Nucl. Phys.* **B718** (2005) 319–338, [hep-ph/0503107].
- [97] **E949** Collaboration, A. V. Artamonov et al., *New measurement of the $K^+ \rightarrow \pi^+ \nu \bar{\nu}$ branching ratio*, *Phys. Rev. Lett.* **101** (2008) 191802, [arXiv:0808.2459].
- [98] **E391a** Collaboration, J. Ahn et al., *Experimental study of the decay $K_L^0 \rightarrow \pi^0 \nu \bar{\nu}$* , *Phys. Rev.* **D81** (2010) 072004, [arXiv:0911.4789].
- [99] G. Buchalla and A. J. Buras, *Qcd corrections to rare k and b decays for arbitrary top quark mass*, *Nucl. Phys.* **B400** (1993) 225–239.

- [100] M. Misiak and J. Urban, *QCD corrections to FCNC decays mediated by Z penguins and W boxes*, *Phys.Lett.* **B451** (1999) 161–169, [[hep-ph/9901278](#)].
- [101] G. Buchalla and A. J. Buras, *The rare decays $K \rightarrow \pi\nu\bar{\nu}$, $B \rightarrow X\nu\bar{\nu}$ and $B \rightarrow \ell^+\ell^-$: An Update*, *Nucl.Phys.* **B548** (1999) 309–327, [[hep-ph/9901288](#)].
- [102] J. Brod, M. Gorbahn, and E. Stamou, *Two-Loop Electroweak Corrections for the $K \rightarrow \pi\nu\bar{\nu}$ Decays*, *Phys. Rev.* **D83** (2011) 034030, [[arXiv:1009.0947](#)].
- [103] M. Gorbahn and U. Haisch, *Charm quark contribution to $K_L \rightarrow \mu^+\mu^-$ at next-to-next-to-leading order*, *Phys. Rev. Lett.* **97** (2006) 122002, [[hep-ph/0605203](#)].
- [104] G. Isidori and R. Unterdorfer, *On the short-distance constraints from $K_{L,S} \rightarrow \mu^+\mu^-$* , *JHEP* **01** (2004) 009, [[hep-ph/0311084](#)].
- [105] C. Bobeth, M. Gorbahn, and E. Stamou, *Electroweak Corrections to $B_{s,d} \rightarrow \ell^+\ell^-$* , *Phys. Rev.* **D89** (2014) 034023, [[arXiv:1311.1348](#)].
- [106] F. Mescia, C. Smith, and S. Trine, *$K_L \rightarrow \pi^0 e^+ e^-$ and $K_L \rightarrow \pi^0 \mu^+ \mu^-$: A binary star on the stage of flavor physics*, *JHEP* **08** (2006) 088, [[hep-ph/0606081](#)].
- [107] **KTeV** Collaboration, A. Alavi-Harati et al., *Search for the Rare Decay $K_L \rightarrow \pi^0 e^+ e^-$* , *Phys. Rev. Lett.* **93** (2004) 021805, [[hep-ex/0309072](#)].
- [108] **KTEV** Collaboration, A. Alavi-Harati et al., *Search for the Decay $K_L \rightarrow \pi^0 \mu^+ \mu^-$* , *Phys. Rev. Lett.* **84** (2000) 5279–5282, [[hep-ex/0001006](#)].
- [109] **RBC, UKQCD** Collaboration, N. H. Christ, X. Feng, A. Portelli, and C. T. Sachrajda, *Prospects for a lattice computation of rare kaon decay amplitudes: $K \rightarrow \pi \ell^+ \ell^-$ decays*, *Phys. Rev.* **D92** (2015), no. 9 094512, [[arXiv:1507.03094](#)].
- [110] M. Blanke et al., *Rare and CP-violating K and B decays in the Littlest Higgs model with T-parity*, *JHEP* **01** (2007) 066, [[hep-ph/0610298](#)].
- [111] A. J. Buras, J. Girrbach-Noe, C. Niehoff, and D. M. Straub, *$B \rightarrow K^{(*)}\nu\bar{\nu}$ decays in the Standard Model and beyond*, *JHEP* **1502** (2015) 184, [[arXiv:1409.4557](#)].
- [112] A. Crivellin, G. D’Ambrosio, M. Hoferichter, and L. C. Tunstall, *Lepton flavor (universality) violation in rare kaon decays*, [arXiv:1601.00970](#).